IMA Journal of Numerical Analysis (2025) **00**, 1–44
https://doi.org/10.1093/imanum/draf101

A priori and *a posteriori* error bounds for the fully mixed FEM formulation of poroelasticity with stress-dependent permeability

Arbaz Khan
Department of Mathematics, Indian Institute of Technology Roorkee (IITR), Roorkee 247667, India

Bishnu P. Lamichhane
School of Information and Physical Sciences, University of Newcastle, University Drive, Newcastle, New South Wales 2308, Australia

Ricardo Ruiz-Baier*
School of Mathematics, Monash University, 9 Rainforest Walk, Melbourne, Victoria 3800, Australia
Universidad Adventista de Chile, Casilla 7-D, Chillán, Chile
Institute for Computer Science and Mathematical Modeling, Sechenov First Moscow State Medical University, Moscow, 119048, Russia
*Corresponding author: ricardo.ruizbaier@monash.edu

AND

Segundo Villa-Fuentes
School of Mathematics, Monash University, 9 Rainforest Walk, Melbourne, Victoria 3800, Australia
Departamento de Matemáticas, Universidad del Bío-Bío, Avenida Collao 1202, Casilla 5-C, Concepción, Chile
Departamento de Ciencias Exactas, Universidad de Los Lagos, Casilla 933, Osorno, Chile

[Received on 19 February 2025; revised on 17 August 2025]

We develop a family of mixed finite element methods for a model of nonlinear poroelasticity where, due to a rewriting of the constitutive equations, the permeability depends on the total poroelastic stress and on the fluid pressure, and therefore we can use the Hellinger–Reissner principle with weakly imposed stress symmetry for Biot's equations. The problem is adequately structured into a coupled system consisting of one saddle-point formulation, one linearized perturbed saddle-point formulation and two off-diagonal perturbations. This system's unique solvability requires assumptions on regularity and Lipschitz continuity of the inverse permeability, and the analysis follows fixed-point arguments and the Babuška–Brezzi theory. The discrete problem is shown uniquely solvable by applying similar fixed-point and saddle-point techniques as for the continuous case. The method is based on the classical PEERS$_k$ elements; it is exactly equilibrium and mass conservative, and it is robust with respect to the nearly incompressible, as well as vanishing storativity limits. We derive *a priori* error estimates; we also propose fully computable residual-based *a posteriori* error indicators, and show that they are reliable and efficient with respect to the natural norms, and robust in the limit of near incompressibility. These *a posteriori* error estimates are used to drive adaptive mesh refinement. The theoretical analysis is supported and illustrated by several numerical examples in two dimensions and three dimensions.

Keywords: mixed finite elements; stress-based formulation; nonlinear poroelasticity; fixed-point operators; error estimates.

1. Introduction

Scope. Nonlinear interaction between flow and the mechanical response of saturated porous media is of great importance in many applications in biophysics, geomechanics and tissue engineering, for example. One of such models is the equations of nonlinear poroelasticity, whose mathematical and numerical properties were studied in detail, for example, in the references Showalter & Su (2001), Cao *et al.* (2013), Gaspar *et al.* (2016), Borregales Reverón *et al.* (2021), van Duijn & Mikelić (2023) and Kraus *et al.* (2024). In addition, in the works Bociu *et al.* (2016), Bociu & Webster (2021) and Bociu *et al.* (2022) it is emphasized that a distinctive property of nonlinear poroelasticity models targeted for, e.g., soft tissue (cartilage, trabecular meshwork, brain matter, etc.) is that the nonlinear permeability (the hydraulic conductivity, defined as how easily pore fluid escapes from the compacted pore spaces), which depends on the evolving total amount of fluid, does not entail a monotone operator, and therefore one cannot readily apply typical tools from monotone saddle-point problems.

More specifically, this work considers deriving mixed finite element (FE) formulations (solving also for other variables of interest), and for this we can cite in particular Gómez-Vargas *et al.* (2023) and Lamichhane *et al.* (2024), where fully mixed formulations based on the Hu–Washizu principle are studied. Writing the poroelasticity equations in terms of the strain tensor was motivated in particular in Lamichhane *et al.* (2024) because the permeability—at least in the regime we focus on here—depends nonlinearly on the total amount of fluid, which is a function of strain.

Novelty and main contributions. The upshot here compared with Lamichhane *et al.* (2024) is that we are able to rewrite the constitutive equation for permeability to depend on the total poroelastic stress and on the fluid pressure (similarly as in, e.g., Barbeiro & Wheeler (2010)). This allows us to revert to the more popular Hellinger–Reissner type of mixed formulations for poroelasticity (Yi, 2014; Lee, 2016; Bærland *et al.*, 2017; Li & Yotov, 2022) (without solving explicitly for the strain). Consequently, another appealing advantage with respect to the formulation in Lamichhane *et al.* (2024) is that, as in the Hellinger–Reissner formulation, the model becomes robust in the nearly incompressibility regime. Also, in contrast to Lamichhane *et al.* (2024), in this work we use a mixed form for the fluid flow (adding the discharge flux as additional unknown), which gives the additional advantage of mass conservativity. This is certainly a key advantage over other models for nonlinear permeability poromechanics: that the formulation is adequately reverted into a form that lends itself to analysis using well-known techniques.

Regarding the well-posedness analysis the aforementioned nonmonotonicity of the permeability suggest, for example, to use a fixed-point argument. We opt for freezing the arguments of permeability, turning the double saddle-point structure with three perturbations coming from the stress trace operator and from the L^2 pressure blocks into two decoupled saddle-point problems whose separate solvability can be established from the classical literature for weakly symmetric elasticity and mixed reaction–diffusion equations. Banach fixed-point theorem is then used to show well-posedness of the overall problem. This analysis needs to verify conditions of ball-mapping and contraction of the fixed-point map, and this imposes a small data assumption, which can be carried over to the external load, mass source, boundary displacement and boundary fluid pressure. Compared with Lamichhane *et al.* (2024) these conditions are less restrictive and imply also a less restrictive discrete analysis (which follows closely the continuous one), due to the analysis being performed using the inverse of the Hooke tensor, which allows us to achieve robustness with respect to the first Lamé parameter λ and also with respect to the storativity coefficient.

Note that at the discrete level we can simply use conforming FE spaces. Discrete inf-sup conditions are already well known for the chosen FE families of PEERS_k and Raviart–Thomas elements used for the solid and fluid sub-problems (but several other inf-sup stable spaces that satisfy a discrete kernel characterization are also possible). We emphasize that, as a consequence of the parameter robustness

of the continuous formulation and of the conformity of the discretization, all estimates hold uniformly in the limit of nearly incompressibility (implying that the formulation is Poisson locking-free), as well as when the constrained storage coefficient vanishes (poroelastic locking-free), and therefore they are free of nonphysical pressure oscillations. These properties are confirmed numerically through a set of computations including mild and extreme parameters, not only testing dependence on Lamé constants and storativity-permeability, but also the Biot–Willis coefficient.

An additional goal of this work is to derive efficient and reliable residual *a posteriori* error estimators for the nonlinear poroelasticity equations. The approach follows a similar treatment as that of Gatica *et al.* (2022) (which focuses on mixed formulations of stress-assisted diffusion equations), with the difference that here we do not need to include augmentation terms for the mixed form of the mixed diffusion problem. The main ingredients in the analysis of these estimates are Helmholtz decompositions and a global inf-sup (together with boundedness and Lipschitz continuity of coupling terms), local inverse and trace estimates, bubble-based localization arguments and properties of Clément and Raviart–Thomas interpolators. See also Álvarez *et al.* (2016) and Elyes *et al.* (2019) for estimators in a similar multiphysics context and, e.g., Carstensen & Dolzmann (1998), Carstensen *et al.* (2000) and Lonsing & Verfürth (2004) for mixed linear elasticity. Note that for the reliability of the estimator the aforementioned Helmholtz decompositions—for both tensor-vector and vector-scalar cases—should be valid for mixed boundary conditions. For this we follow Álvarez *et al.* (2016) and Caucao *et al.* (2022), from which we inherit a convexity assumption on the Neumann sub-boundary (where we impose traction and flux boundary conditions).

Outline. The rest of the paper is organized as follows. The remainder of this section has a collection of preliminary definitions and notational convention, as well as the statement of the governing partial differential equations. The weak formulation and proofs of the uniform boundedness of the bilinear forms and suitable inf-sup conditions are shown in Section 2. The fixed-point analysis of the coupled problem is carried out in Section 3. Section 4 then focuses on the Galerkin discretization, including its well-posedness analysis and definition of specific FE subspaces that provide equilibrium and mass conservativity. In Section 5 we show a Céa estimate and using appropriate approximation properties we derive optimal *a priori* error bounds including also the higher order case. The definition of a residual *a posteriori* error estimator and the proofs of its reliability and efficiency are presented in Section 6. We display in Section 7 some numerical tests that both validate and underline the theoretical properties of the proposed discretizations, and close in Section 8 with a summary and a discussion on possible extensions.

Notation and preliminaries. Let $\mathrm{L}^2(\Omega)$ be the set of all square-integrable functions in $\Omega \subset \mathbb{R}^d$ where $d \in \{2,3\}$ is the spatial dimension, and we denote by $\mathbf{L}^2(\Omega) = \mathrm{L}^2(\Omega)^d$ its vector-valued counterpart and by $\mathbb{L}^2(\Omega) = \mathrm{L}^2(\Omega)^{d\times d}$ its tensor-valued counterpart. We also write

$$\mathbb{L}^2_{\mathrm{skew}}(\Omega) := \{\boldsymbol{\tau} \in \mathbb{L}^2(\Omega) : \boldsymbol{\tau} = -\boldsymbol{\tau}^{\mathrm{t}}\}$$

to represent the skew-symmetric tensors in Ω with each component being square-integrable. Standard notation will be employed for Sobolev spaces $\mathrm{H}^m(\Omega)$ with $m \geq 0$ (and we note that $\mathrm{H}^0(\Omega) = \mathrm{L}^2(\Omega)$). Their norms and seminorms are denoted as $\|\cdot\|_{m,\Omega}$ and $|\cdot|_{m,\Omega}$, respectively (as well as for their vector and tensor-valued counterparts $\mathbf{H}^m(\Omega)$, $\mathbb{H}^m(\Omega)$) see, e.g., Brenner & Scott (1994).

As usual, $\mathbf{I}$ stands for the identity tensor in $\mathbb{R}^{d\times d}$, and $|\cdot|$ denotes the Euclidean norm in $\mathbb{R}^d$. Also, for any vector field $\mathbf{v} = (v_i)_{i=1,d}$ we set the gradient and divergence operators as $\nabla\mathbf{v} := \left(\frac{\partial v_i}{\partial x_j}\right)_{i,j=1,d}$ and $\mathrm{div}\,\mathbf{v} := \sum_{j=1}^{d} \frac{\partial v_j}{\partial x_j}$. In addition, for any tensor fields $\boldsymbol{\tau} = (\tau_{ij})_{i,j=1,d}$ and $\boldsymbol{\zeta} = (\zeta_{ij})_{i,j=1,d}$ we let $\mathbf{div}\,\boldsymbol{\tau}$ be the divergence operator div acting along the rows of $\boldsymbol{\tau}$, and define the transpose, the trace, the tensor

inner product and the deviatoric tensor as $\boldsymbol{\tau}^{\mathrm{t}} := (\tau_{ji})_{i,j=1,d}$, $\mathrm{tr}(\boldsymbol{\tau}) := \sum_{i=1}^{d} \tau_{ii}$, $\boldsymbol{\tau} : \boldsymbol{\zeta} := \sum_{i,j=1}^{n} \tau_{ij}\zeta_{ij}$ and $\boldsymbol{\tau}^{\mathrm{d}} := \boldsymbol{\tau} - \frac{1}{d}\,\mathrm{tr}(\boldsymbol{\tau})\,\mathbf{I}$, respectively. We also recall the Hilbert space

$$\mathbf{H}(\mathrm{div};\Omega) := \left\{ z \in \mathbf{L}^2(\Omega) : \ \mathrm{div}\, z \in \mathrm{L}^2(\Omega) \right\},$$

with norm $\|z\|^2_{\mathrm{div};\Omega} := \|z\|^2_{0,\Omega} + \|\mathrm{div}\, z\|^2_{0,\Omega}$, and introduce its tensor-valued version

$$\mathbb{H}(\mathbf{div};\Omega) := \left\{ \boldsymbol{\tau} \in \mathbb{L}^2(\Omega) : \ \mathbf{div}\, \boldsymbol{\tau} \in \mathbf{L}^2(\Omega) \right\}.$$

Governing equations. Let us consider a fully saturated poroelastic medium (consisting of a mechanically isotropic and homogeneous fluid-solid mixture) occupying the open and bounded domain Ω in $\mathbb{R}^d$; the Lipschitz boundary $\partial\Omega$ is partitioned into disjoint sub-boundaries $\partial\Omega := \overline{\Gamma_{\mathrm{D}}} \cup \overline{\Gamma_{\mathrm{N}}}$, and it is assumed for the sake of simplicity that both sub-boundaries are nonempty $|\Gamma_{\mathrm{D}}| \cdot |\Gamma_{\mathrm{N}}| > 0$. The symbol $\boldsymbol{n}$ will stand for the unit outward normal vector on the boundary. Let $\boldsymbol{f} \in \mathbf{L}^2(\Omega)$ be a prescribed body force per unit of volume (acting on the fluid-structure mixture) and let $g \in L^2(\Omega)$ be a net volumetric fluid production rate.

The equilibrium (balance of linear momentum) for the solid-fluid mixture is written as

$$-\,\mathbf{div}\,\boldsymbol{\sigma} = \boldsymbol{f} \qquad \text{in } \Omega, \tag{1.1}$$

with $\boldsymbol{\sigma}$ being the total Cauchy stress tensor of the mixture (sum of the effective solid and fluid stresses), whose dependence on strain and on fluid pressure is given by the constitutive assumption (or effective stress principle)

$$\boldsymbol{\sigma} = \mathscr{C}\boldsymbol{\varepsilon}(\boldsymbol{u}) - \alpha p \mathbf{I} \qquad \text{in } \Omega. \tag{1.2}$$

Here, the skeleton displacement vector $\boldsymbol{u}$ from the position $\boldsymbol{x} \in \Omega$ is an unknown, the tensor $\boldsymbol{\varepsilon}(\boldsymbol{u}) := \frac{1}{2}(\nabla \boldsymbol{u} + [\nabla \boldsymbol{u}]^{\mathrm{t}})$ is the infinitesimal strain, by $\mathscr{C}$ we denote the fourth-order elasticity tensor, also known as Hooke's tensor (symmetric and positive definite and characterized by $\mathscr{C}\boldsymbol{\tau} := \lambda(\mathrm{tr}\boldsymbol{\tau})\mathbf{I} + 2\mu\,\boldsymbol{\tau}$), λ and μ are the Lamé parameters (assumed constant and positive), $0 \le \alpha \le 1$ is the Biot–Willis parameter and p denotes the Darcy fluid pressure (positive in compression), which is an unknown in the system.

We also consider the balance of angular momentum, which in this context states that the total poroelastic stress is a symmetric tensor $\boldsymbol{\sigma} = \boldsymbol{\sigma}^{\mathrm{t}}$. To weakly impose it is customary to use the rotation tensor

$$\boldsymbol{\rho} = \frac{1}{2}(\nabla \boldsymbol{u} - [\nabla \boldsymbol{u}]^{\mathrm{t}}) = \nabla \boldsymbol{u} - \boldsymbol{\varepsilon}(\boldsymbol{u}). \tag{1.3}$$

The fluid content (due to both fluid saturation and local volume dilation) is given by

$$\zeta = c_0 p + \alpha\, \mathrm{div}\, \boldsymbol{u}, \tag{1.4}$$

where $c_0 \ge 0$ is the constrained specific storage coefficient. Using Darcy's law to describe the discharge velocity in terms of the fluid pressure gradient the balance of mass for the total amount of fluid is

$\partial_t \zeta - \operatorname{div}(\boldsymbol{\kappa}\nabla p) = g$ in $\Omega \times (0, t_{\text{end}})$, where $\boldsymbol{\kappa}$ is the intrinsic permeability tensor of the medium, a nonlinear function of the porosity. In turn, in the limit of small strains, the porosity can be approximated by a linear function of the fluid content ζ (see for example (van Duijn & Mikelić, 2023, section 2.1)), and so, due to (1.4), we can simply write

$$\boldsymbol{\kappa} = \boldsymbol{\kappa}(\boldsymbol{\varepsilon}(\boldsymbol{u}), p).$$

Furthermore, after a backward Euler semidiscretization in time with a constant time step and rescaling appropriately, we only consider the type of equations needed to solve at each time step, and therefore we will concentrate on the form

$$c_0 p + \alpha \operatorname{tr}\boldsymbol{\varepsilon}(\boldsymbol{u}) - \operatorname{div}\left(\boldsymbol{\kappa}(\boldsymbol{\varepsilon}(\boldsymbol{u}), p)\nabla p\right) = g \qquad \text{in } \Omega. \tag{1.5}$$

Typical constitutive relations for permeability are, e.g., exponential or Kozeny–Carman type (cf. Ateshian & Weiss (2010))

$$\boldsymbol{\kappa}(\boldsymbol{\varepsilon}(\boldsymbol{u}), p) = \frac{k_0}{\mu_f}\mathbf{I} + \frac{k_1}{\mu_f}\exp(k_2(c_0 p + \alpha \operatorname{tr}\boldsymbol{\varepsilon}(\boldsymbol{u})))\mathbf{I}, \quad \boldsymbol{\kappa}(\boldsymbol{\varepsilon}(\boldsymbol{u}), p) = \frac{k_0}{\mu_f}\mathbf{I} + \frac{k_1(c_0 p + \alpha \operatorname{tr}\boldsymbol{\varepsilon}(\boldsymbol{u}))^3}{\mu_f(1 - (c_0 p + \alpha \operatorname{tr}\boldsymbol{\varepsilon}(\boldsymbol{u})))^2}\mathbf{I}, \tag{1.6}$$

where μ_f denotes the viscosity of the interstitial fluid and k_0, k_1 *and* k_2 are model constants. We note that in the case of incompressible constituents one has $c_0 = 0$ and $\alpha = 1$, indicating that permeability depends only on the dilation $\operatorname{tr}\boldsymbol{\varepsilon}(\boldsymbol{u}) = \operatorname{div}\boldsymbol{u}$ (see, e.g., Bociu *et al.* (2016)). We also note that even in such a scenario (of incompressible phases) the overall mixture is not necessarily incompressible itself. More precise assumptions on the behaviour of the permeability are postponed to Section 2.2. Next, we note that from (1.2) we can obtain

$$\operatorname{tr}\boldsymbol{\sigma} = (d\lambda + 2\mu)\operatorname{div}\boldsymbol{u} - d\alpha p \quad \text{and} \quad \mathscr{C}^{-1}\boldsymbol{\sigma} + \frac{\alpha}{d\lambda + 2\mu}p\mathbf{I} = \boldsymbol{\varepsilon}(\boldsymbol{u}) \qquad \text{in } \Omega. \tag{1.7}$$

Then, from the first equation in (1.7) we get

$$\operatorname{tr}\boldsymbol{\varepsilon}(\boldsymbol{u}) = \frac{1}{d\lambda + 2\mu}\operatorname{tr}\boldsymbol{\sigma} + \frac{d\alpha}{d\lambda + 2\mu}p,$$

and therefore the dependence of $\boldsymbol{\kappa}$ on $\boldsymbol{\varepsilon}(\boldsymbol{u})$ and p (cf. (1.6)) can be written in terms of $\boldsymbol{\sigma}$ and p as follows:

$$\begin{aligned}
\boldsymbol{\kappa}(\boldsymbol{\sigma}, p) &= \frac{k_0}{\mu_f}\mathbf{I} + \frac{k_1}{\mu_f}\exp\left(\frac{k_2}{d\lambda + 2\mu}\left((c_0(d\lambda + 2\mu) + d\alpha^2)\,p + \alpha \operatorname{tr}\boldsymbol{\sigma}\right)\right)\mathbf{I}, \\
\boldsymbol{\kappa}(\boldsymbol{\sigma}, p) &= \frac{k_0}{\mu_f}\mathbf{I} + \frac{k_1\left((c_0(d\lambda + 2\mu) + d\alpha^2)\,p + \alpha \operatorname{tr}\boldsymbol{\sigma}\right)^3}{(d\lambda + 2\mu)\mu_f\left(d\lambda + 2\mu - ((c_0(d\lambda + 2\mu) + d\alpha^2)\,p + \alpha \operatorname{tr}\boldsymbol{\sigma})\right)^2}\mathbf{I},
\end{aligned} \tag{1.8}$$

and emphasize that the permeability tensor is the same constitutive law on either (1.6) or (1.8), so, making abuse of notation, we have

$$\boldsymbol{\kappa} = \boldsymbol{\kappa}(\zeta) = \boldsymbol{\kappa}(\boldsymbol{\varepsilon}(\boldsymbol{u}), p) = \boldsymbol{\kappa}(\boldsymbol{\sigma}, p).$$

In addition, putting together the second equation in (1.7) and (1.3), we obtain

$$\mathscr{C}^{-1}\boldsymbol{\sigma} + \frac{\alpha}{d\lambda + 2\mu} p\mathbf{I} = \boldsymbol{\nabla u} - \boldsymbol{\rho} \qquad \text{in } \Omega. \tag{1.9}$$

Finally, we introduce the discharge flux $\boldsymbol{\varphi}$ as an unknown defined by the constitutive relation

$$\boldsymbol{\kappa}(\boldsymbol{\sigma}, p)^{-1}\boldsymbol{\varphi} = \nabla p, \tag{1.10}$$

and combining (1.7) and (1.5) we are able to rewrite the mass balance equation as

$$c_0 p + \frac{\alpha}{d\lambda + 2\mu} \mathrm{tr}\boldsymbol{\sigma} + \frac{d\alpha^2}{d\lambda + 2\mu} p - \operatorname{div} \boldsymbol{\varphi} = g \qquad \text{in } \Omega. \tag{1.11}$$

To close the system we consider mixed boundary conditions for a given $\boldsymbol{u}_{\mathrm{D}} \in \mathbf{H}^{1/2}(\Gamma_{\mathrm{D}})$ and $p_{\mathrm{D}} \in \mathrm{H}^{1/2}(\Gamma_{\mathrm{D}})$:

$$\boldsymbol{u} = \boldsymbol{u}_{\mathrm{D}} \quad \text{and} \quad p = p_{\mathrm{D}} \quad \text{on} \quad \Gamma_{\mathrm{D}}, \qquad \boldsymbol{\varphi} \cdot \boldsymbol{n} = 0 \quad \text{and} \quad \boldsymbol{\sigma n} = \mathbf{0} \quad \text{on} \quad \Gamma_{\mathrm{N}}. \tag{1.12}$$

2. Weak formulation and preliminary properties

2.1 *Derivation of weak forms*

Let us define the following spaces:

$$\mathbb{H}_{\mathrm{N}}(\mathbf{div}; \Omega) := \left\{ \boldsymbol{\tau} \in \mathbb{H}(\mathbf{div}; \Omega) : \ \boldsymbol{\tau n} = \mathbf{0} \quad \text{on} \quad \Gamma_{\mathrm{N}} \right\},$$

$$\mathbf{H}_{\mathrm{N}}(\mathrm{div}; \Omega) := \left\{ \boldsymbol{\psi} \in \mathbf{H}(\mathrm{div}; \Omega) : \ \boldsymbol{\psi} \cdot \boldsymbol{n} = 0 \quad \text{on} \quad \Gamma_{\mathrm{N}} \right\}.$$

We test equation (1.1) against $\mathbf{v} \in \mathbf{L}^2(\Omega)$, equation (1.9) against $\boldsymbol{\tau} \in \mathbb{H}_{\mathrm{N}}(\mathbf{div}; \Omega)$, impose the symmetry of $\boldsymbol{\sigma}$ weakly, test equation (1.11) against $q \in \mathrm{L}^2(\Omega)$, equation (1.10) against $\boldsymbol{\psi} \in \mathbf{H}_{\mathrm{N}}(\mathrm{div}; \Omega)$, integrate by parts and use the boundary conditions (1.12) naturally, and then reorder the resulting equations. Then,

we arrive at

$$\int_\Omega \mathscr{C}^{-1}\boldsymbol{\sigma} : \boldsymbol{\tau} + \frac{\alpha}{d\lambda + 2\mu}\int_\Omega p\,\mathrm{tr}\boldsymbol{\tau} + \int_\Omega \boldsymbol{u}\cdot\mathbf{div}\boldsymbol{\tau} + \int_\Omega \boldsymbol{\rho} : \boldsymbol{\tau} = \langle \boldsymbol{\tau}\boldsymbol{n}, \boldsymbol{u}_{\mathrm{D}}\rangle_{\Gamma_{\mathrm{D}}} \qquad \forall\, \boldsymbol{\tau} \in \mathbb{H}_{\mathrm{N}}(\mathbf{div};\Omega),$$

$$\int_\Omega \mathbf{v}\cdot\mathbf{div}\,\boldsymbol{\sigma} = -\int_\Omega \boldsymbol{f}\cdot\mathbf{v} \qquad \forall\, \mathbf{v} \in \mathbf{L}^2(\Omega),$$

$$\int_\Omega \boldsymbol{\sigma} : \boldsymbol{\eta} = 0 \qquad \forall\, \boldsymbol{\eta} \in \mathbb{L}^2_{\mathrm{skew}}(\Omega),$$

$$\int_\Omega \boldsymbol{\kappa}(\boldsymbol{\sigma}, p)^{-1}\boldsymbol{\varphi}\cdot\boldsymbol{\psi} + \int_\Omega p\,\mathrm{div}\,\boldsymbol{\psi} = \langle \boldsymbol{\psi}\cdot\boldsymbol{n}, p_{\mathrm{D}}\rangle_{\Gamma_{\mathrm{D}}} \qquad \forall\, \boldsymbol{\psi} \in \mathbf{H}_{\mathrm{N}}(\mathrm{div};\Omega),$$

$$\left(c_0 + \frac{d\alpha^2}{d\lambda + 2\mu}\right)\int_\Omega p\,q + \frac{\alpha}{d\lambda + 2\mu}\int_\Omega q\,\mathrm{tr}\boldsymbol{\sigma} - \int_\Omega q\,\mathrm{div}\,\boldsymbol{\varphi} = \int_\Omega g\,q \qquad \forall\, q \in \mathrm{L}^2(\Omega),$$

where $\langle\cdot,\cdot\rangle_{\Gamma_{\mathrm{D}}}$ denotes the duality pairing between $\mathrm{H}^{-1/2}(\Gamma_{\mathrm{D}})$ and its dual $\mathrm{H}^{1/2}(\Gamma_{\mathrm{D}})$ with respect to the inner product in $L^2(\Gamma_{\mathrm{D}})$, and we use the same notation, $\langle\cdot,\cdot\rangle_{\Gamma_{\mathrm{D}}}$, in the vector-valued case.

Next, we proceed to introduce the bilinear forms $a : \mathbb{H}_{\mathrm{N}}(\mathbf{div};\Omega)\times\mathbb{H}_{\mathrm{N}}(\mathbf{div};\Omega) \to \mathbb{R}$, $b : \mathbb{H}_{\mathrm{N}}(\mathbf{div};\Omega)\times[\mathbf{L}^2(\Omega)\times\mathbb{L}^2_{\mathrm{skew}}(\Omega)] \to \mathbb{R}$, $c : \mathbb{H}_{\mathrm{N}}(\mathbf{div};\Omega)\times\mathrm{L}^2(\Omega) \to \mathbb{R}$, the nonlinear form $\widetilde{a}_{\widehat{\boldsymbol{\sigma}},\widehat{p}} : \mathbf{H}_{\mathrm{N}}(\mathrm{div};\Omega)\times\mathbf{H}_{\mathrm{N}}(\mathrm{div};\Omega) \to \mathbb{R}$, and the bilinear forms $\widetilde{b} : \mathbf{H}_{\mathrm{N}}(\mathrm{div};\Omega)\times\mathrm{L}^2(\Omega) \to \mathbb{R}$ and $\widetilde{c} : \mathrm{L}^2(\Omega)\times\mathrm{L}^2(\Omega) \to \mathbb{R}$, as follows:

$$a(\boldsymbol{\sigma},\boldsymbol{\tau}) := \textstyle\int_\Omega \mathscr{C}^{-1}\boldsymbol{\sigma} : \boldsymbol{\tau}, \quad b(\boldsymbol{\tau},(\mathbf{v},\boldsymbol{\eta})) := \int_\Omega \mathbf{v}\cdot\mathbf{div}\,\boldsymbol{\tau} + \int_\Omega \boldsymbol{\tau} : \boldsymbol{\eta}, \quad c(\boldsymbol{\tau},q) := \frac{\alpha}{d\lambda+2\mu}\int_\Omega q\,\mathrm{tr}\boldsymbol{\tau},$$

$$\widetilde{a}_{\widehat{\boldsymbol{\sigma}},\widehat{p}}(\boldsymbol{\varphi},\boldsymbol{\psi}) := \textstyle\int_\Omega \boldsymbol{\kappa}(\widehat{\boldsymbol{\sigma}},\widehat{p})^{-1}\boldsymbol{\varphi}\cdot\boldsymbol{\psi}, \quad \widetilde{b}(\boldsymbol{\psi},q) := \int_\Omega q\,\mathrm{div}\,\boldsymbol{\psi}, \quad \widetilde{c}(p,q) := \left(c_0 + \frac{d\alpha^2}{d\lambda+2\mu}\right)\int_\Omega p\,q, \tag{2.1}$$

respectively, and linear functionals $H \in \mathbb{H}_{\mathrm{N}}(\mathbf{div};\Omega)'$, $F \in (\mathbf{L}^2(\Omega)\times\mathbb{L}^2_{\mathrm{skew}}(\Omega))'$, $\widetilde{H} \in \mathbf{H}_{\mathrm{N}}(\mathrm{div};\Omega)'$, $\tilde{F} \in \mathrm{L}^2(\Omega)'$

$$H(\boldsymbol{\tau}) := \langle\boldsymbol{\tau}\boldsymbol{n},\boldsymbol{u}_{\mathrm{D}}\rangle_{\Gamma_{\mathrm{D}}}, \quad F(\mathbf{v},\boldsymbol{\eta}) := -\int_\Omega \boldsymbol{f}\cdot\mathbf{v}, \quad \widetilde{H}(\boldsymbol{\psi}) := \langle\boldsymbol{\psi}\cdot\boldsymbol{n},p_{\mathrm{D}}\rangle_{\Gamma_{\mathrm{D}}}, \quad \tilde{F}(q) := -\int_\Omega g\,q,$$

we arrive at: find $(\boldsymbol{\sigma},\boldsymbol{u},\boldsymbol{\rho},\boldsymbol{\varphi},p) \in \mathbb{H}_{\mathrm{N}}(\mathbf{div};\Omega)\times\mathbf{L}^2(\Omega)\times\mathbb{L}^2_{\mathrm{skew}}(\Omega)\times\mathbf{H}_{\mathrm{N}}(\mathrm{div};\Omega)\times\mathrm{L}^2(\Omega)$, such that

$$a(\boldsymbol{\sigma},\boldsymbol{\tau}) + b(\boldsymbol{\tau},(\boldsymbol{u},\boldsymbol{\rho})) + c(\boldsymbol{\tau},p) = H(\boldsymbol{\tau}) \qquad \forall\,\boldsymbol{\tau} \in \mathbb{H}_{\mathrm{N}}(\mathbf{div};\Omega), \tag{2.2a}$$

$$b(\boldsymbol{\sigma},(\mathbf{v},\boldsymbol{\eta})) = F(\mathbf{v},\boldsymbol{\eta}) \qquad \forall\,\mathbf{v} \in \mathbf{L}^2(\Omega),\ \forall\,\boldsymbol{\eta} \in \mathbb{L}^2_{\mathrm{skew}}(\Omega), \tag{2.2b}$$

$$\widetilde{a}_{\boldsymbol{\sigma},p}(\boldsymbol{\varphi},\boldsymbol{\psi}) + \widetilde{b}(\boldsymbol{\psi},p) = \widetilde{H}(\boldsymbol{\psi}) \qquad \forall\,\boldsymbol{\psi} \in \mathbf{H}_{\mathrm{N}}(\mathrm{div};\Omega), \tag{2.2c}$$

$$\widetilde{b}(\boldsymbol{\varphi},q) - \widetilde{c}(p,q) - c(\boldsymbol{\sigma},q) = \tilde{F}(q) \qquad \forall\,q \in \mathrm{L}^2(\Omega). \tag{2.2d}$$

In what follows we stress that bilinear forms without tildes will refer to the perturbed saddle-point problem of the solid, and bilinear forms with tildes relate with the perturbed saddle-point sub-system of the interstitial fluid. Functions with hats will typically denote fixed quantities (which will be of importance in the fixed-point setting).

2.2 *Stability properties and suitable inf-sup conditions*

For the sake of the analysis we allow the permeability $\boldsymbol{\kappa}(\boldsymbol{\sigma}, p)$ to be anisotropic, but still require $\boldsymbol{\kappa}(\boldsymbol{\sigma}, p)^{-1}$ to be uniformly positive definite in $\mathbb{L}^\infty(\Omega)$ and Lipschitz continuous with respect to $p \in \mathrm{L}^2(\Omega)$. That is, there exist strictly positive constants κ_1, κ_2 such that

$$\kappa_1 |\mathbf{v}|^2 \leq \mathbf{v}^{\mathtt{t}} \boldsymbol{\kappa}(\cdot,\cdot)^{-1}\mathbf{v}, \qquad \|\boldsymbol{\kappa}(\cdot, p_1)^{-1} - \boldsymbol{\kappa}(\cdot, p_2)^{-1}\|_{\mathbb{L}^\infty(\Omega)} \leq \kappa_2 \|p_1 - p_2\|_{0,\Omega}, \tag{2.3}$$

for all $\mathbf{v} \in \mathbb{R}^d \setminus \{\mathbf{0}\}$, and for all $p_1, p_2 \in \mathrm{L}^2(\Omega)$. We observe that the boundedness away from zero and Lipschitz continuity of the permeability (in the pressure) are quite common assumptions on models for nonlinear flow in porous media. For the specific applications we target here (bone, trabecular meshwork and other soft tissues) typical parametric regimes will imply that (2.3) easily holds for the constitutive relations (1.8). We also note that it is possible to consider a more general formulation in a non-Hilbert setting for the fluid sub-problem, leading to $p \in L^s(\Omega)$ and $\boldsymbol{\varphi} \in \mathbf{H}^r(\mathrm{div}_{s'}, \Omega)$ for a range of exponents r, s and $\frac{1}{s} + \frac{1}{s'} = 1$. And, at least for sake of continuity of the bilinear form $\tilde{a}$, the Lipschitz continuity of the inverse permeability can be relaxed and sought for in the space $\mathbb{L}^t(\Omega)$ with $\frac{1}{t} + \frac{1}{2r} = 1$. The coercivity of $\tilde{a}$, however, would require a more restrictive range for the exponents t, r (and in turn for s). It is not clear how this can be extended to a more general form of Lipschitz continuity without disrupting the functional structure of pressure and flux (and therefore also of displacement and stress).

We start by establishing the boundedness of the bilinear forms a, b, c, $\widetilde{b}$, $\widetilde{c}$:

$$\big|a(\boldsymbol{\sigma}, \boldsymbol{\tau})\big| \leq \frac{1}{\mu}\|\boldsymbol{\sigma}\|_{\mathbf{div};\Omega}\|\boldsymbol{\tau}\|_{\mathbf{div};\Omega}, \qquad \big|b(\boldsymbol{\tau}, (\mathbf{v}, \boldsymbol{\eta}))\big| \leq \|\boldsymbol{\tau}\|_{\mathbf{div};\Omega}(\|\mathbf{v}\|_{0,\Omega} + \|\boldsymbol{\eta}\|_{0,\Omega}), \tag{2.4a}$$

$$\big|c(\boldsymbol{\tau}, q)\big| \leq \gamma \|\boldsymbol{\tau}\|_{\mathbf{div};\Omega}\|q\|_{0,\Omega}, \tag{2.4b}$$

$$\big|\widetilde{b}(\boldsymbol{\psi}, q)\big| \leq \|\boldsymbol{\psi}\|_{\mathrm{div};\Omega}\|q\|_{0,\Omega}, \qquad \big|\widetilde{c}(p, q)\big| \leq \widetilde{\gamma}\|p\|_{0,\Omega}\|q\|_{0,\Omega}, \tag{2.4c}$$

where

$$\gamma := \frac{\alpha\sqrt{d}}{d\lambda + 2\mu} \quad \text{and} \quad \widetilde{\gamma} := c_0 + \frac{d\alpha^2}{d\lambda + 2\mu}. \tag{2.5}$$

On the other hand, using Hölder's and trace inequalities we can readily observe that the right-hand side functionals are all bounded

$$\big|H(\boldsymbol{\tau})\big| \leq \|\boldsymbol{u}_{\mathrm{D}}\|_{1/2,\Gamma_{\mathrm{D}}}\|\boldsymbol{\tau}\|_{\mathbf{div};\Omega}, \qquad \big|F(\mathbf{v}, \boldsymbol{\eta})\big| \leq \|\boldsymbol{f}\|_{0,\Omega}\|\mathbf{v}\|_{0,\Omega} \leq \|\boldsymbol{f}\|_{0,\Omega}(\|\mathbf{v}\|_{0,\Omega} + \|\boldsymbol{\eta}\|_{0,\Omega}),$$
$$\big|\widetilde{H}(\boldsymbol{\psi})\big| \leq \|p_{\mathrm{D}}\|_{1/2,\Gamma_{\mathrm{D}}}\|\boldsymbol{\psi}\|_{\mathrm{div};\Omega}, \qquad \big|\tilde{F}(q)\big| \leq \|g\|_{0,\Omega}\|q\|_{0,\Omega}.$$

Let us now denote by $\mathbb{V}$ and $\mathbf{V}$ the kernels of b and $\widetilde{b}$, respectively. They are characterized, respectively, as

$$\mathbb{V} = \left\{ \boldsymbol{\tau} \in \mathbb{H}_{\mathrm{N}}(\mathbf{div}; \Omega) : \quad \mathbf{div}\, \boldsymbol{\tau} = \mathbf{0} \quad \text{and} \quad \boldsymbol{\tau} = \boldsymbol{\tau}^{\mathrm{t}} \quad \text{in} \quad \Omega \right\}, \tag{2.6a}$$

$$\mathbf{V} = \left\{ \boldsymbol{\psi} \in \mathbf{H}_{\mathrm{N}}(\mathrm{div}; \Omega) : \quad \mathrm{div}\, \boldsymbol{\psi} = 0 \quad \text{in}\, \Omega \right\}. \tag{2.6b}$$

From (Álvarez *et al.*, 2015, lemmas 3.1 and 3.2) we easily deduce that there exists $c_a > 0$ such that

$$a(\boldsymbol{\tau}, \boldsymbol{\tau}) \geq c_a \|\boldsymbol{\tau}\|^2_{\mathbf{div};\Omega} \quad \forall\, \boldsymbol{\tau} \in \mathbb{V}. \tag{2.7}$$

REMARK 2.1. From (Gatica, 2006, lemma 2.2) and (Gatica, 2014, lemma 2.2), we have that the ellipticity constant c_a has the form $c_a = \hat{c}\frac{1}{\mu}$, where $\hat{c}$ depends on Γ_{N}, $|\Omega|$, and the Poincaré constant. Based on the above c_a has a nonzero lower bound.

The following inf-sup conditions are well known to hold (see, e.g., Camaño *et al.* (2015)):

$$\sup_{\mathbf{0} \neq \boldsymbol{\tau} \in \mathbb{H}_{\mathrm{N}}(\mathbf{div};\Omega)} \frac{b(\boldsymbol{\tau}, (\mathbf{v}, \boldsymbol{\eta}))}{\|\boldsymbol{\tau}\|_{\mathbf{div};\Omega}} \geq \beta(\|\mathbf{v}\|_{0,\Omega} + \|\boldsymbol{\eta}\|_{0,\Omega}) \quad \forall\, (\mathbf{v}, \boldsymbol{\eta}) \in \mathbf{L}^2(\Omega) \times \mathbb{L}^2_{\mathrm{skew}}(\Omega), \tag{2.8a}$$

$$\sup_{\mathbf{0} \neq \boldsymbol{\psi} \in \mathbf{H}_{\mathrm{N}}(\mathrm{div};\Omega)} \frac{\widetilde{b}(\boldsymbol{\psi}, q)}{\|\psi\|_{\mathrm{div};\Omega}} \geq \widetilde{\beta} \|q\|_{0,\Omega} \quad \forall\, q \in \mathrm{L}^2(\Omega). \tag{2.8b}$$

Finally, we observe that $\widetilde{c}$ is elliptic over $\mathrm{L}^2(\Omega)$

$$\widetilde{c}(q, q) \geq \widetilde{\gamma}\, \|q\|^2_{0,\Omega}. \tag{2.9}$$

REMARK 2.2. Due to the careful choice of the bilinear form $a(\cdot, \cdot)$, constants in continuity estimates (2.4a)–(2.4c) and inf-sup conditions (2.8a) and (2.8b) do not blow up when $\lambda \to \infty$ and $c_0 \to 0$. In particular, the constants γ and $\widetilde{\gamma}$, which depend on λ and c_0 (cf. (2.5)), remain bounded.

3. Analysis of the coupled problem

We now use a combination of the classical Babuška–Brezzi and Banach fixed-point theorems to establish the well-posedness of (2.2) under appropriate assumptions on the data.

3.1 *A fixed-point operator*

We adopt a similar approach to, e.g., Caucao *et al.* (2020b). First, we define a closed ball of $\mathrm{L}^2(\Omega)$ centred at the origin and of given radius $r > 0$

$$\mathrm{W} := \left\{ \widehat{p} \in \mathrm{L}^2(\Omega) : \quad \|\widehat{p}\|_{0,\Omega} \leq r \right\}. \tag{3.1}$$

Then, for a given $(\widehat{\boldsymbol{\sigma}},\widehat{p}) \in \mathbb{H}_{\mathrm{N}}(\mathbf{div};\Omega) \times \mathrm{W}$, due to the assumptions on the nonlinear permeability, we can infer that the form $\widetilde{a}_{\widehat{\boldsymbol{\sigma}},\widehat{p}}$ (cf. (2.1)) is continuous, as well as coercive over $\mathbf{V}$

$$\left|\widetilde{a}_{\widehat{\boldsymbol{\sigma}},\widehat{p}}(\boldsymbol{\varphi},\boldsymbol{\psi})\right| \leq C_{\widetilde{a}}\,\|\boldsymbol{\varphi}\|_{\mathbf{div};\Omega}\|\boldsymbol{\psi}\|_{\mathbf{div};\Omega}, \tag{3.2a}$$

$$\widetilde{a}_{\widehat{\boldsymbol{\sigma}},\widehat{p}}(\boldsymbol{\psi},\boldsymbol{\psi}) \geq \kappa_1\|\boldsymbol{\psi}\|^2_{\mathbf{div};\Omega} \quad \forall\,\boldsymbol{\varphi},\ \boldsymbol{\psi} \in \mathbf{V}. \tag{3.2b}$$

Then, we define the auxiliary operators $\mathbf{R} : \mathrm{W} \subseteq \mathrm{L}^2(\Omega) \to \mathbb{H}_{\mathrm{N}}(\mathbf{div};\Omega) \times (\mathbf{L}^2(\Omega) \times \mathbb{L}^2_{\mathrm{skew}}(\Omega))$ and $\mathbf{S} : \mathbb{H}_{\mathrm{N}}(\mathbf{div};\Omega) \times \mathrm{W} \to \mathbf{H}_{\mathrm{N}}(\mathrm{div};\Omega) \times \mathrm{L}^2(\Omega)$, given by

$$\mathbf{R}(\widehat{p}) := \big(R_1(\widehat{p}),(R_2(\widehat{p}),R_3(\widehat{p}))\big) = (\boldsymbol{\sigma},(\boldsymbol{u},\boldsymbol{\rho})) \quad \forall\,\widehat{p} \in \mathrm{W},$$

with $(\boldsymbol{\sigma},(\boldsymbol{u},\boldsymbol{\rho})) \in \mathbb{H}_{\mathrm{N}}(\mathbf{div};\Omega) \times (\mathbf{L}^2(\Omega) \times \mathbb{L}^2_{\mathrm{skew}}(\Omega))$ satisfying

$$\begin{aligned} a(\boldsymbol{\sigma},\boldsymbol{\tau}) + b(\boldsymbol{\tau},(\boldsymbol{u},\boldsymbol{\rho})) &= H(\boldsymbol{\tau}) - c(\boldsymbol{\tau},\widehat{p}) && \forall\,\boldsymbol{\tau} \in \mathbb{H}_{\mathrm{N}}(\mathbf{div};\Omega), \\ b(\boldsymbol{\sigma},(\mathbf{v},\boldsymbol{\eta})) &= F(\mathbf{v},\boldsymbol{\eta}) && \forall\,(\mathbf{v},\boldsymbol{\eta}) \in \mathbf{L}^2(\Omega) \times \mathbb{L}^2_{\mathrm{skew}}(\Omega), \end{aligned} \tag{3.3}$$

and

$$\mathbf{S}(\widehat{\boldsymbol{\sigma}},\widehat{p}) := \big(S_1(\widehat{\boldsymbol{\sigma}},\widehat{p}),S_2(\widehat{\boldsymbol{\sigma}},\widehat{p})\big) = (\boldsymbol{\varphi},p) \qquad \forall\,(\widehat{\boldsymbol{\sigma}},\widehat{p}) \in \mathbb{H}_{\mathrm{N}}(\mathbf{div};\Omega) \times \mathrm{W},$$

where $(\boldsymbol{\varphi},p)$ is such that

$$\begin{aligned} \widetilde{a}_{\widehat{\boldsymbol{\sigma}},\widehat{p}}(\boldsymbol{\varphi},\boldsymbol{\psi}) + \widetilde{b}(\boldsymbol{\psi},p) &= \widetilde{H}(\boldsymbol{\psi}) && \forall\,\boldsymbol{\psi} \in \mathbf{H}_{\mathrm{N}}(\mathrm{div};\Omega), \\ \widetilde{b}(\boldsymbol{\varphi},q) - \widetilde{c}(p,q) &= \tilde{F}(q) + c(\widehat{\boldsymbol{\sigma}},q) && \forall\,q \in \mathrm{L}^2(\Omega). \end{aligned} \tag{3.4}$$

By virtue of the above, by defining the operator $\mathbf{T} : \mathrm{W} \subseteq \mathrm{L}^2(\Omega) \to \mathrm{L}^2(\Omega)$ as

$$\mathbf{T}(\widehat{p}) := S_2(R_1(\widehat{p}),\widehat{p}), \tag{3.5}$$

it is clear that $(\boldsymbol{\sigma},\boldsymbol{u},\boldsymbol{\rho},\boldsymbol{\varphi},p)$ is a solution to (2.2) if and only if $p \in \mathrm{W}$ solves the fixed-point problem

$$\mathbf{T}(p) = p. \tag{3.6}$$

Thus, in what follows, we focus on proving the unique solvability of (3.6).

3.2 *Well-definedness of* $\mathbf{T}$

From the definition of $\mathbf{T}$ in (3.5) it is evident that its well-definedness requires the well-posedness of problems (3.3) and (3.4). We begin by analysing that of (3.3).

LEMMA 3.1. Let $\widehat{p} \in \mathrm{W}$ (cf. (3.1)). Then, there exists a unique $(\boldsymbol{\sigma}, (\boldsymbol{u}, \boldsymbol{\rho})) \in \mathbb{H}_{\mathrm{N}}(\mathbf{div}; \Omega) \times \mathbf{L}^2(\Omega) \times \mathbb{L}^2_{\mathrm{skew}}(\Omega)$ solution to (3.3). In addition, there exist C_1, $C_2 > 0$, such that

$$\begin{aligned} \|\boldsymbol{\sigma}\|_{\mathbf{div};\Omega} &\leq C_1 \left(\|\boldsymbol{u}_{\mathrm{D}}\|_{1/2,\Gamma_{\mathrm{D}}} + \|\boldsymbol{f}\|_{0,\Omega}\right) + \frac{1}{c_a}\,\gamma\,\|\widehat{p}\|_{0,\Omega}, \\ \|\boldsymbol{u}\|_{0,\Omega} + \|\boldsymbol{\rho}\|_{0,\Omega} &\leq C_2 \left(\|\boldsymbol{u}_{\mathrm{D}}\|_{1/2,\Gamma_{\mathrm{D}}} + \|\boldsymbol{f}\|_{0,\Omega}\right) + \frac{1}{\beta}\left(1 + \frac{1}{\mu c_a}\right)\gamma\,\|\widehat{p}\|_{0,\Omega}. \end{aligned} \tag{3.7}$$

Proof. It is a direct consequence of the Babuška–Brezzi theory (Ern & Guermond, 2004, theorem 2.34), using (2.7) and (2.8a) with

$$C_1 := \left(\frac{1}{c_a} + \frac{1}{\beta}\right)\left(1 + \frac{1}{\mu c_a}\right) \quad \text{and} \quad C_2 := \frac{1}{\beta}\left(1 + \frac{1}{\mu c_a}\right)\left(1 + \frac{1}{\mu\beta}\right); \tag{3.8}$$

we omit further details. □

Next, we provide the well-definedness of $\mathbf{S}$, or equivalently, the well-posedness of (3.4).

LEMMA 3.2. Let $(\widehat{\boldsymbol{\sigma}}, \widehat{p}) \in \mathbb{H}_{\mathrm{N}}(\mathbf{div}; \Omega) \times \mathrm{W}$. Then, there exists a unique $(\boldsymbol{\varphi}, p) \in \mathbf{H}_{\mathrm{N}}(\mathrm{div}; \Omega) \times \mathrm{L}^2(\Omega)$ solution to (3.4). In addition, there exists a constant $\widetilde{C} > 0$, depending on κ_1, $\widetilde{\beta}$, $\widetilde{\gamma}$ and $C_{\widetilde{a}}$, such that

$$\|\boldsymbol{\varphi}\|_{\mathrm{div};\Omega} + \|p\|_{0,\Omega} \leq \widetilde{C}\left(\|g\|_{0,\Omega} + \|p_{\mathrm{D}}\|_{1/2,\Gamma_{\mathrm{D}}} + \gamma\,\|\widehat{\boldsymbol{\sigma}}\|_{\mathbf{div};\Omega}\right). \tag{3.9}$$

Proof. The existence of a unique solution $(\boldsymbol{\varphi}, p)$ to (3.4) follows directly from the properties of the bilinear forms $\widetilde{a}$, $\widetilde{b}$ and $\widetilde{c}$. In particular, by examining conditions (3.2b), (2.9) and (2.8b), the proof can be naturally divided into two cases: if $\widetilde{\gamma} = 0$—which corresponds to $c_0 = 0$ and either $\alpha = 0$ or the fully incompressible case of $\lambda = \infty$—then the classical Babuška–Brezzi theory for unperturbed saddle point problems (see e.g., (Boffi *et al.*, 2013, theorem 4.2.3)) applies, whereas if $\widetilde{\gamma} > 0$, we can readily invoke the theory for perturbed saddle-point problems (with coercive perturbation) stated in (Boffi *et al.*, 2013, theorem 4.3.1). Additional technical details can be omitted. □

REMARK 3.3. It is important to note that, due to the careful choice of the bilinear forms $\widetilde{a}_{\widehat{\boldsymbol{\sigma}},\widehat{p}}$, $\widetilde{b}$, $\widetilde{c}$, the constants in estimates (2.4c) and (2.8b) do not blow up when $\lambda \to \infty$ and $c_0 \to 0$. In particular, the constant $\widetilde{C}$, which depends on the constant $\widetilde{\gamma}$, which in turn depends on λ and c_0, remain bounded.

LEMMA 3.4. Given $r > 0$ let us assume that

$$\widetilde{C}\left(1 + \gamma\, C_1\right)\left(\|g\|_{0,\Omega} + \|p_{\mathrm{D}}\|_{1/2,\Gamma_{\mathrm{D}}} + \|\boldsymbol{u}_{\mathrm{D}}\|_{1/2,\Gamma_{\mathrm{D}}} + \|\boldsymbol{f}\|_{0,\Omega}\right) + \frac{\widetilde{C}}{c_a}\,\gamma^2 r \leq r, \tag{3.10}$$

where C_1, $\widetilde{C}$ and γ are defined in (3.8), (3.9) and (2.5), respectively. Then, for a given $\widehat{p} \in \mathrm{W}$ (cf. (3.1)), there exists a unique $p \in \mathrm{W}$ such that $\mathbf{T}(\widehat{p}) = p$.

Proof. From Lemmas 3.1 and 3.2 we ascertain that the operators $\mathbf{R}$ and $\mathbf{S}$, respectively, are well-defined, thereby ensuring the well-definition of $\mathbf{T}$. Furthermore, from (3.7) and (3.9), for each $\widehat{p} \in \mathrm{W}$,

we deduce that

$$\begin{aligned}\|\mathbf{T}(\widehat{p})\|_{0,\Omega} &= \|S_2(R_1(\widehat{p}),\widehat{p})\|_{0,\Omega}\\ &\leq \widetilde{C}\,(\|g\|_{0,\Omega}+\|p_{\mathrm{D}}\|_{1/2,\Gamma_{\mathrm{D}}})+\widetilde{C}\,\gamma\,\|R_1(\widehat{p})\|_{\mathbf{div};\Omega}\\ &\leq \widetilde{C}\,(\|g\|_{0,\Omega}+\|p_{\mathrm{D}}\|_{1/2,\Gamma_{\mathrm{D}}})+\widetilde{C}\,\gamma\,C_1\,(\|\boldsymbol{u}_{\mathrm{D}}\|_{1/2,\Gamma_{\mathrm{D}}}+\|\boldsymbol{f}\|_{0,\Omega})+\frac{\widetilde{C}}{c_a}\,\gamma^2\|\widehat{p}\|_{0,\Omega};\end{aligned}$$

this, combined with assumption (3.10), implies $\mathbf{T}(\mathrm{W})\subseteq \mathrm{W}$, which concludes the proof. □

Remark 3.5. Note that the argument used in Lemma 3.4 is as follows: for an arbitrary, but fixed $r>0$ we define the ball W (cf. (3.1)). Then, for this fixed r, we assume that the data $\boldsymbol{f}$, g, $\boldsymbol{u}_{\mathrm{D}}$, p_{D} and γ (cf. (2.5)) are sufficiently small to satisfy Hypothesis (3.10). In particular, for the last term on the left-hand side of assumption (3.10), the condition $\dfrac{\widetilde{C}}{c_a}\gamma^2 r\leq r$ is required, which implies that $\gamma^2\leq \dfrac{c_a}{\widetilde{C}}$. As noted in Remarks 2.1 and 3.3 $\dfrac{c_a}{\widetilde{C}}$ admits a positive lower bound. Therefore, it suffices to consider λ sufficiently large (nearly incompressible regime) to ensure that γ^2 is sufficiently small, thereby guaranteeing the feasibility of the condition (3.10).

Remark 3.6. Another option for defining the operator $\mathbf{S}$ (see (3.4)) is to introduce the perturbation $\widetilde{c}$ on the right-hand side of the system, given by

$$\begin{aligned}\widetilde{a}_{\widehat{\boldsymbol{\sigma}},\widehat{p}}(\boldsymbol{\varphi},\boldsymbol{\psi})+\widetilde{b}(\boldsymbol{\psi},p)&=\widetilde{H}(\boldsymbol{\psi}) && \forall\,\boldsymbol{\psi}\in\mathbf{H}_{\mathrm{N}}(\mathrm{div};\Omega),\\ \widetilde{b}(\boldsymbol{\varphi},q)&=\tilde{F}(q)+c(\widehat{\boldsymbol{\sigma}},q)+\widetilde{c}(\widehat{p},q) && \forall\,q\in\mathrm{L}^2(\Omega).\end{aligned}$$

But in this case, the assumption of small data in (3.10) (as well as in other instances, later on) would also involve the storativity parameter c_0, making the analysis slightly more restrictive.

3.3 *Existence and uniqueness of weak solution*

We begin by establishing two lemmas deriving conditions under which the operator $\mathbf{T}$ is a contraction.

Lemma 3.7. Given $\widehat{p}_1,\widehat{p}_2,\in \mathrm{W}$ the following estimate holds:

$$\|R_1(\widehat{p}_1)-R_1(\widehat{p}_2)\|_{\mathbf{div};\Omega}\leq\frac{1}{c_a}\,\gamma\,\|\widehat{p}_1-\widehat{p}_2\|_{0,\Omega}. \tag{3.11}$$

Proof. Let $(\boldsymbol{\sigma}_1,(\boldsymbol{u}_1,\boldsymbol{\rho}_1))$, $(\boldsymbol{\sigma}_2,(\boldsymbol{u}_2,\boldsymbol{\rho}_2))\in\mathbb{H}_{\mathrm{N}}(\mathbf{div};\Omega)\times(\mathbf{L}^2(\Omega)\times\mathbb{L}^2_{\mathrm{skew}}(\Omega))$, such that $\mathbf{R}(\widehat{p}_1)=(\boldsymbol{\sigma}_1,(\boldsymbol{u}_1,\boldsymbol{\rho}_1))$ ad $\mathbf{R}(\widehat{p}_2)=(\boldsymbol{\sigma}_2,(\boldsymbol{u}_2,\boldsymbol{\rho}_2))$. Then, from the definition of $\mathbf{R}$ (cf. (3.3)), we have

$$\begin{aligned}a(\boldsymbol{\sigma}_1-\boldsymbol{\sigma}_2,\boldsymbol{\tau})+b(\boldsymbol{\tau},(\boldsymbol{u}_1-\boldsymbol{u}_2,\boldsymbol{\rho}_1-\boldsymbol{\rho}_2))&=-c(\boldsymbol{\tau},\widehat{p}_1-\widehat{p}_2) && \forall\,\boldsymbol{\tau}\in\mathbb{H}_{\mathrm{N}}(\mathbf{div};\Omega),\\ b(\boldsymbol{\sigma}_1-\boldsymbol{\sigma}_2,(\mathbf{v},\boldsymbol{\eta}))&=0 && \forall\,(\mathbf{v},\boldsymbol{\eta})\in\mathbf{L}^2(\Omega)\times\mathbb{L}^2_{\mathrm{skew}}(\Omega).\end{aligned} \tag{3.12}$$

Since $\boldsymbol{\sigma}_1 - \boldsymbol{\sigma}_2 \in \mathbb{V}$ (cf. (2.6a)) taking $\boldsymbol{\tau} = \boldsymbol{\sigma}_1 - \boldsymbol{\sigma}_2$ in (3.12), and utilizing the ellipticity of a on $\mathbb{V}$ (cf. (2.7)), along with the bound of c (cf. (2.4b)), we obtain

$$c_a \|\boldsymbol{\sigma}_1 - \boldsymbol{\sigma}_2\|^2_{\mathbf{div};\Omega} \leq a(\boldsymbol{\sigma}_1 - \boldsymbol{\sigma}_2, \boldsymbol{\sigma}_1 - \boldsymbol{\sigma}_2) = -c(\boldsymbol{\sigma}_1 - \boldsymbol{\sigma}_2, \widehat{p}_1 - \widehat{p}_2) \leq \gamma \, \|\boldsymbol{\sigma}_1 - \boldsymbol{\sigma}_2\|_{\mathbf{div};\Omega} \|\widehat{p}_1 - \widehat{p}_2\|_{0,\Omega},$$

which concludes the proof. □

LEMMA 3.8. Given $(\widehat{\boldsymbol{\sigma}}_1, \widehat{p}_1)$, $(\widehat{\boldsymbol{\sigma}}_2, \widehat{p}_2), \in \mathbb{H}_{\mathrm{N}}(\mathbf{div}; \Omega) \times \mathrm{W}$ the following estimate holds:

$$\begin{aligned} &\|S_2(\widehat{\boldsymbol{\sigma}}_1, \widehat{p}_1) - S_2(\widehat{\boldsymbol{\sigma}}_2, \widehat{p}_2)\|_{0,\Omega} \qquad (3.13)\\ &\leq \frac{2\kappa_2 \widetilde{C}}{\min\{\widetilde{\gamma}, \kappa_1\}} \left(\|g\|_{0,\Omega} + \|p_{\mathrm{D}}\|_{1/2,\Gamma_{\mathrm{D}}} + \gamma \|\widehat{\boldsymbol{\sigma}}_2\|_{\mathbf{div};\Omega} \right) \|\widehat{p}_1 - \widehat{p}_2\|_{0,\Omega} + \frac{2}{\min\{\widetilde{\gamma}, \kappa_1\}} \gamma \, \|\widehat{\boldsymbol{\sigma}}_1 - \widehat{\boldsymbol{\sigma}}_2\|_{\mathbf{div};\Omega}. \end{aligned}$$

Note that $\min\{\tilde{\gamma}, \kappa_1\}$ enters in the denominator of the estimate, but we have assumed that κ_1 is strictly positive and it does not degenerate to zero.

Proof. Let $(\boldsymbol{\varphi}_1, p_1)$, $(\boldsymbol{\varphi}_2, p_2) \in \mathbf{H}_{\mathrm{N}}(\mathrm{div}; \Omega) \times \mathrm{L}^2(\Omega)$, such that $\mathbf{S}(\widehat{\boldsymbol{\sigma}}_1, \widehat{p}_1) = (\boldsymbol{\varphi}_1, p_1)$ and $\mathbf{S}(\widehat{\boldsymbol{\sigma}}_2, \widehat{p}_2) = (\boldsymbol{\varphi}_2, p_2)$. Then, from the definition of $\mathbf{S}$ (cf. (3.4)), and employing similar arguments to those in Lemma 3.7, we have

$$\widetilde{a}_{\widehat{\boldsymbol{\sigma}}_1, \widehat{p}_1}(\boldsymbol{\varphi}_1, \boldsymbol{\varphi}_1 - \boldsymbol{\varphi}_2) - \widetilde{a}_{\widehat{\boldsymbol{\sigma}}_2, \widehat{p}_2}(\boldsymbol{\varphi}_2, \boldsymbol{\varphi}_1 - \boldsymbol{\varphi}_2) + \widetilde{c}(p_1 - p_2, p_1 - p_2) = -c(\widehat{\boldsymbol{\sigma}}_1 - \widehat{\boldsymbol{\sigma}}_2, p_1 - p_2);$$

by adding $\pm \widetilde{a}_{\widehat{\boldsymbol{\sigma}}_1, \widehat{p}_1}(\boldsymbol{\varphi}_2, \boldsymbol{\varphi}_1 - \boldsymbol{\varphi}_2)$ in the last equation, we obtain

$$\begin{aligned} &\widetilde{a}_{\widehat{\boldsymbol{\sigma}}_1, \widehat{p}_1}(\boldsymbol{\varphi}_1 - \boldsymbol{\varphi}_2, \boldsymbol{\varphi}_1 - \boldsymbol{\varphi}_2) + \widetilde{c}(p_1 - p_2, p_1 - p_2)\\ &\qquad = \widetilde{a}_{\widehat{\boldsymbol{\sigma}}_2, \widehat{p}_2}(\boldsymbol{\varphi}_2, \boldsymbol{\varphi}_1 - \boldsymbol{\varphi}_2) - \widetilde{a}_{\widehat{\boldsymbol{\sigma}}_1, \widehat{p}_1}(\boldsymbol{\varphi}_2, \boldsymbol{\varphi}_1 - \boldsymbol{\varphi}_2) - c(\widehat{\boldsymbol{\sigma}}_1 - \widehat{\boldsymbol{\sigma}}_2, p_1 - p_2). \end{aligned}$$

Then, using the first assumption for $\boldsymbol{\kappa}$ (cf. (2.3)), the ellipticity of $\widetilde{c}$ (see (2.9)), the definition of $\widetilde{a}_{\widehat{\boldsymbol{\sigma}}, \widehat{p}}$ (cf. (2.1)) and the continuity of the form c (see (2.4b)) we deduce

$$\begin{aligned} \kappa_1 \|\boldsymbol{\varphi}_1 - \boldsymbol{\varphi}_2\|^2_{0,\Omega} + \widetilde{\gamma} \|p_1 - p_2\|^2_{0,\Omega} &\leq \widetilde{a}_{\widehat{\boldsymbol{\sigma}}_1, \widehat{p}_1}(\boldsymbol{\varphi}_1 - \boldsymbol{\varphi}_2, \boldsymbol{\varphi}_1 - \boldsymbol{\varphi}_2) + \widetilde{c}(p_1 - p_2, p_1 - p_2)\\ &= \textstyle\int_\Omega (\boldsymbol{\kappa}(\widehat{\boldsymbol{\sigma}}_2, \widehat{p}_2)^{-1} - \boldsymbol{\kappa}(\widehat{\boldsymbol{\sigma}}_1, \widehat{p}_1)^{-1}) \, \boldsymbol{\varphi}_2 \cdot (\boldsymbol{\varphi}_1 - \boldsymbol{\varphi}_2) - c(\widehat{\boldsymbol{\sigma}}_1 - \widehat{\boldsymbol{\sigma}}_2, p_1 - p_2)\\ &\leq \|\boldsymbol{\kappa}(\widehat{\boldsymbol{\sigma}}_2, \widehat{p}_2)^{-1} - \boldsymbol{\kappa}(\widehat{\boldsymbol{\sigma}}_1, \widehat{p}_1)^{-1}\|_{\mathbb{L}^\infty(\Omega)} \, \|\boldsymbol{\varphi}_2\|_{0,\Omega} \|\boldsymbol{\varphi}_1 - \boldsymbol{\varphi}_2\|_{0,\Omega} + \gamma \, \|\widehat{\boldsymbol{\sigma}}_1 - \widehat{\boldsymbol{\sigma}}_2\|_{\mathbf{div};\Omega} \|p_1 - p_2\|_{0,\Omega}. \end{aligned}$$

From the last equation, by utilizing the second assumption regarding $\boldsymbol{\kappa}$ (see (2.3)), we obtain

$$\begin{aligned} \tfrac{1}{2} \min\{\widetilde{\gamma}, \kappa_1\} (\|\boldsymbol{\varphi}_1 - \boldsymbol{\varphi}_2\|_{0,\Omega} + \|p_1 - p_2\|_{0,\Omega})^2 &\leq \kappa_1 \|\boldsymbol{\varphi}_1 - \boldsymbol{\varphi}_2\|^2_{0,\Omega} + \widetilde{\gamma} \|p_1 - p_2\|^2_{0,\Omega}\\ &\leq \kappa_2 \|\widehat{p}_2 - \widehat{p}_1\|_{0,\Omega} \|\boldsymbol{\varphi}_2\|_{0,\Omega} \|\boldsymbol{\varphi}_1 - \boldsymbol{\varphi}_2\|_{0,\Omega} + \gamma \, \|\widehat{\boldsymbol{\sigma}}_1 - \widehat{\boldsymbol{\sigma}}_2\|_{\mathbf{div};\Omega} \|p_1 - p_2\|_{0,\Omega}\\ &\leq \left(\kappa_2 \|\widehat{p}_2 - \widehat{p}_1\|_{0,\Omega} \|\boldsymbol{\varphi}_2\|_{0,\Omega} + \gamma \, \|\widehat{\boldsymbol{\sigma}}_1 - \widehat{\boldsymbol{\sigma}}_2\|_{\mathbf{div};\Omega}\right) \left(\|\boldsymbol{\varphi}_1 - \boldsymbol{\varphi}_2\|_{0,\Omega} + \|p_1 - p_2\|_{0,\Omega}\right); \end{aligned}$$

the last, together with the fact that $\boldsymbol{\varphi}_2$ satisfies (3.9), leads to the following bound:

$$\begin{aligned}\tfrac{1}{2}\min\{\widetilde{\gamma},\kappa_1\}(\|\boldsymbol{\varphi}_1-\boldsymbol{\varphi}_2\|_{0,\Omega}+\|p_1-p_2\|_{0,\Omega}) &\leq \kappa_2\|\widehat{p}_2-\widehat{p}_1\|_{0,\Omega}\|\boldsymbol{\varphi}_2\|_{0,\Omega}+\gamma\,\|\widehat{\boldsymbol{\sigma}}_1-\widehat{\boldsymbol{\sigma}}_2\|_{\mathbf{div};\Omega}\\ &\leq \kappa_2\|\widehat{p}_2-\widehat{p}_1\|_{0,\Omega}\widetilde{C}\,(\|g\|_{0,\Omega}+\|p_{\mathrm{D}}\|_{1/2,\Gamma_{\mathrm{D}}}+\gamma\|\widehat{\boldsymbol{\sigma}}_2\|_{\mathbf{div};\Omega})+\gamma\,\|\widehat{\boldsymbol{\sigma}}_1-\widehat{\boldsymbol{\sigma}}_2\|_{\mathbf{div};\Omega},\end{aligned}$$

and this yields (3.13), concluding the proof. □

The following theorem presents the main result of this section, establishing the existence and uniqueness of the solution to the fixed-point problem (3.6), or equivalently, of (2.2).

THEOREM 3.9. Given $r>0$, assume that $\boldsymbol{f}\in\mathbf{L}^2(\Omega)$, $g\in L^2(\Omega)$, $\boldsymbol{u}_{\mathrm{D}}\in\mathbf{H}^{1/2}(\Gamma_{\mathrm{D}})$, $p_{\mathrm{D}}\in\mathrm{H}^{1/2}(\Gamma_{\mathrm{D}})$ and γ satisfies

$$\frac{2\max\{1,\,\kappa_2\}}{\min\{\widetilde{\gamma},\,\kappa_1\,,r\}}\left\{\widetilde{C}(1+C_1\gamma)(\|g\|_{0,\Omega}+\|p_{\mathrm{D}}\|_{1/2,\Gamma_{\mathrm{D}}}+\|\boldsymbol{u}_{\mathrm{D}}\|_{1/2,\Gamma_{\mathrm{D}}}+\|\boldsymbol{f}\|_{0,\Omega})+\frac{\gamma^2}{c_a}\left(\frac{1}{\kappa_2}+\widetilde{C}\,r\right)\right\}<1. \tag{3.14}$$

Then, $\mathbf{T}$ (cf. (3.5)) has a unique fixed point $p\in\mathrm{W}$. Equivalently, (2.2) has a unique solution $(\boldsymbol{\sigma},\boldsymbol{u},\boldsymbol{\rho},\boldsymbol{\varphi},p)\in\mathbb{H}_{\mathrm{N}}(\mathbf{div};\Omega)\times\mathbf{L}^2(\Omega)\times\mathbb{L}^2_{\mathrm{skew}}(\Omega)\times\mathbf{H}_{\mathrm{N}}(\mathrm{div};\Omega)\times\mathrm{W}$. In addition, there exists $C>0$, such that

$$\begin{aligned}&\|\boldsymbol{\sigma}\|_{\mathbf{div};\Omega}+\|\boldsymbol{u}\|_{0,\Omega}+\|\boldsymbol{\rho}\|_{0,\Omega}+\|\boldsymbol{\varphi}\|_{\mathrm{div};\Omega}+\|p\|_{0,\Omega}\\ &\qquad\leq C(\|g\|_{0,\Omega}+\|p_{\mathrm{D}}\|_{1/2,\Gamma_{\mathrm{D}}}+\|\boldsymbol{u}_{\mathrm{D}}\|_{1/2,\Gamma_{\mathrm{D}}}+\|\boldsymbol{f}\|_{0,\Omega}+\gamma\,r\,).\end{aligned} \tag{3.15}$$

Proof. Recall that (3.14) ensures the well-definedness of $\mathbf{T}$. Let $\widehat{p}_1,\widehat{p}_2,p_1,p_2\in\mathrm{W}$, such that $\mathbf{T}(\widehat{p}_1)=p_1$ and $\mathbf{T}(\widehat{p}_2)=p_2$. From the definition of $\mathbf{T}$ (see (3.5)), and the estimates (3.13) and (3.11), we deduce

$$\begin{aligned}\|p_1-p_2\|_{0,\Omega}&=\|\mathbf{T}(\widehat{p}_1)-\mathbf{T}(\widehat{p}_2)\|_{0,\Omega}=\|S_2(R_1(\widehat{p}_1),\widehat{p}_1)-S_2(R_1(\widehat{p}_2),\widehat{p}_2)\|_{0,\Omega}\\ &\leq\frac{2\kappa_2\,\widetilde{C}}{\min\{\widetilde{\gamma},\,\kappa_1\}}\left(\|g\|_{0,\Omega}+\|p_{\mathrm{D}}\|_{1/2,\Gamma_{\mathrm{D}}}+\gamma\|R_1(\widehat{p}_2)\|_{\mathbf{div};\Omega}\right)\|\widehat{p}_1-\widehat{p}_2\|_{0,\Omega}\\ &\quad+\frac{2}{\min\{\widetilde{\gamma},\,\kappa_1\}}\,\gamma\,\|R_1(\widehat{p}_1)-R_1(\widehat{p}_2)\|_{\mathbf{div};\Omega}\\ &\leq\frac{2\kappa_2\,\widetilde{C}}{\min\{\widetilde{\gamma},\,\kappa_1\}}\left(\|g\|_{0,\Omega}+\|p_{\mathrm{D}}\|_{1/2,\Gamma_{\mathrm{D}}}\right)\|\widehat{p}_1-\widehat{p}_2\|_{0,\Omega}+\frac{2\kappa_2\,\widetilde{C}}{\min\{\widetilde{\gamma},\,\kappa_1\}}\gamma\,\|R_1(\widehat{p}_2)\|_{\mathbf{div};\Omega}\|\widehat{p}_1-\widehat{p}_2\|_{0,\Omega}\\ &\quad+\frac{2}{c_a\,\min\{\widetilde{\gamma},\,\kappa_1\}}\,\gamma^2\,\|\widehat{p}_1-\widehat{p}_2\|_{0,\Omega};\end{aligned}$$

the above, along with the fact that $R_1(\widehat{p}_2)$ satisfies (3.7) and $\widehat{p}_2 \in \mathrm{W}$, implies

$$\begin{aligned}\|p_1 - p_2\|_{0,\Omega} &\leq \frac{2\kappa_2\,\widetilde{C}}{\min\{\widetilde{\gamma},\,\kappa_1\}}\left(\|g\|_{0,\Omega} + \|p_{\mathrm{D}}\|_{1/2,\Gamma_{\mathrm{D}}}\right)\|\widehat{p}_1 - \widehat{p}_2\|_{0,\Omega} + \frac{2}{c_a\,\min\{\widetilde{\gamma},\,\kappa_1\}}\,\gamma^2\,\|\widehat{p}_1 - \widehat{p}_2\|_{0,\Omega}\\ &\quad + \frac{2\kappa_2\,\widetilde{C}}{\min\{\widetilde{\gamma},\,\kappa_1\}}\gamma\left(C_1\,(\|\boldsymbol{u}_{\mathrm{D}}\|_{1/2,\Gamma_{\mathrm{D}}} + \|\boldsymbol{f}\|_{0,\Omega}) + \frac{1}{c_a}\,\gamma\,r\right)\|\widehat{p}_1 - \widehat{p}_2\|_{0,\Omega}\\ &\leq \frac{2}{\min\{\widetilde{\gamma},\,\kappa_1\}}\left\{\kappa_2\,\widetilde{C}(1 + C_1\gamma)(\|g\|_{0,\Omega} + \|p_{\mathrm{D}}\|_{1/2,\Gamma_{\mathrm{D}}} + \|\boldsymbol{u}_{\mathrm{D}}\|_{1/2,\Gamma_{\mathrm{D}}} + \|\boldsymbol{f}\|_{0,\Omega})\right.\\ &\quad \left. + \frac{\gamma^2}{c_a}(1 + \kappa_2\,\widetilde{C}\,r)\right\}\|\widehat{p}_1 - \widehat{p}_2\|_{0,\Omega},\end{aligned}$$

which together with (3.14) and the Banach fixed-point theorem yields that $\mathbf{T}$ has a unique fixed point in W. Finally, (3.15) is derived analogously to the estimates in (3.7) and (3.9), which completes the proof. □

Remark 3.10. The operator $\mathbf{T}$ (see (3.5)) could be also defined, for example $\mathbf{T} : \mathbf{W} \to \mathbf{W}$, with $\mathbf{W} := \left\{(\widehat{\boldsymbol{\sigma}},\widehat{p}) \in \mathbb{H}_{\mathrm{N}}(\mathbf{div};\Omega) \times \mathrm{L}^2(\Omega) : \quad \|\widehat{\boldsymbol{\sigma}}\|_{\mathbf{div};\Omega} + \|\widehat{p}\|_{0,\Omega} \leq r\right\}$ and $\mathbf{T}(\widehat{\boldsymbol{\sigma}},\widehat{p}) := (R_1(\widehat{p}), S_2(\widehat{\boldsymbol{\sigma}},\widehat{p})) = (\boldsymbol{\sigma},p)$, with R_1 and S_2 defined as in (3.3) and (3.4), respectively.

4. FE discretization

In this section we present and analyse the Galerkin scheme for problem (2.2). An advantage of this scheme is that the well-posedness analysis can be straightforwardly extended from the continuous problem to the discrete case. Therefore, we can omit many of the rather standard details.

4.1 *FE spaces and Galerkin scheme*

Let us consider a regular partition $\mathscr{T}_h$ of $\bar{\Omega}$ made up of triangles K (in $\mathbb{R}^2$) or tetrahedra K (in $\mathbb{R}^3$) of diameter h_K, and denote the mesh size by $h := \max\{h_K : K \in \mathscr{T}_h\}$. Given an integer $\ell \geq 0$ and $K \in \mathscr{T}_h$ we first let $\mathrm{P}_\ell(K)$ be the space of polynomials of degree $\leq \ell$ defined on K, whose vector and tensor versions are denoted $\mathbf{P}_\ell(K) := [\mathrm{P}_\ell(K)]^d$ and $\mathbb{P}_\ell(K) = [\mathrm{P}_\ell(K)]^{d\times d}$, respectively. Also, we let $\mathbf{RT}_\ell(K) := \mathbf{P}_\ell(K) \oplus \mathrm{P}_\ell(K)\,\boldsymbol{x}$ be the local Raviart–Thomas space of order ℓ defined on K, where $\boldsymbol{x}$ stands for a generic vector in $\mathbb{R}^d$, and denote by $\mathbb{RT}_k(K)$ the tensor-valued counterpart of this space.

For each $K \in \mathscr{T}_h$ we consider the bubble space of order k, defined as

$$\mathbf{B}_k(K) := \begin{cases}\mathrm{curl}(b_K)\mathrm{P}_k(K) & \text{in} \quad \mathbb{R}^2,\\ \nabla \times (b_K\mathbf{P}_k(K)) & \text{in} \quad \mathbb{R}^3,\end{cases}$$

where b_K is a suitably normalized cubic polynomial on K, which vanishes on the boundary of K (see Ern & Guermond (2004)).

We recall the classical PEERS$_k$ elements (cf. Arnold *et al.* (1984)) to define the discrete subspaces for the stress tensor $\boldsymbol{\sigma}$, the displacement $\boldsymbol{u}$ and the rotation tensor $\boldsymbol{\rho}$

$$\begin{aligned}
\mathbb{H}_h^{\boldsymbol{\sigma}} &:= \left\{ \boldsymbol{\tau}_h \in \mathbb{H}_{\mathrm{N}}(\mathbf{div};\Omega) : \quad \boldsymbol{\tau}_h|_K \in \mathbb{RT}_k(K) \oplus [\mathbf{B}_k(K)]^d \quad \forall\, K \in \mathscr{T}_h \right\}, \\
\mathbf{H}_h^{\boldsymbol{u}} &:= \left\{ \mathbf{v}_h \in \mathbf{L}^2(\Omega) : \quad \mathbf{v}_h|_K \in \mathbf{P}_k(K) \quad \forall\, K \in \mathscr{T}_h \right\}, \\
\mathbb{H}_h^{\boldsymbol{\rho}} &:= \left\{ \boldsymbol{\eta}_h \in \mathbb{L}^2_{\mathrm{skew}}(\Omega) \cap \mathbb{C}(\overline{\Omega}) \quad \text{and} \quad \boldsymbol{\eta}_h|_K \in \mathbb{P}_{k+1}(K) \quad \forall\, K \in \mathscr{T}_h \right\},
\end{aligned} \tag{4.1}$$

where $\mathbb{C}(\overline{\Omega})$ denotes the space of continuous tensor fields, and the following estimates are proven for the PEERS$_k$ elements (cf. (Lonsing & Verfürth, 2004, remark 3.3))

$$\sup_{\mathbf{0}\neq\boldsymbol{\tau}_h\in\mathbb{H}_h^{\boldsymbol{\sigma}}} \frac{b(\boldsymbol{\tau}_h,(\mathbf{v}_h,\boldsymbol{\eta}_h))}{\|\boldsymbol{\tau}_h\|_{\mathbf{div};\Omega}} \geq \beta^*(\|\mathbf{v}_h\|_{0,\Omega} + \|\boldsymbol{\eta}_h\|_{0,\Omega}) \quad \forall\,(\mathbf{v}_h,\boldsymbol{\eta}_h) \in \mathbf{H}_h^{\boldsymbol{u}} \times \mathbb{H}_h^{\boldsymbol{\rho}}, \tag{4.2a}$$

$$a(\boldsymbol{\tau}_h,\boldsymbol{\tau}_h) \geq c_a \|\boldsymbol{\tau}_h\|^2_{\mathbf{div};\Omega} \quad \forall\, \boldsymbol{\tau}_h \in \mathbb{V}_h, \tag{4.2b}$$

where $\mathbb{V}_h$ denotes the discrete kernel of b, that is,

$$\mathbb{V}_h := \left\{ \boldsymbol{\tau}_h \in \mathbb{H}_h^{\boldsymbol{\sigma}} : \quad b(\boldsymbol{\tau}_h,(\mathbf{v}_h,\boldsymbol{\eta}_h)) = 0 \quad \forall\,(\mathbf{v}_h,\boldsymbol{\eta}_h) \in \mathbf{H}_h^{\boldsymbol{u}} \times \mathbb{H}_h^{\boldsymbol{\rho}} \right\}.$$

Additionally, for $\boldsymbol{\varphi}$ and the pressure p, we define the FE subspaces

$$\begin{aligned}
\mathbf{H}_h^{\boldsymbol{\varphi}} &:= \left\{ \boldsymbol{\psi}_h \in \mathbf{H}_{\mathrm{N}}(\mathrm{div};\Omega) : \ \boldsymbol{\psi}_h|_K \in \mathbf{RT}_k(K) \quad \forall\, K \in \mathscr{T}_h \right\}, \\
\mathrm{H}_h^{p} &:= \left\{ q_h \in \mathrm{L}^2(\Omega) : \ q_h|_K \in \mathrm{P}_k(K) \quad \forall\, K \in \mathscr{T}_h \right\},
\end{aligned} \tag{4.3}$$

and it is well known that $\widetilde{b}$ satisfies the inf-sup condition (see, e.g., (Caucao *et al.*, 2020a, lemma 4.6))

$$\sup_{\mathbf{0}\neq\boldsymbol{\psi}_h\in\mathbf{H}_h^{\boldsymbol{\varphi}}} \frac{\widetilde{b}(\boldsymbol{\psi}_h,q_h)}{\|\boldsymbol{\psi}_h\|_{\mathrm{div};\Omega}} \geq \widetilde{\beta}^* \|q_h\|_{0,\Omega} \quad \forall\, q_h \in \mathrm{H}_h^p. \tag{4.4}$$

Note that it is of course possible to consider other conforming and inf-sup stable spaces such as Arnold–Falk–Winther and Brezzi–Douglas–Marini instead of (4.1) and (4.3), respectively. The Galerkin scheme for (2.2) reads the following: find $(\boldsymbol{\sigma}_h,\boldsymbol{u}_h,\boldsymbol{\rho}_h,\boldsymbol{\varphi}_h,p_h) \in \mathbb{H}_h^{\boldsymbol{\sigma}} \times \mathbf{H}_h^{\boldsymbol{u}} \times \mathbb{H}_h^{\boldsymbol{\rho}} \times \mathbf{H}_h^{\boldsymbol{\varphi}} \times \mathrm{H}_h^p$, such that

$$\begin{aligned}
a(\boldsymbol{\sigma}_h,\boldsymbol{\tau}_h) + b(\boldsymbol{\tau}_h,(\boldsymbol{u}_h,\boldsymbol{\rho}_h)) + c(\boldsymbol{\tau}_h,p_h) &= H(\boldsymbol{\tau}_h) && \forall\, \boldsymbol{\tau}_h \in \mathbb{H}_h^{\boldsymbol{\sigma}}, \\
b(\boldsymbol{\sigma}_h,(\mathbf{v}_h,\boldsymbol{\eta}_h)) &= F(\mathbf{v}_h,\boldsymbol{\eta}_h) && \forall (\mathbf{v}_h,\boldsymbol{\eta}_h) \in \mathbf{H}_h^{\boldsymbol{u}} \times \mathbb{H}_h^{\boldsymbol{\rho}}, \\
\widetilde{a}_{\boldsymbol{\sigma}_h,p_h}(\boldsymbol{\varphi}_h,\boldsymbol{\psi}_h) + \widetilde{b}(\boldsymbol{\psi}_h,p_h) &= \widetilde{H}(\boldsymbol{\psi}_h) && \forall\, \boldsymbol{\psi}_h \in \mathbf{H}_h^{\boldsymbol{\varphi}}, \\
\widetilde{b}(\boldsymbol{\varphi}_h,q_h) - \widetilde{c}(p_h,q_h) - c(\boldsymbol{\sigma}_h,q_h) &= \tilde{F}(q_h) && \forall\, q_h \in \mathrm{H}_h^p.
\end{aligned} \tag{4.5}$$

4.2 *Analysis of the discrete problem*

In this section we analyse the Galerkin scheme (4.5). It is worth noting that establishing well-posedness can be readily achieved by extending the results derived for the continuous problem to the discrete setting. Firstly, and similarly to the continuous case, we define the following set:

$$\mathrm{W}_h := \left\{ \widehat{p}_h \in \mathrm{H}^p_h : \quad \|\widehat{p}_h\|_{0,\Omega} \leq r \right\}.$$

Next, for a fixed $\widehat{p}_h$ in W_h, we have that the bilinear form $\widetilde{a}_{\boldsymbol{\sigma}_h,p_h}$ satisfies

$$\widetilde{a}_{\widehat{\boldsymbol{\sigma}}_h,\widehat{p}_h}(\boldsymbol{\psi}_h,\boldsymbol{\psi}_h) \geq \kappa_1 \|\boldsymbol{\psi}_h\|^2_{\mathrm{div};\Omega} \quad \forall\, \boldsymbol{\psi}_h \in \mathbf{V}_h, \tag{4.6}$$

where $\mathbf{V}_h$ is the discrete kernel of $\widetilde{b}$

$$\mathbf{V}_h := \left\{ \boldsymbol{\psi}_h \in \mathbf{H}^{\boldsymbol{\varphi}}_h : \quad \widetilde{b}(\boldsymbol{\psi}_h, q_h) = 0 \quad \forall\, q_h \in \mathrm{H}^p_h \right\}.$$

Additionally, we define the discrete operators $\mathbf{R}_h : \mathrm{W}_h \subseteq \mathrm{H}^p_h \to \mathbb{H}^{\boldsymbol{\sigma}}_h \times (\mathbf{H}^{\boldsymbol{u}}_h \times \mathbb{H}^{\boldsymbol{\rho}}_h)$ and $\mathbf{S}_h : \mathbb{H}^{\boldsymbol{\sigma}}_h \times \mathrm{W}_h \to \mathbf{H}^{\boldsymbol{\varphi}}_h \times \mathrm{H}^p_h$, respectively, by

$$\mathbf{R}_h(\widehat{p}_h) := \big(R_{1,h}(\widehat{p}_h), (R_{2,h}(\widehat{p}_h), R_{3,h}(\widehat{p}_h))\big) = (\boldsymbol{\sigma}_h, (\boldsymbol{u}_h, \boldsymbol{\rho}_h)) \quad \forall\, \widehat{p}_h \in \mathrm{W}_h,$$

where $(\boldsymbol{\sigma}_h, (\boldsymbol{u}_h, \boldsymbol{\rho}_h)) \in \mathbb{H}^{\boldsymbol{\sigma}}_h \times (\mathbf{H}^{\boldsymbol{u}}_h \times \mathbb{H}^{\boldsymbol{\rho}}_h)$ is the unique solution of

$$\begin{aligned} a(\boldsymbol{\sigma}_h,\boldsymbol{\tau}_h) + b(\boldsymbol{\tau}_h,(\boldsymbol{u}_h,\boldsymbol{\rho}_h)) &= H(\boldsymbol{\tau}_h) - c(\boldsymbol{\tau}_h,\widehat{p}_h) && \forall\, \boldsymbol{\tau}_h \in \mathbb{H}^{\boldsymbol{\sigma}}_h, \\ b(\boldsymbol{\sigma}_h,(\mathbf{v}_h,\boldsymbol{\eta}_h)) &= F(\mathbf{v}_h,\boldsymbol{\eta}_h) && \forall\, (\mathbf{v}_h,\boldsymbol{\eta}_h) \in \mathbf{H}^{\boldsymbol{u}}_h \times \mathbb{H}^{\boldsymbol{\rho}}_h, \end{aligned} \tag{4.7}$$

and

$$\mathbf{S}_h(\widehat{\boldsymbol{\sigma}}_h,\widehat{p}_h) := \big(S_{1,h}(\widehat{\boldsymbol{\sigma}}_h,\widehat{p}_h), S_{2,h}(\widehat{\boldsymbol{\sigma}}_h,\widehat{p}_h)\big) = (\boldsymbol{\varphi}_h, p_h) \quad \forall\, (\widehat{\boldsymbol{\sigma}}_h,\widehat{p}_h) \in \mathbb{H}^{\boldsymbol{\sigma}}_h \times \mathrm{W}_h,$$

where $(\boldsymbol{\varphi}_h, p_h)$ is the unique tuple in $\mathbf{H}^{\boldsymbol{\varphi}}_h \times \mathrm{H}^p_h$ such that

$$\begin{aligned} \widetilde{a}_{\widehat{\boldsymbol{\sigma}}_h,\widehat{p}_h}(\boldsymbol{\varphi}_h,\boldsymbol{\psi}_h) + \widetilde{b}(\boldsymbol{\psi}_h,p_h) &= \widetilde{H}(\boldsymbol{\psi}_h) && \forall\, \boldsymbol{\psi}_h \in \mathbf{H}^{\boldsymbol{\varphi}}_h, \\ \widetilde{b}(\boldsymbol{\varphi}_h,q_h) - \widetilde{c}(p_h,q_h) &= \widetilde{F}(q_h) + c(\widehat{\boldsymbol{\sigma}}_h,q_h) && \forall\, q_h \in \mathrm{H}^p_h. \end{aligned}$$

Employing properties (4.2a), (4.2b), (4.4), (4.6) and (2.9), and proceeding exactly as for the continuous case (Lemmas 3.1 and 3.2), it can be easily deduced that both operators are well defined. Then, analogously to the continuous case, we define the following fixed-point operator:

$$\mathbf{T}_h : \mathrm{W}_h \subseteq \mathrm{H}^p_h \to \mathrm{H}^p_h, \quad \widehat{p}_h \mapsto \mathbf{T}_h(\widehat{p}_h) := S_{2,h}(R_{1,h}(\widehat{p}_h),\widehat{p}_h), \tag{4.8}$$

which is clearly well defined (since R_h and S_h are). Further, it can be easily deduced that $\mathbf{T}_h(\mathrm{W}_h) \subseteq \mathrm{W}_h$ if

$$\widetilde{C}^* \left(1 + \gamma\, C_1^*\right) \left(\|g\|_{0,\Omega} + \|p_{\mathrm{D}}\|_{1/2,\Gamma_{\mathrm{D}}} + \|\boldsymbol{u}_{\mathrm{D}}\|_{1/2,\Gamma_{\mathrm{D}}} + \|\boldsymbol{f}\|_{0,\Omega} \right) + \frac{\widetilde{C}^*}{c_a}\, \gamma^2 r \leq r, \tag{4.9}$$

where $\widetilde{C}^*$ and C_1^* (depending on c_a, μ, κ_1, κ_2, $C_{\widetilde{a}}$, β^*, $\widetilde{\beta}^*$) are the discrete versions of the constants $\widetilde{C}$ and C_1 (cf. (3.7) and (3.9)). Finally, it is clear that $(\boldsymbol{\sigma}_h, \boldsymbol{u}_h, \boldsymbol{\rho}_h, \boldsymbol{\varphi}_h, p_h)$ is a solution to (4.5) if and only if p_h satisfies

$$\mathbf{T}_h(p_h) = p_h. \tag{4.10}$$

The main outcome of this section is presented in the following theorem, establishing the existence and uniqueness of a solution to the fixed-point problem (4.10), equivalently proving the well-posedness of problem (4.5).

THEOREM 4.1. Given $r > 0$, assume that the data and γ satisfy

$$\frac{2\max\{1,\, \kappa_2\}}{\min\{\widetilde{\gamma},\, \kappa_1\,, r\}} \left\{ \widetilde{C}^*(1 + C_1^*\gamma)(\|g\|_{0,\Omega} + \|p_{\mathrm{D}}\|_{1/2,\Gamma_{\mathrm{D}}} + \|\boldsymbol{u}_{\mathrm{D}}\|_{1/2,\Gamma_{\mathrm{D}}} + \|\boldsymbol{f}\|_{0,\Omega}) + \frac{\gamma^2}{c_a} \left(\frac{1}{\kappa_2} + \widetilde{C}^*\, r \right) \right\} < 1. \tag{4.11}$$

Then, $\mathbf{T}_h$ (cf. (4.8)) has a unique fixed point $p_h \in \mathrm{W}_h$. Equivalently, problem (4.5) has a unique solution $(\boldsymbol{\sigma}_h, \boldsymbol{u}_h, \boldsymbol{\rho}_h, \boldsymbol{\varphi}_h, p_h) \in \mathbb{H}_h^{\boldsymbol{\sigma}} \times \mathbf{H}_h^{\boldsymbol{u}} \times \mathbb{H}_h^{\boldsymbol{\rho}} \times \mathbf{H}_h^{\boldsymbol{\varphi}} \times \mathrm{W}_h$. In addition, there exists $C^* > 0$, such that

$$\begin{aligned} &\|\boldsymbol{\sigma}_h\|_{\mathbf{div};\Omega} + \|\boldsymbol{u}_h\|_{0,\Omega} + \|\boldsymbol{\rho}_h\|_{0,\Omega} + \|\boldsymbol{\varphi}_h\|_{\mathrm{div};\Omega} + \|p_h\|_{0,\Omega} \\ &\qquad \leq C^*(\|g\|_{0,\Omega} + \|p_{\mathrm{D}}\|_{1/2,\Gamma_{\mathrm{D}}} + \|\boldsymbol{u}_{\mathrm{D}}\|_{1/2,\Gamma_{\mathrm{D}}} + \|\boldsymbol{f}\|_{0,\Omega} + \gamma\, r). \end{aligned} \tag{4.12}$$

Proof. First, we observe that, similar to the continuous case (as seen in the proof of Theorem 3.9), assumption (4.11) ensures the well-definedness of $\mathbf{T}_h$ and that $\mathbf{T}_h(\mathrm{W}_h) \subseteq \mathrm{W}_h$. Now, by adapting the arguments used in Section 3.3 (cf. Lemmas 3.7 and 3.8), one can derive the following estimates:

$$\|R_{1,h}(\widehat{p}_1) - R_{1,h}(\widehat{p}_2)\|_{\mathbf{div};\Omega} \leq \frac{1}{c_a}\, \gamma\, \|\widehat{p}_1 - \widehat{p}_2\|_{0,\Omega},$$

$$\begin{aligned} \|S_{2,h}(\widehat{\boldsymbol{\sigma}}_1, \widehat{p}_1) - S_{2,h}(\widehat{\boldsymbol{\sigma}}_2, \widehat{p}_2)\|_{0,\Omega} &\leq \frac{2\kappa_2\, \widetilde{C}^*}{\min\{\widetilde{\gamma},\, \kappa_1\}} \left(\|g\|_{0,\Omega} + \|p_{\mathrm{D}}\|_{1/2,\Gamma_{\mathrm{D}}} + \gamma\, \|\widehat{\boldsymbol{\sigma}}_2\|_{\mathbf{div};\Omega} \right) \|\widehat{p}_1 - \widehat{p}_2\|_{0,\Omega} \\ &\quad + \frac{2}{\min\{\widetilde{\gamma},\, \kappa_1\}}\, \gamma\, \|\widehat{\boldsymbol{\sigma}}_1 - \widehat{\boldsymbol{\sigma}}_2\|_{\mathbf{div};\Omega}, \end{aligned}$$

for all $\widehat{p}_1, \widehat{p}_2 \in \mathrm{W}_h$ and $\widehat{\boldsymbol{\sigma}}_1, \widehat{\boldsymbol{\sigma}}_2 \in \mathbb{H}_h^{\boldsymbol{\sigma}}$, which, together with the definition of $\mathbf{T}_h$ (see (4.8)), yield

$$\|\mathbf{T}_h(\widehat{p}_1) - \mathbf{T}_h(\widehat{p}_2)\|_{0,\Omega} \leq \frac{2}{\min\{\widetilde{\gamma},\, \kappa_1\}} \left\{ \kappa_2\, \widetilde{C}^*(1 + C_1^* \gamma)(\|g\|_{0,\Omega} + \|p_{\mathrm{D}}\|_{1/2,\Gamma_{\mathrm{D}}} + \|\boldsymbol{u}_{\mathrm{D}}\|_{1/2,\Gamma_{\mathrm{D}}} + \|\boldsymbol{f}\|_{0,\Omega}) \right.$$
$$\left. + \frac{\gamma^2}{c_a}(1 + \kappa_2\, \widetilde{C}^*\, r) \right\} \|\widehat{p}_1 - \widehat{p}_2\|_{0,\Omega},$$

for all $\widehat{p}_1, \widehat{p}_2 \in \mathrm{W}_h$. In this way, using estimate (4.11), we obtain that $\mathbf{T}_h$ is a contraction mapping on W_h, thus problem (4.10), or equivalently (4.5), is well-posed. Finally, analogously to the proof of Theorem 3.9 (see also Lemmas 3.7 and 3.8) we can obtain (4.12), which concludes the proof. □

5. *A priori* error estimates

In this section we aim to provide the convergence of the Galerkin scheme (4.5) and derive the corresponding rate of convergence. From now on we assume that the hypotheses of Theorem 3.9 and Theorem 4.1 hold.

5.1 *Preliminaries*

Let the tuples $(\boldsymbol{\sigma}, \boldsymbol{u}, \boldsymbol{\rho}, \boldsymbol{\varphi}, p) \in \mathbb{H}_{\mathrm{N}}(\mathbf{div}; \Omega) \times \mathbf{L}^2(\Omega) \times \mathbb{L}^2_{\mathrm{skew}}(\Omega) \times \mathbf{H}_{\mathrm{N}}(\mathrm{div}; \Omega) \times \mathrm{L}^2(\Omega)$ and $(\boldsymbol{\sigma}_h, \boldsymbol{u}_h, \boldsymbol{\rho}_h, \boldsymbol{\varphi}_h, p_h) \in \mathbb{H}_h^{\boldsymbol{\sigma}} \times \mathbf{H}_h^{\boldsymbol{u}} \times \mathbb{H}_h^{\boldsymbol{\rho}} \times \mathbf{H}_h^{\boldsymbol{\varphi}} \times \mathrm{H}_h^p$ be the unique solutions of (3.3) and (4.7), respectively.

Let us write $\mathrm{e}_{\boldsymbol{\sigma}} = \boldsymbol{\sigma} - \boldsymbol{\sigma}_h$, $\mathrm{e}_{\boldsymbol{u}} = \boldsymbol{u} - \boldsymbol{u}_h$, $\mathrm{e}_{\boldsymbol{\rho}} = \boldsymbol{\rho} - \boldsymbol{\rho}_h$, $\mathrm{e}_{\boldsymbol{\varphi}} = \boldsymbol{\varphi} - \boldsymbol{\varphi}_h$ and $\mathrm{e}_p = p - p_h$. As usual, for a given $(\widehat{\boldsymbol{\tau}}_h, (\widehat{\mathbf{v}}_h, \widehat{\boldsymbol{\eta}}_h)) \in \mathbb{H}_h^{\boldsymbol{\sigma}} \times (\mathbf{H}_h^{\boldsymbol{u}} \times \mathbb{H}_h^{\boldsymbol{\rho}})$ and $(\widehat{\boldsymbol{\psi}}_h, \widehat{q}_h) \in \mathbf{H}_h^{\boldsymbol{\varphi}} \times \mathrm{H}_h^p$, we shall then decompose these errors into

$$\mathrm{e}_{\boldsymbol{\sigma}} = \boldsymbol{\xi}_{\boldsymbol{\sigma}} + \boldsymbol{\chi}_{\boldsymbol{\sigma}}, \quad \mathrm{e}_{\boldsymbol{u}} = \boldsymbol{\xi}_{\boldsymbol{u}} + \boldsymbol{\chi}_{\boldsymbol{u}}, \quad \mathrm{e}_{\boldsymbol{\rho}} = \boldsymbol{\xi}_{\boldsymbol{\rho}} + \boldsymbol{\chi}_{\boldsymbol{\rho}}, \quad \mathrm{e}_{\boldsymbol{\varphi}} = \boldsymbol{\xi}_{\boldsymbol{\varphi}} + \boldsymbol{\chi}_{\boldsymbol{\varphi}}, \quad \mathrm{e}_p = \xi_p + \chi_p, \tag{5.1}$$

with $\boldsymbol{\xi}_{\boldsymbol{\sigma}} := \boldsymbol{\sigma} - \widehat{\boldsymbol{\tau}}_h$, $\boldsymbol{\chi}_{\boldsymbol{\sigma}} := \widehat{\boldsymbol{\tau}}_h - \boldsymbol{\sigma}_h$, $\boldsymbol{\xi}_{\boldsymbol{u}} := \boldsymbol{u} - \widehat{\mathbf{v}}_h$, $\boldsymbol{\chi}_{\boldsymbol{u}} := \widehat{\mathbf{v}}_h - \boldsymbol{u}_h$, $\boldsymbol{\xi}_{\boldsymbol{\rho}} := \boldsymbol{\rho} - \widehat{\boldsymbol{\eta}}_h$, $\boldsymbol{\chi}_{\boldsymbol{\rho}} := \widehat{\boldsymbol{\eta}}_h - \boldsymbol{\rho}_h$, $\boldsymbol{\xi}_{\boldsymbol{\varphi}} := \boldsymbol{\varphi} - \widehat{\boldsymbol{\psi}}_h$, $\boldsymbol{\chi}_{\boldsymbol{\varphi}} := \widehat{\boldsymbol{\psi}}_h - \boldsymbol{\varphi}_h$, $\xi_p := p - \widehat{q}_h$ and $\chi_p := \widehat{q}_h - p_h$.

Considering the first two equations of problems (2.2) and (4.5) the following identities hold:

$$\begin{aligned} a(\boldsymbol{\sigma}, \boldsymbol{\tau}) + b(\boldsymbol{\tau}, (\boldsymbol{u}, \boldsymbol{\rho})) &= H(\boldsymbol{\tau}) - c(\boldsymbol{\tau}, p) && \forall\, \boldsymbol{\tau} \in \mathbb{H}_{\mathrm{N}}(\mathbf{div}; \Omega), \\ b(\boldsymbol{\sigma}, (\mathbf{v}, \boldsymbol{\eta})) &= F(\mathbf{v}, \boldsymbol{\eta}) && \forall\, \mathbf{v} \in \mathbf{L}^2(\Omega),\ \forall\, \boldsymbol{\eta} \in \mathbb{L}^2_{\mathrm{skew}}(\Omega), \end{aligned}$$

and

$$\begin{aligned} a(\boldsymbol{\sigma}_h, \boldsymbol{\tau}_h) + b(\boldsymbol{\tau}_h, (\boldsymbol{u}_h, \boldsymbol{\rho}_h)) &= H(\boldsymbol{\tau}_h) - c(\boldsymbol{\tau}_h, p_h) && \forall\, \boldsymbol{\tau}_h \in \mathbb{H}_h^{\boldsymbol{\sigma}}, \\ b(\boldsymbol{\sigma}_h, (\mathbf{v}_h, \boldsymbol{\eta}_h)) &= F(\mathbf{v}_h, \boldsymbol{\eta}_h) && \forall (\mathbf{v}_h, \boldsymbol{\eta}_h) \in \mathbf{H}_h^{\boldsymbol{u}} \times \mathbb{H}_h^{\boldsymbol{\rho}}. \end{aligned}$$

From these relations we can obtain that for all $(\boldsymbol{\tau}_h, (\mathbf{v}_h, \boldsymbol{\rho}_h)) \in \mathbb{H}_h^{\boldsymbol{\sigma}} \times (\mathbf{H}_h^{\boldsymbol{u}} \times \mathbb{H}_h^{\boldsymbol{\rho}})$ there holds

$$\begin{aligned} a(\mathrm{e}_{\boldsymbol{\sigma}}, \boldsymbol{\tau}_h) + b(\boldsymbol{\tau}_h, (\mathrm{e}_{\boldsymbol{u}}, \mathrm{e}_{\boldsymbol{\rho}})) &= -c(\boldsymbol{\tau}_h, \mathrm{e}_p), \\ b(\mathrm{e}_{\boldsymbol{\sigma}}, (\mathbf{v}_h, \boldsymbol{\eta}_h)) &= 0, \end{aligned}$$

which, together with the definition of the errors in (5.1), implies that

$$\begin{aligned} &a(\boldsymbol{\chi}_{\boldsymbol{\sigma}}, \boldsymbol{\tau}_h) + b(\boldsymbol{\tau}_h, (\boldsymbol{\chi}_{\boldsymbol{u}}, \boldsymbol{\chi}_{\boldsymbol{\rho}})) + b(\boldsymbol{\chi}_{\boldsymbol{\sigma}}, (\mathbf{v}_h, \boldsymbol{\eta}_h)) \\ &\qquad = -a(\boldsymbol{\xi}_{\boldsymbol{\sigma}}, \boldsymbol{\tau}_h) - b(\boldsymbol{\tau}_h, (\boldsymbol{\xi}_{\boldsymbol{u}}, \boldsymbol{\xi}_{\boldsymbol{\rho}})) - b(\boldsymbol{\xi}_{\boldsymbol{\sigma}}, (\mathbf{v}_h, \boldsymbol{\eta}_h)) - c(\boldsymbol{\tau}_h, \boldsymbol{\chi}_p) - c(\boldsymbol{\tau}_h, \boldsymbol{\xi}_p), \end{aligned} \tag{5.2}$$

for all $(\boldsymbol{\tau}_h, (\mathbf{v}_h, \boldsymbol{\rho}_h)) \in \mathbb{H}_h^{\boldsymbol{\sigma}} \times (\mathbf{H}_h^{\boldsymbol{u}} \times \mathbb{H}_h^{\boldsymbol{\rho}})$.

Next, considering the last two equations of both problems (2.2) and (4.5), we obtain

$$\begin{aligned} \widetilde{a}_{\boldsymbol{\sigma},p}(\boldsymbol{\varphi}, \boldsymbol{\psi}) + \widetilde{b}(\boldsymbol{\psi}, p) &= \widetilde{H}(\boldsymbol{\psi}) && \forall\, \boldsymbol{\psi} \in \mathbf{H}_{\mathrm{N}}(\mathrm{div}; \Omega), \\ \widetilde{b}(\boldsymbol{\varphi}, q) - \widetilde{c}(p, q) &= \tilde{F}(q) + c(\boldsymbol{\sigma}, q) && \forall\, q \in \mathrm{L}^2(\Omega), \end{aligned}$$

and

$$\begin{aligned} \widetilde{a}_{\boldsymbol{\sigma}_h,p_h}(\boldsymbol{\varphi}_h, \boldsymbol{\psi}_h) + \widetilde{b}(\boldsymbol{\psi}_h, p_h) &= \widetilde{H}(\boldsymbol{\psi}_h) && \forall\, \boldsymbol{\psi}_h \in \mathbf{H}_h^{\boldsymbol{\varphi}}, \\ \widetilde{b}(\boldsymbol{\varphi}_h, q_h) - \widetilde{c}(p_h, q_h) &= \tilde{F}(q_h) + c(\boldsymbol{\sigma}_h, q_h) && \forall\, q_h \in \mathrm{H}_h^p. \end{aligned}$$

Then, using arguments similar to those in Lemma 3.8, by adding $\pm\widetilde{a}_{\boldsymbol{\sigma}_h,p_h}(\boldsymbol{\varphi}, \boldsymbol{\psi}_h)$, we have

$$\begin{aligned} &\widetilde{a}_{\boldsymbol{\sigma}_h,p_h}(\mathrm{e}_{\boldsymbol{\varphi}_h}, \boldsymbol{\psi}_h) + \widetilde{b}(\boldsymbol{\psi}_h, \mathrm{e}_{p_h}) + \widetilde{b}(\mathrm{e}_{\boldsymbol{\varphi}_h}, q_h) - \widetilde{c}(\mathrm{e}_{p_h}, q_h) \\ &\qquad = -\int_\Omega \left(\boldsymbol{\kappa}(\boldsymbol{\sigma}, p)^{-1} - \boldsymbol{\kappa}(\boldsymbol{\sigma}_h, p_h)^{-1}\right) \boldsymbol{\varphi} \cdot \boldsymbol{\psi}_h + c(\mathrm{e}_{\boldsymbol{\sigma}}, q_h), \end{aligned}$$

which together with (5.1), implies that

$$\begin{aligned} &\widetilde{a}_{\boldsymbol{\sigma}_h,p_h}(\boldsymbol{\chi}_{\boldsymbol{\varphi}}, \boldsymbol{\psi}_h) + \widetilde{b}(\boldsymbol{\psi}_h, \chi_{p_h}) + \widetilde{b}(\boldsymbol{\chi}_{\boldsymbol{\varphi}}, q_h) - \widetilde{c}(\chi_p, q_h) + \widetilde{a}_{\boldsymbol{\sigma}_h,p_h}(\boldsymbol{\xi}_{\boldsymbol{\varphi}}, \boldsymbol{\psi}_h) \\ &\qquad = -\widetilde{b}(\boldsymbol{\psi}_h, \xi_p) - \widetilde{b}(\boldsymbol{\xi}_{\boldsymbol{\varphi}}, q_h) + \widetilde{c}(\xi_p, q_h) - \int_\Omega \left(\boldsymbol{\kappa}(\boldsymbol{\sigma}, p)^{-1} - \boldsymbol{\kappa}(\boldsymbol{\sigma}_h, p_h)^{-1}\right) \boldsymbol{\varphi} \cdot \boldsymbol{\psi}_h + c(\mathrm{e}_{\boldsymbol{\sigma}}, q_h). \end{aligned} \tag{5.3}$$

5.2 *Derivation of Céa estimates*

LEMMA 5.1. There exist C_3^*, $C_4^* > 0$, independent of h, such that

$$\|\boldsymbol{\chi}_{\boldsymbol{\sigma}}\|_{\mathbf{div};\Omega} + \|\boldsymbol{\chi}_{\boldsymbol{u}}\|_{0,\Omega} + \|\boldsymbol{\chi}_{\boldsymbol{\rho}}\|_{0,\Omega} \leq C_3^*(\|\boldsymbol{\xi}_{\boldsymbol{\sigma}}\|_{\mathbf{div};\Omega} + \|\boldsymbol{\xi}_{\boldsymbol{u}}\|_{0,\Omega} + \|\boldsymbol{\xi}_{\boldsymbol{\rho}}\|_{0,\Omega} + \|\boldsymbol{\xi}_p\|_{0,\Omega}) + C_4^*\gamma\|\chi_p\|_{0,\Omega}. \tag{5.4}$$

Proof. From the properties of a and b (refer to (4.2b) and (4.2a)), and (Ern & Guermond, 2004, proposition 2.36), we derive the following discrete global inf-sup condition:

$$\begin{aligned}&\|\boldsymbol{\chi}_{\boldsymbol{\sigma}}\|_{\mathbf{div};\Omega}+\|\boldsymbol{\chi}_{\boldsymbol{u}}\|_{0,\Omega}+\|\boldsymbol{\chi}_{\boldsymbol{\rho}}\|_{0,\Omega}\\&\quad\leq(C_1^*+C_2^*)\sup_{\mathbf{0}\neq(\boldsymbol{\tau}_h,\mathbf{v}_h,\boldsymbol{\psi}_h)\in\mathbb{H}_h^{\boldsymbol{\sigma}}\times\mathbf{H}_h^{\boldsymbol{u}}\times\mathbb{H}_h^{\boldsymbol{\rho}}}\frac{a(\boldsymbol{\chi}_{\boldsymbol{\sigma}},\boldsymbol{\tau}_h)+b(\boldsymbol{\tau}_h,(\boldsymbol{\chi}_{\boldsymbol{u}},\boldsymbol{\chi}_{\boldsymbol{\rho}}))+b(\boldsymbol{\chi}_{\boldsymbol{\sigma}},(\mathbf{v}_h,\boldsymbol{\eta}_h))}{\|\boldsymbol{\tau}_h\|_{\mathbf{div};\Omega}+\|\mathbf{v}_h\|_{0,\Omega}+\|\boldsymbol{\eta}_h\|_{0,\Omega}},\end{aligned}$$

where C_1^*, $C_2^*>0$ independent of h are the discrete version of the constants C_1, C_2 defined in (3.8). Then, combining the last inequality with (5.2), and the continuity properties of a and b (see (2.4a)), we obtain

$$\begin{aligned}&\|\boldsymbol{\chi}_{\boldsymbol{\sigma}}\|_{\mathbf{div};\Omega}+\|\boldsymbol{\chi}_{\boldsymbol{u}}\|_{0,\Omega}+\|\boldsymbol{\chi}_{\boldsymbol{\rho}}\|_{0,\Omega}\\&\quad\leq(C_1^*+C_2^*)\left(\frac{1}{\mu}\|\boldsymbol{\xi}_{\boldsymbol{\sigma}}\|_{\mathbf{div};\Omega}+\|\boldsymbol{\xi}_{\boldsymbol{u}}\|_{0,\Omega}+\|\boldsymbol{\xi}_{\boldsymbol{\rho}}\|_{0,\Omega}+\|\boldsymbol{\xi}_{\boldsymbol{\sigma}}\|_{\mathbf{div};\Omega}+\gamma\|\chi_p\|_{0,\Omega}+\gamma\|\xi_p\|_{0,\Omega}\right),\end{aligned}$$

which implies (5.4) with $C_3^*:=(C_1^*+C_2^*)(\frac{1}{\mu}+1+\gamma)$ and $C_4^*:=C_1^*+C_2^*$. Note also that the error estimate is robust with respect to λ. □

LEMMA 5.2. There exist $\widetilde{C}_5^*$, $\widetilde{C}_6^*>0$, independent of h, such that

$$\begin{aligned}\|\boldsymbol{\chi}_{\boldsymbol{\varphi}}\|_{\mathrm{div};\Omega}+\|\chi_p\|_{0,\Omega}&\leq\widetilde{C}_5^*\left(\|\boldsymbol{\xi}_{\boldsymbol{\varphi}}\|_{\mathrm{div};\Omega}+\|\xi_p\|_{0,\Omega}+\|\boldsymbol{\xi}_{\boldsymbol{\sigma}}\|_{\mathbf{div};\Omega}\right)\\&+\widetilde{C}_6^*\left((\|g\|_{0,\Omega}+\|p_{\mathrm{D}}\|_{1/2,\Gamma_{\mathrm{D}}}+\|\boldsymbol{u}_{\mathrm{D}}\|_{1/2,\Gamma_{\mathrm{D}}}+\|\boldsymbol{f}\|_{0,\Omega}+\gamma\,r)\|\chi_p\|_{0,\Omega}+\gamma\|\boldsymbol{\chi}_{\boldsymbol{\sigma}}\|_{\mathbf{div};\Omega}\right).\end{aligned}\tag{5.5}$$

Proof. Similarly to Lemma 5.1, using the properties of $\widetilde{a}$, $\widetilde{b}$ and $\widetilde{c}$ (refer to (4.6), (4.4) and (2.9)), and (Correa & Gatica, 2022, theorem 3.4), we derive the following discrete global inf-sup condition:

$$\|\boldsymbol{\chi}_{\boldsymbol{\varphi}}\|_{\mathrm{div};\Omega}+\|\chi_p\|_{0,\Omega}\leq 2\widetilde{C}^*\sup_{\mathbf{0}\neq(\boldsymbol{\psi}_h,q_h)\in\mathbf{H}_h^{\boldsymbol{\varphi}}\times\mathrm{H}_h^p}\frac{\widetilde{a}_{\boldsymbol{\sigma}_h,p_h}(\boldsymbol{\chi}_{\boldsymbol{\varphi}},\boldsymbol{\psi}_h)+\widetilde{b}(\boldsymbol{\psi}_h,\chi_p)+\widetilde{b}(\boldsymbol{\chi}_{\boldsymbol{\varphi}},q_h)-\widetilde{c}(\chi_p,q_h)}{\|\boldsymbol{\psi}_h\|_{\mathrm{div};\Omega}+\|q_h\|_{0,\Omega}},$$

with $\widetilde{C}^*$ defined as in (4.9). Then, using the equation (5.3), the bound properties of $\widetilde{a}$, $\widetilde{b}$ and $\widetilde{c}$ (see (3.2a) and (2.4c)) and the second assumption for $\boldsymbol{\kappa}$ (cf. (2.3)), we obtain

$$\begin{aligned}&\|\boldsymbol{\chi}_{\boldsymbol{\varphi}}\|_{\mathrm{div};\Omega}+\|\chi_p\|_{0,\Omega}\\&\quad\leq 2\widetilde{C}^*(C_{\widetilde{a}}\|\boldsymbol{\xi}_{\boldsymbol{\varphi}}\|_{\mathrm{div};\Omega}+\|\xi_p\|_{0,\Omega}+\|\boldsymbol{\xi}_{\boldsymbol{\varphi}}\|_{\mathrm{div};\Omega}+\widetilde{\gamma}\|\xi_p\|_{0,\Omega}\\&\qquad+\|\boldsymbol{\kappa}(\boldsymbol{\sigma},p)^{-1}-\boldsymbol{\kappa}(\boldsymbol{\sigma}_h,p_h)^{-1}\|_{\mathbb{L}^\infty(\Omega)}\|\boldsymbol{\varphi}\|_{\mathrm{div};\Omega}+\gamma\|\mathrm{e}_{\boldsymbol{\sigma}}\|_{\mathbf{div};\Omega})\\&\quad\leq 2\widetilde{C}^*(C_{\widetilde{a}}\|\boldsymbol{\xi}_{\boldsymbol{\varphi}}\|_{\mathrm{div};\Omega}+\|\xi_p\|_{0,\Omega}+\|\boldsymbol{\xi}_{\boldsymbol{\varphi}}\|_{\mathrm{div};\Omega}+\widetilde{\gamma}\|\xi_p\|_{0,\Omega}+\kappa_2\|\mathrm{e}_p\|_{0,\Omega}\|\boldsymbol{\varphi}\|_{\mathrm{div};\Omega}+\gamma\|\mathrm{e}_{\boldsymbol{\sigma}}\|_{\mathbf{div};\Omega});\end{aligned}$$

hence, using the fact that $\boldsymbol{\varphi}$ satisfies (3.15) and the error decomposition (5.1), we have

$$\begin{aligned}\|\boldsymbol{\chi}_{\boldsymbol{\varphi}}\|_{\mathrm{div};\Omega}+\|\chi_p\|_{0,\Omega} &\leq 2\widetilde{C}^*(C_{\widetilde{a}}\|\boldsymbol{\xi}_{\boldsymbol{\varphi}}\|_{\mathrm{div};\Omega}+\|\xi_p\|_{0,\Omega}+\|\boldsymbol{\xi}_{\boldsymbol{\varphi}}\|_{\mathrm{div};\Omega}+\widetilde{\gamma}\|\xi_p\|_{0,\Omega}+\kappa_2\|\xi_p\|_{0,\Omega}\|\boldsymbol{\varphi}\|_{\mathrm{div};\Omega}\\ &\quad+\gamma\|\boldsymbol{\xi}_{\boldsymbol{\sigma}}\|_{\mathbf{div};\Omega})+2\widetilde{C}^*(\kappa_2\|\chi_p\|_{0,\Omega}\|\boldsymbol{\varphi}\|_{\mathrm{div};\Omega}+\gamma\|\boldsymbol{\chi}_{\boldsymbol{\sigma}}\|_{\mathbf{div};\Omega})\\ &\leq \widetilde{C}_5^*\,(\|\boldsymbol{\xi}_{\boldsymbol{\varphi}}\|_{\mathrm{div};\Omega}+\|\xi_p\|_{0,\Omega}+\|\boldsymbol{\xi}_{\boldsymbol{\sigma}}\|_{\mathbf{div};\Omega})\\ &\quad+2\widetilde{C}^*\big(\kappa_2 C(\|g\|_{0,\Omega}+\|p_{\mathrm{D}}\|_{1/2,\Gamma_{\mathrm{D}}}+\|\boldsymbol{u}_{\mathrm{D}}\|_{1/2,\Gamma_{\mathrm{D}}}+\|\boldsymbol{f}\|_{0,\Omega}+\gamma\, r)\|\chi_p\|_{0,\Omega}\\ &\quad+\gamma\|\boldsymbol{\chi}_{\boldsymbol{\sigma}}\|_{\mathbf{div};\Omega}\big);\end{aligned}$$

the last equation implies (5.5), with $\widetilde{C}_5^* := 2\widetilde{C}^*\big(C_{\widetilde{a}}+1+\widetilde{\gamma}+\gamma+\kappa_2 C(\|g\|_{0,\Omega}+\|p_{\mathrm{D}}\|_{1/2,\Gamma_{\mathrm{D}}}+\|\boldsymbol{u}_{\mathrm{D}}\|_{1/2,\Gamma_{\mathrm{D}}}+\|\boldsymbol{f}\|_{0,\Omega}+\gamma\, r)\big)$ and $\widetilde{C}_6^* := 2\widetilde{C}^*(\kappa_2 C+1)$, and concludes the proof. □

THEOREM 5.3. Assume that

$$(C_4^*+\widetilde{C}_6^*+\widetilde{C}_6^* r)\gamma+\widetilde{C}_6^*(\|g\|_{0,\Omega}+\|p_{\mathrm{D}}\|_{1/2,\Gamma_{\mathrm{D}}}+\|\boldsymbol{u}_{\mathrm{D}}\|_{1/2,\Gamma_{\mathrm{D}}}+\|\boldsymbol{f}\|_{0,\Omega})\leq\frac{1}{2},\tag{5.6}$$

with C_4^* and $\widetilde{C}_6^*$ being the constants in Lemmas 5.1 and 5.2. Furthermore, assume that the hypotheses of Theorem 3.9 and Theorem 4.1 hold. Let $(\boldsymbol{\sigma},\boldsymbol{u},\boldsymbol{\rho},\boldsymbol{\varphi},p)\in\mathbb{H}_{\mathrm{N}}(\mathbf{div};\Omega)\times\mathbf{L}^2(\Omega)\times\mathbb{L}^2_{\mathrm{skew}}(\Omega)\times\mathbf{H}_{\mathrm{N}}(\mathrm{div};\Omega)\times\mathrm{L}^2(\Omega)$ and $(\boldsymbol{\sigma}_h,\boldsymbol{u}_h,\boldsymbol{\rho}_h,\boldsymbol{\varphi}_h,p_h)\in\mathbb{H}_h^{\boldsymbol{\sigma}}\times\mathbf{H}_h^{\boldsymbol{u}}\times\mathbb{H}_h^{\boldsymbol{\rho}}\times\mathbf{H}_h^{\boldsymbol{\varphi}}\times\mathrm{H}_h^p$ be the unique solutions of (2.2) and (4.5), respectively. Then, there exists $C_{\mathrm{Céa}}>0$, independent of h, such that

$$\begin{aligned}&\|\mathbf{e}_{\boldsymbol{\sigma}}\|_{\mathbf{div};\Omega}+\|\mathbf{e}_{\boldsymbol{u}}\|_{0,\Omega}+\|\mathbf{e}_{\boldsymbol{\rho}}\|_{0,\Omega}+\|\mathbf{e}_{\boldsymbol{\varphi}}\|_{\mathrm{div};\Omega}+\|\mathbf{e}_p\|_{0,\Omega}\\ &\qquad\leq C_{\mathrm{Céa}}\,\mathrm{dist}\,\big((\boldsymbol{\sigma},\boldsymbol{u},\boldsymbol{\rho},\boldsymbol{\varphi},p),\,\mathbb{H}_h^{\boldsymbol{\sigma}}\times\mathbf{H}_h^{\boldsymbol{u}}\times\mathbb{H}_h^{\boldsymbol{\rho}}\times\mathbf{H}_h^{\boldsymbol{\varphi}}\times\mathrm{H}_h^p\big).\end{aligned}\tag{5.7}$$

Proof. Combining (5.4) and (5.5), and using the assumption (5.6), we deduce

$$\begin{aligned}&\|\boldsymbol{\chi}_{\boldsymbol{\sigma}}\|_{\mathbf{div};\Omega}+\|\boldsymbol{\chi}_{\boldsymbol{u}}\|_{0,\Omega}+\|\boldsymbol{\chi}_{\boldsymbol{\rho}}\|_{0,\Omega}+\|\boldsymbol{\chi}_{\boldsymbol{\varphi}}\|_{\mathrm{div};\Omega}+\|\chi_p\|_{0,\Omega}\\ &\quad\leq C_3^*(\|\boldsymbol{\xi}_{\boldsymbol{\sigma}}\|_{\mathbf{div};\Omega}+\|\boldsymbol{\xi}_{\boldsymbol{u}}\|_{0,\Omega}+\|\boldsymbol{\xi}_{\boldsymbol{\rho}}\|_{0,\Omega}+\|\xi_p\|_{0,\Omega})\\ &\qquad+\widetilde{C}_5^*\,(\|\boldsymbol{\xi}_{\boldsymbol{\varphi}}\|_{\mathrm{div};\Omega}+\|\xi_p\|_{0,\Omega}+\|\boldsymbol{\xi}_{\boldsymbol{\sigma}}\|_{\mathbf{div};\Omega})+\frac{1}{2}\|\chi_p\|_{0,\Omega}+\frac{1}{2}\|\boldsymbol{\chi}_{\boldsymbol{\sigma}}\|_{\mathbf{div};\Omega}.\end{aligned}$$

And from the latter inequality, we obtain

$$\begin{aligned}&\|\boldsymbol{\chi}_{\boldsymbol{\sigma}}\|_{\mathbf{div};\Omega}+\|\boldsymbol{\chi}_{\boldsymbol{u}}\|_{0,\Omega}+\|\boldsymbol{\chi}_{\boldsymbol{\rho}}\|_{0,\Omega}+\|\boldsymbol{\chi}_{\boldsymbol{\varphi}}\|_{\mathrm{div};\Omega}+\|\chi_p\|_{0,\Omega}\\ &\qquad\leq 2(C_3^*+\widetilde{C}_5^*)(\|\boldsymbol{\xi}_{\boldsymbol{\sigma}}\|_{\mathbf{div};\Omega}+\|\boldsymbol{\xi}_{\boldsymbol{u}}\|_{0,\Omega}+\|\boldsymbol{\xi}_{\boldsymbol{\rho}}\|_{0,\Omega}+\|\boldsymbol{\xi}_{\boldsymbol{\varphi}}\|_{\mathrm{div};\Omega}+\|\xi_p\|_{0,\Omega}).\end{aligned}\tag{5.8}$$

In this way, from (5.1), (5.8) and the triangle inequality, we obtain

$$\begin{aligned}
&\|\mathbf{e}_{\boldsymbol{\sigma}}\|_{\mathbf{div};\Omega} + \|\mathbf{e}_{\boldsymbol{u}}\|_{0,\Omega} + \|\mathbf{e}_{\boldsymbol{\rho}}\|_{0,\Omega} + \|\mathbf{e}_{\boldsymbol{\varphi}}\|_{\mathrm{div};\Omega} + \|\mathrm{e}_{p}\|_{0,\Omega} \\
&\quad \leq \|\boldsymbol{\chi}_{\boldsymbol{\sigma}}\|_{\mathbf{div};\Omega} + \|\boldsymbol{\xi}_{\boldsymbol{\sigma}}\|_{\mathbf{div};\Omega} + \|\boldsymbol{\chi}_{\boldsymbol{u}}\|_{0,\Omega} + \|\boldsymbol{\xi}_{\boldsymbol{u}}\|_{0,\Omega} \\
&\qquad + \|\boldsymbol{\chi}_{\boldsymbol{\rho}}\|_{0,\Omega} + \|\boldsymbol{\xi}_{\boldsymbol{\rho}}\|_{0,\Omega} + \|\boldsymbol{\chi}_{\boldsymbol{\varphi}}\|_{\mathrm{div};\Omega} + \|\boldsymbol{\xi}_{\boldsymbol{\varphi}}\|_{\mathrm{div};\Omega} + \|\chi_{p}\|_{0,\Omega} + \|\xi_{p}\|_{0,\Omega} \\
&\quad \leq (2C_3^* + 2\widetilde{C}_5^* + 1)\left(\|\boldsymbol{\xi}_{\boldsymbol{\sigma}}\|_{\mathbf{div};\Omega} + \|\boldsymbol{\xi}_{\boldsymbol{u}}\|_{0,\Omega} + \|\boldsymbol{\xi}_{\boldsymbol{\rho}}\|_{0,\Omega} + \|\boldsymbol{\xi}_{\boldsymbol{\varphi}}\|_{\mathrm{div};\Omega} + \|\xi_{p}\|_{0,\Omega}\right),
\end{aligned}$$

which, combined with the fact that $(\widehat{\boldsymbol{\tau}}_h, (\widehat{\mathbf{v}}_h, \widehat{\boldsymbol{\eta}}_h)) \in \mathbb{H}_h^{\boldsymbol{\sigma}} \times (\mathbf{H}_h^{\boldsymbol{u}} \times \mathbb{H}_h^{\boldsymbol{\rho}})$ and $(\widehat{\boldsymbol{\psi}}_h, \widehat{q}_h) \in \mathbf{H}_h^{\boldsymbol{\varphi}} \times \mathrm{H}_h^{p}$ are arbitrary (see (5.1)), concludes the proof. □

5.3 *Rates of convergence*

In order to establish the rate of convergence of the Galerkin scheme (4.5) we first recall the following approximation properties associated with the FE spaces specified in Section 4.1.

For each $0 < m \leq k+1$ and for each $\boldsymbol{\tau} \in \mathbb{H}^m(\Omega) \cap \mathbb{H}_{\mathrm{N}}(\mathbf{div};\Omega)$ with $\mathbf{div}\,\boldsymbol{\tau} \in \mathbf{H}^m(\Omega)$, $\mathbf{v} \in \mathbf{H}^m(\Omega)$, $\boldsymbol{\eta} \in \mathbb{H}^m(\Omega) \cap \mathbb{L}^2_{\mathrm{skew}}(\Omega)$, $\boldsymbol{\psi} \in \mathbf{H}^m(\Omega) \cap \mathbf{H}_{\mathrm{N}}(\mathrm{div};\Omega)$ with $\mathrm{div}\,\mathbf{v} \in \mathrm{H}^m(\Omega)$, and $q \in \mathrm{H}^m(\Omega)$ there holds

$$\mathrm{dist}\left(\boldsymbol{\tau}, \mathbb{H}_h^{\boldsymbol{\sigma}}\right) := \inf_{\boldsymbol{\tau}_h \in \mathbb{H}_h^{\boldsymbol{\sigma}}} \|\boldsymbol{\tau} - \boldsymbol{\tau}_h\|_{\mathbf{div};\Omega} \lesssim h^m \left\{\|\boldsymbol{\tau}\|_{m,\Omega} + \|\mathbf{div}\,\boldsymbol{\tau}\|_{m,\Omega}\right\}, \tag{5.9a}$$

$$\mathrm{dist}\left(\mathbf{v}, \mathbf{H}_h^{\boldsymbol{u}}\right) := \inf_{\mathbf{v}_h \in \mathbf{H}_h^{\boldsymbol{u}}} \|\mathbf{v} - \mathbf{v}_h\|_{0,\Omega} \lesssim h^m \|\mathbf{v}\|_{m,\Omega}, \tag{5.9b}$$

$$\mathrm{dist}\left(\boldsymbol{\eta}, \mathbb{H}_h^{\boldsymbol{\rho}}\right) := \inf_{\boldsymbol{\eta}_h \in \mathbb{H}_h^{\boldsymbol{\rho}}} \|\boldsymbol{\eta} - \boldsymbol{\eta}_h\|_{0,\Omega} \lesssim h^m \|\boldsymbol{\eta}\|_{m,\Omega}, \tag{5.9c}$$

$$\mathrm{dist}\left(\boldsymbol{\psi}, \mathbf{H}_h^{\boldsymbol{\varphi}}\right) := \inf_{\boldsymbol{\psi}_h \in \mathbf{H}_h^{\boldsymbol{\varphi}}} \|\boldsymbol{\psi} - \boldsymbol{\psi}_h\|_{\mathrm{div};\Omega} \lesssim h^m \left\{\|\boldsymbol{\psi}\|_{m,\Omega} + \|\mathrm{div}\,\boldsymbol{\psi}\|_{m,\Omega}\right\}, \tag{5.9d}$$

$$\mathrm{dist}\left(q, \mathrm{H}_h^{p}\right) := \inf_{q_h \in \mathrm{H}_h^{p}} \|q - q_h\|_{0,\Omega} \lesssim h^m \|q\|_{m,\Omega}. \tag{5.9e}$$

For (5.9a), (5.9b) and (5.9c) we refer to (Gatica *et al.*, 2013, theorem 2.4), whereas (5.9d) and (5.9e) are provided in (Gatica, 2014, theorem 3.6) and (Ern & Guermond, 2004, proposition 1.134), respectively. With these steps we are now in a position to state the rates of convergence associated with the Galerkin scheme (4.5).

THEOREM 5.4. Assume that the hypotheses of Theorem 5.3 hold and let $(\boldsymbol{\sigma}, \boldsymbol{u}, \boldsymbol{\rho}, \boldsymbol{\varphi}, p) \in \mathbb{H}_{\mathrm{N}}(\mathbf{div};\Omega) \times \mathbf{L}^2(\Omega) \times \mathbb{L}^2_{\mathrm{skew}}(\Omega) \times \mathbf{H}_{\mathrm{N}}(\mathrm{div};\Omega) \times \mathrm{L}^2(\Omega)$ and $(\boldsymbol{\sigma}_h, \boldsymbol{u}_h, \boldsymbol{\rho}_h, \boldsymbol{\varphi}_h, p_h) \in \mathbb{H}_h^{\boldsymbol{\sigma}} \times \mathbf{H}_h^{\boldsymbol{u}} \times \mathbb{H}_h^{\boldsymbol{\rho}} \times \mathbf{H}_h^{\boldsymbol{\varphi}} \times \mathrm{H}_h^{p}$ be the unique solutions of the continuous and discrete problems (2.2) and (4.5), respectively. Assume further that $\boldsymbol{\sigma} \in \mathbb{H}^m(\Omega)$, $\mathbf{div}\,\boldsymbol{\sigma} \in \mathbf{H}^m(\Omega)$, $\boldsymbol{u} \in \mathbf{H}^m(\Omega)$, $\boldsymbol{\rho} \in \mathbb{H}^m(\Omega)$, $\boldsymbol{\varphi} \in \mathbf{H}^m(\Omega)$, $\mathrm{div}\,\boldsymbol{\varphi} \in \mathrm{H}^m(\Omega)$ and $p \in \mathrm{H}^m(\Omega)$, for $1 \leq m \leq k+1$. Then, there exists $C_{\mathrm{rate}} > 0$, independent of h, such that

$$\begin{aligned}
&\|\mathbf{e}_{\boldsymbol{\sigma}}\|_{\mathbf{div};\Omega} + \|\mathbf{e}_{\boldsymbol{u}}\|_{0,\Omega} + \|\mathbf{e}_{\boldsymbol{\rho}}\|_{0,\Omega} + \|\mathbf{e}_{\boldsymbol{\varphi}}\|_{\mathrm{div};\Omega} + \|\mathbf{e}_{p}\|_{0,\Omega} \\
&\quad \leq C_{\mathrm{rate}}\, h^m \left\{\|\boldsymbol{\sigma}\|_{m,\Omega} + \|\mathbf{div}\,\boldsymbol{\sigma}\|_{m,\Omega} + \|\boldsymbol{u}\|_{m,\Omega} + \|\boldsymbol{\rho}\|_{m,\Omega} + \|\boldsymbol{\varphi}\|_{m,\Omega} + \|\mathrm{div}\,\boldsymbol{\varphi}\|_{m,\Omega} + \|p\|_{m,\Omega}\right\}.
\end{aligned}$$

Proof. The result follows from Céa estimate (5.7) and the approximation properties (5.9). □

REMARK 5.5. Similarly to Lamichhane *et al.* (2024) the analysis developed in Sections 2–5 can be adapted to a formulation without the variable $\boldsymbol{\rho}$ ($\boldsymbol{\rho}_h$ in the discrete problem), imposing symmetry of $\boldsymbol{\sigma}$ by taking $\boldsymbol{\sigma} \in \mathbb{H}_{\mathrm{sym}}(\mathbf{div};\Omega) := \left\{\boldsymbol{\tau} \in \mathbb{L}^2_{\mathrm{sym}}(\Omega) : \mathbf{div}\,\boldsymbol{\tau} \in \mathbf{L}^2(\Omega)\right\}$ and $\mathbb{L}^2_{\mathrm{sym}}(\Omega) := \{\boldsymbol{\tau} \in \mathbb{L}^2(\Omega) : \boldsymbol{\tau} = \boldsymbol{\tau}^{\mathrm{t}}\}$, utilizing results from (Lamichhane *et al.*, 2024, section 2.2) ((Lamichhane *et al.*, 2024, section 4.1) for the discrete problem), and adapting the strategy used in, e.g., (Lamichhane *et al.*, 2024, sections 3 and 4).

6. *A posteriori* error estimates

In this section we derive residual-based *a posteriori* error estimates and demonstrate the reliability and efficiency of the proposed estimators. Mainly due to notational convenience we confine our analysis to the two-dimensional case. The extension to three-dimensional case should be quite straightforward (see, e.g., Caucao *et al.* (2023)). Similarly to (Camaño *et al.*, 2022, section 4) we introduce additional notation. Let $\mathscr{E}_h$ be the set of edges of $\mathscr{T}_h$, whose corresponding diameters are denoted h_E, and define

$$\mathscr{E}_h(\star) := \left\{E \in \mathscr{E}_h : E \subseteq \star\right\}, \quad \star \in \{\Omega, \Gamma_{\mathrm{D}}, \Gamma_{\mathrm{N}}\}.$$

On each $E \in \mathscr{E}_h$ we also define the unit normal vector $\boldsymbol{n}_E := (n_1, n_2)^{\mathrm{t}}$ and the tangential vector $\boldsymbol{s}_E := (-n_2, n_1)^{\mathrm{t}}$. However, when no confusion arises we will simply write $\boldsymbol{n}$ and $\boldsymbol{s}$ instead of $\boldsymbol{n}_E$ and $\boldsymbol{s}_E$, respectively. Also, by $\frac{\mathrm{d}}{\mathrm{ds}}$ we denote the tangential derivative. The usual jump operator $[\![\cdot]\!]$ across internal edges are defined for piecewise continuous matrix, vector or scalar-valued functions. For sufficiently smooth scalar ψ, vector $\mathbf{v} := (v_1, v_2)^{\mathrm{t}}$ and tensor fields $\boldsymbol{\tau} := (\tau_{ij})_{1\le i,j\le 2}$ we let

$$\mathrm{curl}\,(\psi) := \left(\frac{\partial \psi}{\partial x_2}, -\frac{\partial \psi}{\partial x_1}\right)^{\mathrm{t}}, \quad \mathrm{rot}\,(\mathbf{v}) := \frac{\partial v_2}{\partial x_1} - \frac{\partial v_1}{\partial x_2}, \quad \mathbf{curl}\,(\mathbf{v}) = \begin{pmatrix} \mathrm{curl}\,(v_1)^{\mathrm{t}} \\ \mathrm{curl}\,(v_2)^{\mathrm{t}} \end{pmatrix},$$

$$\text{and} \quad \underline{\mathbf{curl}}\,(\boldsymbol{\tau}) = \begin{pmatrix} \mathrm{rot}\,(\boldsymbol{\tau}_1) \\ \mathrm{rot}\,(\boldsymbol{\tau}_2) \end{pmatrix}.$$

In addition, we denote by Π_h the Raviart–Thomas interpolator and by I_h the Clément operator (see, e.g., (Álvarez *et al.*, 2016, section 3) for their properties). In what follows we denote by $\boldsymbol{\Pi}_h$ the tensor version of Π_h, which is defined row-wise by Π_h and by $\mathbf{I}_h$ the corresponding vector version of I_h, which is defined componentwise by I_h.

In what follows we will assume that the hypotheses of Theorems 3.9 and 4.1 are satisfied. Let $\boldsymbol{\sigma}_h$, $\boldsymbol{u}_h$, $\boldsymbol{\rho}_h$, $\boldsymbol{\varphi}_h$, p_h denote the FE solutions of (4.5). We define the residual-based and fully computable local contributions to the error estimator Ξ^2_K, defined as the sum of $\Xi^2_{s,K}$ and $\Xi^2_{f,K}$, where $\Xi_{s,K}$ and $\Xi_{f,K}$ pertain

to the solid (mixed elasticity) and fluid (mixed Darcy) components, respectively:

$$\begin{aligned}\Xi_{s,K}^2 := \|\boldsymbol{f} + \mathbf{div}\boldsymbol{\sigma}_h\|_{0,K}^2 + \|\boldsymbol{\sigma}_h - \boldsymbol{\sigma}_h^{\mathrm{t}}\|_{0,K}^2 + h_K^2 \left\| \mathscr{C}^{-1}\boldsymbol{\sigma}_h + \frac{\alpha}{d\lambda + 2\mu} p_h \mathbf{I} - \nabla \boldsymbol{u}_h + \boldsymbol{\rho}_h \right\|_{0,K}^2 \\ + h_K^2 \left\| \underline{\mathbf{curl}} \left(\mathscr{C}^{-1}\boldsymbol{\sigma}_h + \frac{\alpha}{d\lambda + 2\mu} p_h \mathbf{I} + \boldsymbol{\rho}_h \right) \right\|_{0,K}^2 + \sum_{E \in \partial K \cap \mathscr{E}_h(\Gamma_{\mathrm{D}})} h_E \|\boldsymbol{u}_{\mathrm{D}} - \boldsymbol{u}_h\|_{0,E}^2 \\ + \sum_{E \in \partial K \cap \mathscr{E}_h(\Omega)} h_E \left\| \left[\!\left[\left(\mathscr{C}^{-1}\boldsymbol{\sigma}_h + \frac{\alpha}{d\lambda + 2\mu} p_h \mathbf{I} + \boldsymbol{\rho}_h \right) \boldsymbol{s} \right]\!\right] \right\|_{0,E}^2 \\ + \sum_{E \in \partial K \cap \mathscr{E}_h(\Gamma_{\mathrm{D}})} h_E \left\| \left(\mathscr{C}^{-1}\boldsymbol{\sigma}_h + \frac{\alpha}{d\lambda + 2\mu} p_h \mathbf{I} + \boldsymbol{\rho}_h \right) \boldsymbol{s} - \frac{\mathrm{d}\boldsymbol{u}_{\mathrm{D}}}{\mathrm{d}\boldsymbol{s}} \right\|_{0,E}^2, \end{aligned} \tag{6.1a}$$

$$\begin{aligned}\Xi_{f,K}^2 := \left\| c_0 p_h + \frac{\alpha}{d\lambda + 2\mu} \mathrm{tr}\boldsymbol{\sigma}_h + \frac{d\alpha^2}{d\lambda + 2\mu} p_h - \mathrm{div}\boldsymbol{\varphi}_h - g \right\|_{0,K}^2 + h_K^2 \left\| \boldsymbol{\kappa}(\boldsymbol{\sigma}_h, p_h)^{-1}\boldsymbol{\varphi}_h - \nabla p_h \right\|_{0,K}^2 \\ + h_K^2 \|\mathrm{rot}\,(\boldsymbol{\kappa}(\boldsymbol{\sigma}_h, p_h)^{-1}\boldsymbol{\varphi}_h)\|_{0,K}^2 + \sum_{E \in \partial K \cap \mathscr{E}_h(\Omega)} h_E \|[\![(\boldsymbol{\kappa}(\boldsymbol{\sigma}_h, p_h)^{-1}\boldsymbol{\varphi}_h) \cdot \boldsymbol{s}]\!]\|_{0,E}^2 \\ + \sum_{E \in \partial K \cap \mathscr{E}_h(\Gamma_{\mathrm{D}})} h_E \left\| \boldsymbol{\kappa}(\boldsymbol{\sigma}_h, p_h)^{-1}\boldsymbol{\varphi}_h \cdot \boldsymbol{s} - \frac{\mathrm{d}p_{\mathrm{D}}}{\mathrm{d}\boldsymbol{s}} \right\|_{0,E}^2 + \sum_{E \in \partial K \cap \mathscr{E}_h(\Gamma_{\mathrm{D}})} h_E \|p_{\mathrm{D}} - p_h\|_{0,E}^2. \end{aligned} \tag{6.1b}$$

Then, we define the global estimator

$$\Xi^2 := \sum_{K \in \mathscr{T}_h} \Xi_{s,K}^2 + \Xi_{f,K}^2. \tag{6.2}$$

6.1 *Reliability of the* a posteriori *error estimator*

First, we prove preliminary results that will be key in showing the reliability of the global estimator.

LEMMA 6.1. There exists $C_1 > 0$, such that

$$\|\boldsymbol{\sigma} - \boldsymbol{\sigma}_h\|_{\mathbf{div};\Omega} + \|\boldsymbol{u} - \boldsymbol{u}_h\|_{0,\Omega} + \|\boldsymbol{\rho} - \boldsymbol{\rho}_h\|_{0,\Omega} \leq C_1 \left(\|\mathscr{R}_1\| + \|\boldsymbol{f} + \mathbf{div}(\boldsymbol{\sigma}_h)\|_{0,\Omega} + \|\boldsymbol{\sigma}_h - \boldsymbol{\sigma}_h^t\|_{0,\Omega} \right),$$

where

$$\mathscr{R}_1(\boldsymbol{\tau}) := a(\boldsymbol{\sigma} - \boldsymbol{\sigma}_h, \boldsymbol{\tau}) + b(\boldsymbol{\tau}, (\boldsymbol{u} - \boldsymbol{u}_h, \boldsymbol{\rho} - \boldsymbol{\rho}_h)), \tag{6.3}$$

with $\mathscr{R}_1(\boldsymbol{\tau}_h) = -c(\boldsymbol{\tau}_h, p - p_h)$ for all $\boldsymbol{\tau}_h \in \mathbb{H}_h^{\boldsymbol{\sigma}}$, and $||\mathscr{R}_1|| = \sup_{\mathbf{0} \neq \boldsymbol{\tau} \in \mathbb{H}_{\mathrm{N}}(\mathbf{div};\Omega)} \frac{\mathscr{R}_1(\boldsymbol{\tau})}{\|\boldsymbol{\tau}\|_{\mathbf{div};\Omega}}$.

Proof. Using the properties of bilinear forms a and b, as outlined in equations (2.7) and (2.8a), along with the insight from (Ern & Guermond, 2004, proposition 2.36), there exists $C_1 > 0$, depending on

μ, c_a, β such that

$$\|\mathsf{e}_{\boldsymbol{\sigma}}\|_{\mathbf{div};\Omega}+\|\mathsf{e}_{\boldsymbol{u}}\|_{0,\Omega}+\|\mathsf{e}_{\boldsymbol{\rho}}\|_{0,\Omega} \leq C_1 \sup_{\substack{\mathbf{0}\neq(\boldsymbol{\tau},\mathbf{v},\boldsymbol{\eta})\\ \in\mathbb{H}_{\mathrm{N}}(\mathbf{div};\Omega)\times\mathbf{L}^2(\Omega)\times\mathbb{L}^2_{\mathrm{skew}}(\Omega)}} \frac{a(\mathsf{e}_{\boldsymbol{\sigma}},\boldsymbol{\tau})+b(\boldsymbol{\tau},(\mathsf{e}_{\boldsymbol{u}},\mathsf{e}_{\boldsymbol{\rho}}))+b(\mathsf{e}_{\boldsymbol{\sigma}},(\mathbf{v},\boldsymbol{\eta}))}{\|\boldsymbol{\tau}\|_{\mathbf{div};\Omega}+\|\mathbf{v}\|_{0,\Omega}+\|\boldsymbol{\eta}\|_{0,\Omega}}$$

$$\leq C_1 \left(\sup_{\mathbf{0}\neq\boldsymbol{\tau}\in\mathbb{H}_{\mathrm{N}}(\mathbf{div};\Omega)} \frac{\mathscr{R}_1(\boldsymbol{\tau})}{\|\boldsymbol{\tau}\|_{\mathbf{div};\Omega}} + \sup_{\mathbf{0}\neq(\mathbf{v},\boldsymbol{\eta})\in\mathbf{L}^2(\Omega)\times\mathbb{L}^2_{\mathrm{skew}}(\Omega)} \frac{b(\mathsf{e}_{\boldsymbol{\sigma}},(\mathbf{v},\boldsymbol{\eta}))}{\|\mathbf{v}\|_{0,\Omega}+\|\boldsymbol{\eta}\|_{0,\Omega}} \right).$$

Then, recalling the definitions of the bilinear form b (cf. (2.1)), using the equation (2.2b), along with the fact that $\int_\Omega \boldsymbol{\sigma}_h : \boldsymbol{\eta} = \frac{1}{2}\int_\Omega(\boldsymbol{\sigma}_h - \boldsymbol{\sigma}_h^{\mathrm{t}}) : \boldsymbol{\eta}$ for $\boldsymbol{\eta} \in \mathbb{L}^2_{\mathrm{skew}}(\Omega)$, the following estimate holds:

$$|b(\mathsf{e}_{\boldsymbol{\sigma}},(\mathbf{v},\boldsymbol{\eta}))| \leq (||\boldsymbol{f}+\mathbf{div}\,\boldsymbol{\sigma}_h||_{0,\Omega}+||\boldsymbol{\sigma}_h-\boldsymbol{\sigma}_h^{\mathrm{t}}||_{0,\Omega})(\|\mathbf{v}\|_{0,\Omega}+\|\boldsymbol{\eta}\|_{0,\Omega}),$$

and this gives the asserted inequality. □

LEMMA 6.2. There exists $C_2 > 0$ such that

$$\|\boldsymbol{\varphi}-\boldsymbol{\varphi}_h\|_{\mathrm{div};\Omega}+\|p-p_h\|_{0,\Omega}$$
$$\leq C_2\left(\|\mathscr{R}_2\|+\left\|g-c_0p_h-\frac{\alpha}{d\lambda+2\mu}\,\mathrm{tr}\boldsymbol{\sigma}_h-\frac{d\alpha^2}{d\lambda+2\mu}p_h+\mathrm{div}\boldsymbol{\varphi}_h\right\|_{0,\Omega}+\gamma\|\boldsymbol{\sigma}-\boldsymbol{\sigma}_h\|_{\mathbf{div};\Omega}\right),$$

where

$$\mathscr{R}_2(\boldsymbol{\psi}) := \widetilde{a}_{\boldsymbol{\sigma},p}(\boldsymbol{\varphi}-\boldsymbol{\varphi}_h,\boldsymbol{\psi})+\widetilde{b}(\boldsymbol{\psi},p-p_h)$$

satisfies $\mathscr{R}_2(\boldsymbol{\psi}_h)=0$ for all $\boldsymbol{\psi}_h \in \mathbf{H}_h^{\boldsymbol{\varphi}}$, and $||\mathscr{R}_2|| = \sup_{\mathbf{0}\neq\boldsymbol{\psi}\in\mathbf{H}_{\mathrm{N}}(\mathrm{div};\Omega)} \frac{\mathscr{R}_2(\boldsymbol{\psi})}{\|\boldsymbol{\psi}\|_{\mathrm{div};\Omega}}$.

Proof. Similarly to Lemma 5.1, using the properties of bilinear forms $\widetilde{a}_{\boldsymbol{\sigma},p}$ and $\widetilde{b}$ (as outlined in equations (3.2b), (2.8b) and (2.9)), along with the insight from (Correa & Gatica, 2022, theorem 3.4), we establish that there exists $C_2 > 0$, depending on κ_1, κ_2, $C_{\widetilde{a}}$, $\widetilde{\gamma}$, $\widetilde{\beta}$ such that

$$\|\mathsf{e}_{\boldsymbol{\varphi}}\|_{\mathrm{div};\Omega}+\|\mathsf{e}_p\|_{0,\Omega} \leq C_2 \sup_{\mathbf{0}\neq(\boldsymbol{\psi},q)\in\mathbf{H}_{\mathrm{N}}(\mathrm{div};\Omega)\times\mathrm{L}^2(\Omega)} \frac{\widetilde{a}_{\boldsymbol{\sigma},p}(\mathsf{e}_{\boldsymbol{\varphi}},\boldsymbol{\psi})+\widetilde{b}(\boldsymbol{\psi},\mathsf{e}_p)+\widetilde{b}(\mathsf{e}_{\boldsymbol{\varphi}},q)-\widetilde{c}(\mathsf{e}_p,q)}{\|\boldsymbol{\psi}\|_{\mathrm{div};\Omega}+\|q\|_{0,\Omega}}$$
$$\leq C_2\left(\sup_{\mathbf{0}\neq\boldsymbol{\psi}\in\mathbf{H}_{\mathrm{N}}(\mathrm{div};\Omega)}\frac{\mathscr{R}_2(\boldsymbol{\psi})}{\|\boldsymbol{\psi}\|_{\mathrm{div};\Omega}}+\sup_{0\neq q\in\mathrm{L}^2(\Omega)}\frac{\widetilde{b}(\mathsf{e}_{\boldsymbol{\varphi}},q)-\widetilde{c}(\mathsf{e}_p,q)}{\|q\|_{0,\Omega}}\right).$$

Hence, recalling the definitions of $\widetilde{b}$, $\widetilde{c}$, adding $\pm\, c\,(\boldsymbol{\sigma}_h,p)$ and using (2.2d) we arrive at

$$|\widetilde{b}(\mathsf{e}_{\boldsymbol{\varphi}},q)-\widetilde{c}(\mathsf{e}_p,q)| \leq \left\|g-c_0p_h-\frac{\alpha}{d\lambda+2\mu}\mathrm{tr}\,\boldsymbol{\sigma}_h-\frac{d\alpha^2}{d\lambda+2\mu}p_h\right.$$
$$\left.+\,\mathrm{div}\boldsymbol{\varphi}_h\right\|_{0,\Omega}\|q\|_{0,\Omega}+\gamma\|\boldsymbol{\sigma}-\boldsymbol{\sigma}_h\|_{\mathbf{div};\Omega}\|q\|_{0,\Omega},$$

and therefore we obtain the desired result. □

Throughout the rest of this section we provide suitable upper bounds for $\mathscr{R}_1$ and $\mathscr{R}_2$. We begin by establishing the corresponding estimates for $\mathscr{R}_1$, which are based on a suitable Helmholtz decomposition of the space $\mathbb{H}_{\mathrm{N}}(\mathbf{div};\Omega)$ (see (Álvarez *et al.*, 2016, lemma 3.9) for details), along with the following two technical results.

LEMMA 6.3. Let us denote $\hat{\boldsymbol{\xi}} := \boldsymbol{\xi} - \boldsymbol{\Pi}_h(\boldsymbol{\xi})$. There exists a positive constant C_3, independent of h, such that for each $\boldsymbol{\xi} \in \mathbb{H}^1(\Omega)$ there holds

$$|\mathscr{R}_1(\hat{\boldsymbol{\xi}})| \leq -c(\hat{\boldsymbol{\xi}}, p - p_h) + C_3 \left(\sum_{K \in \mathscr{T}_h} h_K^2 \left\| \mathscr{C}^{-1}\boldsymbol{\sigma}_h + \frac{\alpha}{d\lambda + 2\mu} p_h \mathbf{I} - \nabla \boldsymbol{u}_h + \boldsymbol{\rho}_h \right\|_{0,K}^2 + \sum_{E \in \mathscr{E}_h(\Gamma_{\mathrm{D}})} h_E \|\boldsymbol{u}_{\mathrm{D}} - \boldsymbol{u}_h\|_{0,E}^2 \right)^{1/2} \|\boldsymbol{\xi}\|_{1,\Omega}.$$

Proof. From the definition of $\mathscr{R}_1$ (cf. (6.3)), adding $\pm\, c\,(\hat{\boldsymbol{\xi}}, p_h)$ and using equation (2.2a), we have

$$\begin{aligned} \mathscr{R}_1(\hat{\boldsymbol{\xi}}) &= H(\hat{\boldsymbol{\xi}}) - c(\hat{\boldsymbol{\xi}}, p) - a(\boldsymbol{\sigma}_h, \hat{\boldsymbol{\xi}}) - b(\hat{\boldsymbol{\xi}}, (\boldsymbol{u}_h, \boldsymbol{\rho}_h)) \\ &= \langle (\hat{\boldsymbol{\xi}})\boldsymbol{n}, \boldsymbol{u}_{\mathrm{D}} \rangle_{\Gamma_{\mathrm{D}}} - \frac{\alpha}{d\lambda + 2\mu} \int_\Omega (p - p_h) \operatorname{tr}(\hat{\boldsymbol{\xi}}) - \frac{\alpha}{d\lambda + 2\mu} \int_\Omega p_h \operatorname{tr}(\hat{\boldsymbol{\xi}}) \\ &\quad - \int_\Omega \mathscr{C}^{-1}\boldsymbol{\sigma}_h : (\hat{\boldsymbol{\xi}}) - \int_\Omega \boldsymbol{\rho}_h : (\hat{\boldsymbol{\xi}}) - \int_\Omega \boldsymbol{u}_h \cdot \mathbf{div}(\hat{\boldsymbol{\xi}}); \end{aligned}$$

then, applying a local integration by parts to the last term above, using the identity $\int_E \boldsymbol{\Pi}_h(\boldsymbol{\tau})\boldsymbol{n} \cdot \boldsymbol{\xi} = \int_E \boldsymbol{\tau}\boldsymbol{n} \cdot \boldsymbol{\xi}$, for all $\boldsymbol{\xi} \in \mathbf{P}_k(E)$, for all edge E of $\mathscr{T}_h$, the fact that $\boldsymbol{u}_{\mathrm{D}} \in \mathbf{L}^2(\Gamma_{\mathrm{D}})$ and the Cauchy–Schwarz inequality, we obtain

$$\begin{aligned} \mathscr{R}_1(\hat{\boldsymbol{\xi}}) &= \sum_{K \in \mathscr{T}_h} \int_K \left(-\mathscr{C}^{-1}\boldsymbol{\sigma}_h - \frac{\alpha}{d\lambda + 2\mu} p_h \mathbf{I} + \nabla \boldsymbol{u}_h - \boldsymbol{\rho}_h \right) : \hat{\boldsymbol{\xi}} \\ &\quad + \sum_{E \in \mathscr{E}_h(\Gamma_{\mathrm{D}})} \langle \hat{\boldsymbol{\xi}}\boldsymbol{n}, \boldsymbol{u}_{\mathrm{D}} - \boldsymbol{u}_h \rangle_E - \frac{\alpha}{d\lambda + 2\mu} \int_\Omega (p - p_h) \operatorname{tr}(\hat{\boldsymbol{\xi}}) \\ &\leq \sum_{K \in \mathscr{T}_h} \left\| \mathscr{C}^{-1}\boldsymbol{\sigma}_h + \frac{\alpha}{d\lambda + 2\mu} p_h \mathbf{I} - \nabla \boldsymbol{u}_h + \boldsymbol{\rho}_h \right\|_{0,K} \|\hat{\boldsymbol{\xi}}\|_{0,K} \\ &\quad + \sum_{E \in \mathscr{E}_h(\Gamma_{\mathrm{D}})} \|\boldsymbol{u}_{\mathrm{D}} - \boldsymbol{u}_h\|_{0,E} \|\hat{\boldsymbol{\xi}}\|_{0,E} - c(\hat{\boldsymbol{\xi}}, p - p_h). \end{aligned}$$

Therefore, using the approximations properties of $\boldsymbol{\Pi}_h$ (see, e.g., (Álvarez *et al.*, 2016, section 3)) and the Cauchy–Schwarz inequality, we obtain the desired result. □

LEMMA 6.4. Let $\boldsymbol{\chi} \in \mathbf{H}^1_{\Gamma_N}(\Omega) := \{\boldsymbol{w} \in \mathbf{H}^1(\Omega) : \boldsymbol{w} = \mathbf{0} \text{ on } \Gamma_N\}$ denote $\hat{\boldsymbol{\chi}} := \boldsymbol{\chi} - \mathbf{I}_h\boldsymbol{\chi}$, and assume that $\boldsymbol{u}_D \in \mathbf{H}^1(\Gamma_D)$. Then, there exists $C_4 > 0$, independent of h, such that

$$
\begin{aligned}
|\mathscr{R}_1(\mathbf{curl}\,(\hat{\boldsymbol{\chi}}))| \leq & -c(\mathbf{curl}\,(\hat{\boldsymbol{\chi}}), p - p_h) \\
& + C_4 \Bigg(\sum_{K \in \mathscr{T}_h} h_K^2 \left\| \underline{\mathbf{curl}} \left(\mathscr{C}^{-1}\boldsymbol{\sigma}_h + \frac{\alpha}{d\lambda + 2\mu} p_h \mathbf{I} + \boldsymbol{\rho}_h \right) \right\|^2_{0,K} \\
& + \sum_{E \in \mathscr{E}_h(\Omega)} h_E \left\| \left[\!\left[\left(\mathscr{C}^{-1}\boldsymbol{\sigma}_h + \frac{\alpha}{d\lambda + 2\mu} p_h \mathbf{I} + \boldsymbol{\rho}_h \right) \boldsymbol{s} \right]\!\right] \right\|^2_{0,E} \\
& + \sum_{E \in \mathscr{E}_h(\Gamma_D)} h_E \left\| \left(C^{-1}\boldsymbol{\sigma}_h + \frac{\alpha}{d\lambda + 2\mu} p_h \mathbf{I} + \boldsymbol{\rho}_h \right) \boldsymbol{s} - \frac{\mathrm{d}\boldsymbol{u}_D}{\mathrm{d}\boldsymbol{s}} \right\|^2_{0,E} \Bigg)^{1/2} \|\boldsymbol{\chi}\|_{1,\Omega}.
\end{aligned}
$$

Proof. Similarly to Lemma 6.3, adding $\pm\, c\,(\mathbf{curl}\,(\hat{\boldsymbol{\chi}}), p_h)$, we have

$$
\begin{aligned}
\mathscr{R}_1(\mathbf{curl}\,(\hat{\boldsymbol{\chi}})) &= H(\mathbf{curl}\,(\hat{\boldsymbol{\chi}})) - c(\mathbf{curl}\,(\hat{\boldsymbol{\chi}}), p) - a(\boldsymbol{\sigma}_h, \mathbf{curl}\,(\hat{\boldsymbol{\chi}})) - b(\mathbf{curl}\,(\hat{\boldsymbol{\chi}}), (\boldsymbol{u}_h, \boldsymbol{\rho}_h)) \\
&= \langle (\mathbf{curl}\,(\hat{\boldsymbol{\chi}}))\boldsymbol{n}, \boldsymbol{u}_D \rangle_{\Gamma_D} - \frac{\alpha}{d\lambda + 2\mu} \int_\Omega (p - p_h)\, \mathrm{tr}(\mathbf{curl}\,(\hat{\boldsymbol{\chi}})) \\
&\quad - \int_\Omega \mathscr{C}^{-1}\boldsymbol{\sigma}_h : \mathbf{curl}\,(\hat{\boldsymbol{\chi}}) - \int_\Omega \boldsymbol{\rho}_h : \mathbf{curl}\,(\hat{\boldsymbol{\chi}}) - \frac{\alpha}{d\lambda + 2\mu} \int_\Omega p_h\, \mathrm{tr}(\mathbf{curl}\,(\hat{\boldsymbol{\chi}})).
\end{aligned}
$$

Then, applying a local integration by parts, using that $\boldsymbol{u}_D \in \mathbf{H}^1(\Gamma_D)$, the identity $\langle \mathbf{curl}\,(\hat{\boldsymbol{\chi}})\boldsymbol{n}, \boldsymbol{u}_D \rangle_{\Gamma_D} = -\langle \hat{\boldsymbol{\chi}}, \frac{\mathrm{d}\boldsymbol{u}_D}{\mathrm{d}\boldsymbol{s}} \rangle_{\Gamma_D}$ and the Cauchy–Schwarz inequality, we obtain

$$
\begin{aligned}
\mathscr{R}_1(\mathbf{curl}\,(\hat{\boldsymbol{\chi}})) = & - \sum_{K \in \mathscr{T}_h} \int_K \underline{\mathbf{curl}} \left(\mathscr{C}^{-1}\boldsymbol{\sigma}_h + \frac{\alpha}{d\lambda + 2\mu} p_h \mathbf{I} + \boldsymbol{\rho}_h \right) : \hat{\boldsymbol{\chi}} \\
& + \sum_{E \in \mathscr{E}_h(\Omega)} \int_E \left[\!\left[\left(\mathscr{C}^{-1}\boldsymbol{\sigma}_h + \frac{\alpha}{d\lambda + 2\mu} p_h \mathbf{I} + \boldsymbol{\rho}_h \right) \boldsymbol{s} \right]\!\right] \cdot \hat{\boldsymbol{\chi}} - \frac{\alpha}{d\lambda + 2\mu} \int_\Omega (p - p_h)\, \mathrm{tr}(\mathbf{curl}\,(\hat{\boldsymbol{\chi}})) \\
& + \sum_{E \in \mathscr{E}_h(\Gamma_D)} \int_E \left(\mathscr{C}^{-1}\boldsymbol{\sigma}_h + \frac{\alpha}{d\lambda + 2\mu} p_h \mathbf{I} + \boldsymbol{\rho}_h - \nabla \boldsymbol{u}_D \right) \boldsymbol{s} \cdot \hat{\boldsymbol{\chi}} \\
\leq & \sum_{K \in \mathscr{T}_h} \left\| \underline{\mathbf{curl}} \left(\mathscr{C}^{-1}\boldsymbol{\sigma}_h + \frac{\alpha}{d\lambda + 2\mu} p_h \mathbf{I} + \boldsymbol{\rho}_h \right) \right\|_{0,K} \|\hat{\boldsymbol{\chi}}\|_{0,K} - c(\mathbf{curl}\,(\hat{\boldsymbol{\chi}}), p - p_h) \\
& + \sum_{E \in \mathscr{E}_h(\Omega)} \left\| \left[\!\left[\left(\mathscr{C}^{-1}\boldsymbol{\sigma}_h + \frac{\alpha}{d\lambda + 2\mu} p_h \mathbf{I} + \boldsymbol{\rho}_h \right) \boldsymbol{s} \right]\!\right] \right\|_{0,E} \|\hat{\boldsymbol{\chi}}\|_{0,E} \\
& + \sum_{E \in \mathscr{E}_h(\Gamma_D)} \left\| \left(\mathscr{C}^{-1}\boldsymbol{\sigma}_h + \frac{\alpha}{d\lambda + 2\mu} p_h \mathbf{I} + \boldsymbol{\rho}_h \right) \boldsymbol{s} - \frac{\mathrm{d}\boldsymbol{u}_D}{\mathrm{d}\boldsymbol{s}} \right\|_{0,E} \|\hat{\boldsymbol{\chi}}\|_{0,E}.
\end{aligned}
$$

As in the previous result, the approximation properties of the Clément interpolation (see, e.g., (Álvarez *et al.*, 2016, section 3)) in conjunction with the Cauchy–Schwarz inequality produces the desired result. □

The following lemma establishes the desired estimate for $\mathscr{R}_1$.

LEMMA 6.5. Assume that there exists a convex domain B such that $\Omega \subseteq B$ and $\Gamma_{\mathrm{N}} \subseteq \partial B$, and that $\boldsymbol{u}_{\mathrm{D}} \in \mathbf{H}^1(\Gamma_{\mathrm{D}})$. Then, there exists a constant $C_5 > 0$, independent of h, such that

$$\|\boldsymbol{\sigma} - \boldsymbol{\sigma}_h\|_{\mathbf{div};\Omega} + \|\boldsymbol{u} - \boldsymbol{u}_h\|_{0,\Omega} + \|\boldsymbol{\rho} - \boldsymbol{\rho}_h\|_{0,\Omega} \leq C_5 \left\{ \sum_{T \in \mathscr{T}_h} \Xi_{s,K}^2 \right\}^{1/2} + \gamma \|p - p_h\|_{0,\Omega}.$$

Proof. Let $\boldsymbol{\tau} \in \mathbb{H}_{\mathrm{N}}(\mathbf{div};\Omega)$. From (Álvarez *et al.*, 2016, lemma 3.9) there exist $\boldsymbol{\xi} \in \mathbb{H}^1(\Omega)$ and $\boldsymbol{\chi} \in \mathbf{H}^1_{\Gamma_{\mathrm{N}}}(\Omega)$, such that

$$\boldsymbol{\tau} = \boldsymbol{\xi} + \mathbf{curl}\, \boldsymbol{\chi} \quad \text{and} \quad \|\boldsymbol{\xi}\|_{1,\Omega} + \|\boldsymbol{\chi}\|_{1,\Omega} \leq C_{\mathrm{Helm}} \|\boldsymbol{\tau}\|_{\mathbf{div};\Omega}. \tag{6.4}$$

Using that $\mathscr{R}_1(\boldsymbol{\tau}_h) = -c(\boldsymbol{\tau}_h, p - p_h)$ for all $\boldsymbol{\tau}_h \in \mathbb{H}_h^{\boldsymbol{\sigma}}$, we have

$$\mathscr{R}_1(\boldsymbol{\tau}) = \mathscr{R}_1(\boldsymbol{\tau} - \boldsymbol{\tau}_h) - c(\boldsymbol{\tau}_h, p - p_h) \quad \forall\, \boldsymbol{\tau}_h \in \mathbb{H}_h^{\boldsymbol{\sigma}}.$$

In particular, this holds for $\boldsymbol{\tau}_h$ defined as $\boldsymbol{\tau}_h = \boldsymbol{\Pi}_h \boldsymbol{\xi} + \mathbf{curl}\,(\mathbf{I}_h \boldsymbol{\chi})$, whence

$$\mathscr{R}_1(\boldsymbol{\tau}) = \mathscr{R}_1(\boldsymbol{\xi} - \boldsymbol{\Pi}_h \boldsymbol{\xi}) + \mathscr{R}_1(\mathrm{curl}\,(\boldsymbol{\chi} - \mathbf{I}_h \boldsymbol{\chi})) - c(\boldsymbol{\tau}_h, p - p_h).$$

Hence, the proof follows from Lemmas 6.1, 6.3 and 6.4, and estimate (6.4). □

The following lemma establishes the estimate for $\mathscr{R}_2$.

LEMMA 6.6. Assume that there exists a convex domain B such that $\Omega \subseteq B$ and $\Gamma_{\mathrm{N}} \subseteq \partial B$, and that $p_{\mathrm{D}} \in \mathrm{H}^1(\Gamma_{\mathrm{D}})$. Then, there exists a constant $C_8 > 0$, independent of h, such that

$$\|\boldsymbol{\varphi} - \boldsymbol{\varphi}_h\|_{\mathrm{div};\Omega} + \|p - p_h\|_{0,\Omega} \leq C_8 \left\{ \sum_{T \in \mathscr{T}_h} \Xi_{f,K}^2 \right\}^{1/2} + C_8 \left(\|\boldsymbol{\varphi}_h\|_{0,\Omega} \|p - p_h\|_{0,\Omega} + \gamma \|\boldsymbol{\sigma} - \boldsymbol{\sigma}_h\|_{0,\Omega} \right).$$

Proof. It follows the steps of Lemma 6.5. From (Caucao *et al.*, 2022, lemma 4.4), we have that for all $\boldsymbol{\psi} \in \mathbf{H}_{\mathrm{N}}(\mathrm{div};\Omega)$ there exist $\boldsymbol{z} \in \mathbf{H}^1(\Omega)$ and $\phi \in \mathrm{H}^1_{\Gamma_{\mathrm{N}}}(\Omega)$, such that $\boldsymbol{\psi} = \boldsymbol{z} + \mathrm{curl}\,\phi$ and $\|\boldsymbol{z}\|_{1,\Omega} + \|\phi\|_{1,\Omega} \leq \widetilde{C}_{\mathrm{Helm}} \|\boldsymbol{\psi}\|_{\mathbf{div};\Omega}$. Thus, proceeding similarly to Lemmas 6.3 and 6.4, denoting $\hat{\boldsymbol{z}} := \boldsymbol{z} - \boldsymbol{\Pi}_h(\boldsymbol{z})$ and $\hat{\phi} := \phi - I_h \phi$, applying local integration by parts and the approximation properties of $\boldsymbol{\Pi}_h$ and I_h along with the Cauchy–Schwarz inequality, and the second estimate in (2.2), we obtain the following

estimates:

$$
\begin{aligned}
|\mathscr{R}_2(\boldsymbol{z}-\Pi_h(\boldsymbol{z}))| \;&\leq \kappa_2 \|p-p_h\|_{0,\Omega}\,\|\boldsymbol{\varphi}_h\|_{0,\Omega}\,\|\hat{\boldsymbol{z}}\|_{1,\Omega}\\
&+C_6\Big(\textstyle\sum_{K\in\mathscr{T}_h} h_K^2\|\boldsymbol{\kappa}(\boldsymbol{\sigma}_h,p_h)^{-1}\boldsymbol{\varphi}_h-\nabla p_h\|_{0,K}^2+\sum_{E\in\mathscr{E}_h(\Gamma_{\mathrm{D}})} h_E\|p_{\mathrm{D}}-p_h\|_{0,E}^2\Big)^{1/2}\|\boldsymbol{z}\|_{1,\Omega},\\
|\mathscr{R}_2(\mathrm{curl}\,(\phi-I_h\phi))| &\leq \kappa_2\|\boldsymbol{\varphi}_h\|_{0,\Omega}\|p-p_h\|_{0,\Omega}\|\hat{\phi}\|_{1,\Omega}\\
&+C_7\Big(\textstyle\sum_{K\in\mathscr{T}_h} h_K^2\|\mathrm{rot}\,(\boldsymbol{\kappa}(\boldsymbol{\sigma}_h,p_h)^{-1}\boldsymbol{\varphi}_h)\|_{0,K}^2+\sum_{E\in\mathscr{E}_h(\Omega)} h_E\|[\![(\boldsymbol{\kappa}(\boldsymbol{\sigma}_h,p_h)^{-1}\boldsymbol{\varphi}_h)\cdot\boldsymbol{s}]\!]\|_{0,E}^2\\
&+\textstyle\sum_{E\in\mathscr{E}_h(\Gamma_{\mathrm{D}})} h_E\|\boldsymbol{\kappa}(\boldsymbol{\sigma}_h,p_h)^{-1}\boldsymbol{\varphi}_h\cdot\boldsymbol{s}-\frac{\mathrm{d}p_{\mathrm{D}}}{\mathrm{d}\boldsymbol{s}}\|_{0,E}^2\Big)^{1/2}\|\phi\|_{1,\Omega}.
\end{aligned}
\tag{6.5}
$$

Then, noting that $\mathscr{R}_2(\boldsymbol{\psi}_h)=0$ for all $\boldsymbol{\psi}_h\in\mathbf{H}_h^{\boldsymbol{\varphi}}$, and defining $\boldsymbol{\psi}_h$ as $\boldsymbol{\psi}_h=\Pi_h\boldsymbol{z}+\mathrm{curl}\,(I_h\phi)$, we have

$$
\mathscr{R}_2(\boldsymbol{\psi})=\mathscr{R}_2(\boldsymbol{\psi}-\boldsymbol{\psi}_h)=\mathscr{R}_2(\boldsymbol{z}-\Pi_h\boldsymbol{z})+\mathscr{R}_2(\mathrm{curl}\,(\phi-I_h\phi)).
$$

Hence, the proof follows from Lemma 6.2, estimates (6.5), and the Helmholtz decomposition of $\mathbf{H}_{\mathrm{N}}(\mathrm{div};\Omega)$, with C_8, depending on C_2, κ_2, $\widetilde{C}_{\mathrm{Helm}}$ and the stability constants of Π_h and I_h. □

Finally, we state the main reliability bound for the proposed estimator.

THEOREM 6.7. Assume the hypotheses stated in Theorem 5.3 and Lemmas 6.5–6.6. Let $(\boldsymbol{\sigma},\boldsymbol{u},\boldsymbol{\rho},\boldsymbol{\varphi},p)\in\mathbb{H}_{\mathrm{N}}(\mathbf{div};\Omega)\times\mathbf{L}^2(\Omega)\times\mathbb{L}^2_{\mathrm{skew}}(\Omega)\times\mathbf{H}_{\mathrm{N}}(\mathrm{div};\Omega)\times\mathrm{L}^2(\Omega)$ and $(\boldsymbol{\sigma}_h,\boldsymbol{u}_h,\boldsymbol{\rho}_h,\boldsymbol{\varphi}_h,p_h)\in\mathbb{H}_h^{\boldsymbol{\sigma}}\times\mathbf{H}_h^{\boldsymbol{u}}\times\mathbb{H}_h^{\boldsymbol{\rho}}\times\mathbf{H}_h^{\boldsymbol{\varphi}}\times\mathrm{H}_h^{p}$ be the unique solutions of (2.2) and (4.5), respectively. Assume further that

$$
(1+C_8)\gamma+C_8C^*(\|g\|_{0,\Omega}+\|p_{\mathrm{D}}\|_{1/2,\Gamma_{\mathrm{D}}}+\|\boldsymbol{u}_{\mathrm{D}}\|_{1/2,\Gamma_{\mathrm{D}}}+\|\boldsymbol{f}\|_{0,\Omega}+\gamma\,r)\leq\frac{1}{2}.
\tag{6.6}
$$

Then, there exists $C_{\mathrm{rel}}>0$, independent of h, such that

$$
\|\mathrm{e}_{\boldsymbol{\sigma}}\|_{\mathbf{div};\Omega}+\|\mathrm{e}_{\boldsymbol{u}}\|_{0,\Omega}+\|\mathrm{e}_{\boldsymbol{\rho}}\|_{0,\Omega}+\|\mathrm{e}_{\boldsymbol{\varphi}}\|_{\mathrm{div};\Omega}+\|\mathrm{e}_p\|_{0,\Omega}\leq C_{\mathrm{rel}}\,\Xi.
$$

Proof. It follows directly from Lemmas 6.5 and 6.6, using the fact that $\boldsymbol{\varphi}_h$ satisfies the estimate (4.12), and the assumption (6.6). □

Note that, using the same arguments as in Remark 3.3, the constant C_2 appearing in Lemma 6.2 also remains bounded. Consequently, the constant C_8, which depends on C_2, κ_2, $\widetilde{C}_{\mathrm{Helm}}$ and the stability constants of Π_h and I_h, also remains bounded. Therefore, for the first term on the left-hand side of assumption (6.6), $(1+C_8)\gamma$, the condition $(1+C_8)\gamma\leq 1/2$ is required. Since C_8 remains bounded, by using the same arguments as in Remark 3.5, we can ensure the feasibility of assumption (6.6).

6.2 *Efficiency of the a* posteriori *error estimator*

In this section we derive the efficiency estimate of the estimator defined in (6.2). The main result of this section is stated as follows.

THEOREM 6.8. There exists $C_{\rm eff} > 0$, independent of h, such that

$$C_{\rm eff}\,\Xi \;\leq\; \|\boldsymbol{\sigma}-\boldsymbol{\sigma}_h\|_{\mathbf{div};\Omega} + \|\boldsymbol{u}-\boldsymbol{u}_h\|_{0,\Omega} + \|\boldsymbol{\rho}-\boldsymbol{\rho}_h\|_{0,\Omega} + \|\boldsymbol{\varphi}-\boldsymbol{\varphi}_h\|_{\mathrm{div};\Omega} + \|p-p_h\|_{0,\Omega} + \text{h.o.t.}, \tag{6.7}$$

where h.o.t. stands for one or several terms of higher order.

We begin with the estimates for the zero-order terms appearing in the definition of $\Xi_{s,K}$ (cf. (6.1a)).

LEMMA 6.9. For all $K \in \mathscr{T}_h$ there holds

$$\|\boldsymbol{f}+\mathbf{div}\boldsymbol{\sigma}_h\|_{0,K} \lesssim \|\boldsymbol{\sigma}-\boldsymbol{\sigma}_h\|_{\mathbf{div};K} \quad \text{and} \quad \|\boldsymbol{\sigma}_h-\boldsymbol{\sigma}_h^{\mathrm{t}}\|_{0,K} \lesssim \|\boldsymbol{\sigma}-\boldsymbol{\sigma}_h\|_{\mathbf{div};K}.$$

Proof. By employing the same arguments as in (Camaño *et al.*, 2022, theorem 3.2) we can conclude that $\boldsymbol{f} = -\mathbf{div}\,\boldsymbol{\sigma}$, which, together with the symmetry of $\boldsymbol{\sigma}$, implies the desired result. Further details are omitted. □

In order to derive the upper bounds for the remaining terms defining the error estimator $\Xi_{s,K}$, we use results from Carstensen & Dolzmann (1998), inverse inequalities and the localization technique based on element-bubble and edge-bubble functions. The main properties that we will use can be found in (Gatica *et al.*, 2022, lemmas 4.4–4.7).

LEMMA 6.10. For all $K \in \mathscr{T}_h$ there holds

$$\begin{aligned} h_K \left\| \mathscr{C}^{-1}\boldsymbol{\sigma}_h + \frac{\alpha}{d\lambda+2\mu} p_h \mathbf{I} - \nabla \boldsymbol{u}_h + \boldsymbol{\rho}_h \right\|_{0,K} \\ \lesssim h_K \left(\|\boldsymbol{\sigma}-\boldsymbol{\sigma}_h\|_{\mathbf{div};K} + \|\boldsymbol{\rho}-\boldsymbol{\rho}_h\|_{0,K} + \|p-p_h\|_{0,K} \right) + \|\boldsymbol{u}-\boldsymbol{u}_h\|_{0,K}. \end{aligned}$$

Proof. It follows from an application of (Gatica *et al.*, 2022, lemma 4.4) with $\boldsymbol{q} = \mathscr{C}^{-1}\boldsymbol{\sigma}_h + \frac{\alpha}{d\lambda+2\mu} p_h \mathbf{I} - \nabla \boldsymbol{u}_h + \boldsymbol{\rho}_h$, using that $\mathscr{C}^{-1}\boldsymbol{\sigma} + \frac{\alpha}{d\lambda+2\mu} p\mathbf{I} = \nabla \boldsymbol{u} - \boldsymbol{\rho}$ and (Gatica *et al.*, 2022, lemma 4.5). We refer to (Carstensen & Dolzmann, 1998, lemma 6.6) for further details. □

LEMMA 6.11. For all $K \in \mathscr{T}_h$ and $E \in \mathscr{E}_h(\Omega)$ there holds

$$\begin{aligned} h_K \left\| \underline{\mathbf{curl}} \left(\mathscr{C}^{-1}\boldsymbol{\sigma}_h + \frac{\alpha}{d\lambda+2\mu} p_h \mathbf{I} + \boldsymbol{\rho}_h \right) \right\|_{0,K} &\lesssim \|\boldsymbol{\sigma}-\boldsymbol{\sigma}_h\|_{\mathbf{div};K} + \|\boldsymbol{\rho}-\boldsymbol{\rho}_h\|_{0,K} + \|p-p_h\|_{0,K}, \\ h_E^{1/2} \left\| \left[\!\left[\left(\mathscr{C}^{-1}\boldsymbol{\sigma}_h + \frac{\alpha}{d\lambda+2\mu} p_h \mathbf{I} + \boldsymbol{\rho}_h \right) \boldsymbol{s} \right]\!\right] \right\|_{0,E} &\lesssim \|\boldsymbol{\sigma}-\boldsymbol{\sigma}_h\|_{\mathbf{div};\omega_E} + \|\boldsymbol{\rho}-\boldsymbol{\rho}_h\|_{0,\omega_E} + \|p-p_h\|_{0,\omega_E}, \end{aligned}$$

where the patch of elements sharing the edge E is denoted as $\omega_E := \cup\{K' \in \mathscr{T}_h : E \in \mathscr{E}_h(K')\}$.

Proof. It suffices to apply (Gatica *et al.*, 2022, lemma 4.7) with $\boldsymbol{\xi} := \mathscr{C}^{-1}\boldsymbol{\sigma} + \frac{\alpha}{d\lambda+2\mu} p\mathbf{I} + \boldsymbol{\rho} = \nabla \boldsymbol{u}$ and $\boldsymbol{\xi}_h := \mathscr{C}^{-1}\boldsymbol{\sigma}_h + \frac{\alpha}{d\lambda+2\mu} p_h \mathbf{I} + \boldsymbol{\rho}_h$. □

LEMMA 6.12. Assume that $\boldsymbol{u}_{\mathrm{D}}$ is piecewise polynomial. Then, for all $E \in \mathscr{E}_h(\Gamma_{\mathrm{D}})$, there holds

$$h_E^{1/2} \left\| \left(\mathscr{C}^{-1}\boldsymbol{\sigma}_h + \frac{\alpha}{d\lambda + 2\mu} p_h \mathbf{I} + \boldsymbol{\rho}_h \right) \boldsymbol{s} - \tfrac{\mathrm{d}\boldsymbol{u}_{\mathrm{D}}}{\mathrm{d}s} \right\|_{0,E} \lesssim \|\boldsymbol{\sigma} - \boldsymbol{\sigma}_h\|_{\mathbf{div};K_E} + \|\boldsymbol{\rho} - \boldsymbol{\rho}_h\|_{0,K_E} + \|p - p_h\|_{0,K_E},$$

$$h_E^{1/2} \|\boldsymbol{u}_{\mathrm{D}} - \boldsymbol{u}_h\|_{0,E} \lesssim h_{K_E} \left(\|\boldsymbol{\sigma} - \boldsymbol{\sigma}_h\|_{\mathbf{div};K_E} + \|\boldsymbol{\rho} - \boldsymbol{\rho}_h\|_{0,K_E} + \|p - p_h\|_{0,K_E} \right) + \|\boldsymbol{u} - \boldsymbol{u}_h\|_{0,K_E},$$

where K_E is a triangle in $\mathscr{T}_h$ that contains E on its boundary.

Proof. The first estimate follows as in (Gatica *et al.*, 2022, lemma 4.18), defining $\boldsymbol{\xi}$ and $\boldsymbol{\xi}_h$ as in Lemma 6.11. On the other hand, the second estimate follows from an application of the discrete trace inequality (see (Gatica *et al.*, 2022, lemma 4.6)), using that $\mathscr{C}^{-1}\boldsymbol{\sigma} + \dfrac{\alpha}{d\lambda + 2\mu} p\mathbf{I} = \nabla \boldsymbol{u} - \boldsymbol{\rho}$, and the fact that $\boldsymbol{u} = \boldsymbol{u}_{\mathrm{D}}$ on Γ_{D}. See also (Gatica *et al.*, 2010, lemma 4.14). □

A direct application of Lemmas 6.9–6.12 yields

$$\sum_{K \in \mathscr{T}_h} \Xi_{s,K} \lesssim \|\mathsf{e}_{\boldsymbol{\sigma}}\|_{\mathbf{div};\Omega} + \|\mathsf{e}_{\boldsymbol{u}}\|_{0,\Omega} + \|\mathsf{e}_{\boldsymbol{\rho}}\|_{0,\Omega} + \|\mathsf{e}_{\boldsymbol{\varphi}}\|_{\mathrm{div};\Omega} + \|\mathsf{e}_p\|_{0,\Omega}. \tag{6.8}$$

Similarly, using the same arguments as in Lemmas 6.9–6.12, along with algebraic manipulations as in Section 5, assuming that p_{D} is piecewise polynomial, together with the Lipschitz continuity of $\boldsymbol{\kappa}$ (cf. (2.3)), we can bound each of the terms that appear in the estimator $\Xi_{f,K}$ and obtain the following result:

$$\sum_{K \in \mathscr{T}_h} \Xi_{f,K} \lesssim \|\mathsf{e}_{\boldsymbol{\sigma}}\|_{\mathbf{div};\Omega} + \|\mathsf{e}_{\boldsymbol{u}}\|_{0,\Omega} + \|\mathsf{e}_{\boldsymbol{\rho}}\|_{0,\Omega} + \|\mathsf{e}_{\boldsymbol{\varphi}}\|_{\mathrm{div};\Omega} + \|\mathsf{e}_p\|_{0,\Omega}. \tag{6.9}$$

We remark that the efficiency of Ξ (cf. (6.2)) in Theorem 6.8 is now a straightforward consequence of estimates (6.8) and (6.9). In turn, we emphasize that the resulting constant, denoted by $C_{\mathrm{eff}} > 0$, is independent of h.

REMARK 6.13. For simplicity, we have assumed that $\boldsymbol{u}_{\mathrm{D}}$ and p_{D} are piecewise polynomial in the derivation of (6.8) and (6.9). However, similar estimates can also be obtained by assuming $\boldsymbol{u}_{\mathrm{D}}$ and p_{D} are sufficiently smooth (taking, for example, $\boldsymbol{u}_{\mathrm{D}} \in \mathbf{H}^1(\Gamma_{\mathrm{D}})$ and $p_{\mathrm{D}} \in \mathrm{H}^1(\Gamma_{\mathrm{D}})$, as in Lemmas 6.5–6.6), and proceeding as in (Caucao *et al.*, 2016, section 6.2). In such cases, higher-order terms, stemming from errors in the polynomial approximations, would appear in (6.8) and (6.9), accounting for the presence of h.o.t., in (6.7).

REMARK 6.14. We conclude this section by noting that the *a posteriori* error estimation analysis developed here can be adapted to the three-dimensional case. In particular, in (Gatica, 2020, theorem 3.2) and (Caucao *et al.*, 2022, lemma 4.4) one can find the suitable Helmholtz decompositions for the spaces $\mathbb{H}_{\mathrm{N}}(\mathbf{div};\Omega)$ and $\mathbf{H}_{\mathrm{N}}(\mathrm{div};\Omega)$, respectively.

7. Numerical results

The computational examples in this section verify the theoretical properties (optimal convergence, equilibrium and mass conservativity and parameter robustness) of the proposed schemes. The implementation

has been carried out using the FE library FEniCS (Alnæs *et al.*, 2015). The nonlinear systems were solved with Newton–Raphson's method with a residual tolerance of 10^{-7}, and the linear systems were solved using the sparse LU factorization of MUMPS (Amestoy *et al.*, 2000).

Nonhomogeneous essential conditions for flux and stress (for given $\varphi_N \in H^{-1/2}(\Gamma_N)$ and $\boldsymbol{\sigma}_N \in \mathbf{H}^{-1/2}(\Gamma_N)$) can be incorporated in the continuous and discrete analysis by using a classical lifting argument (see, for example, (Ern & Guermond, 2004, remark 32.5)). Regarding implementation it suffices to assign tags for the corresponding sub-boundary and define the test space without the corresponding degrees of freedom, and then provide a boundary datum on the trial space. In FEniCS this is simply done by passing the d components of the nonhomogeneous given traction to each of the row spaces of stress (and the given nonhomogeneous flux vector to the flux space) through `DirichletBC`.

7.1 *Optimal convergence to smooth solutions and conservativity in two dimensions*

We first consider a simple planar problem setup with manufactured exact solution. We take the unit square domain $\Omega = (0,1)^2$, the bottom and left segments represent Γ_D and the top and right sides are Γ_N. We choose the body load $\boldsymbol{f}$, mass source g, boundary displacement $\boldsymbol{u}_D$, boundary pressure p_D, as well as (not necessarily homogeneous, but standard arguments can be used to extend the theory to the inhomogeneous case) boundary data $\boldsymbol{\varphi} \cdot \boldsymbol{n} = \varphi_N$ and $\boldsymbol{\sigma n} = \boldsymbol{\sigma}_N$, such that the exact displacement and fluid pressure are

$$\boldsymbol{u}(x,y) = \frac{1}{20}\begin{pmatrix} \cos\left[\frac{3\pi}{2}(x+y)\right] \\ \sin\left[\frac{3\pi}{2}(x-y)\right] \end{pmatrix}, \quad p(x,y) = \sin(\pi x)\sin(\pi y).$$

These exact primary variables are used to construct exact mixed variables of stress, rotation and discharge flux. We choose the second constitutive relation for the permeability in (1.8) and choose the following arbitrary model parameters (all nondimensional) $k_0 = k_1 = c_0 = \alpha = 0.1$, $\lambda = \mu = \mu_f = 1$. These values indicate a mild permeability variation and it is expected that the nonlinear solver (in this case, Newton–Raphson) converges in only a few iterations. We construct six levels of uniform mesh refinement of the domain, on which we compute approximate solutions and the associated errors for each primal and mixed variable in their natural norms. Convergence rates are calculated as usual:

$$\text{rate} = \log(e/\widehat{e})[\log(h/\widehat{h})]^{-1},$$

where e and $\widehat{e}$ denote errors produced on two consecutive meshes of sizes h and $\widehat{h}$, respectively. Table 1 reports on this error history focusing on the methods defined by the PEERS$_k$ family with $k = 0$ and $k = 1$, showing a $O(h^{k+1})$ convergence for all unknowns as expected from the theoretical error bound of Theorem 5.4 (except for the rotation approximation that shows a slight superconvergence for the lowest-order case and only in two dimensions—a well-known phenomenon associated with PEERS$_k$ elements). With the purpose of illustrating the character of the chosen manufactured solution and the parameter regime we show sample discrete solutions in Fig. 1.

We also exemplify the equilibrium and mass conservativity of the formulation. To do so we represent the loss of equilibrium and mass as

$$\texttt{equ}_h := \left\| \mathscr{P}_h[\mathbf{div}(\boldsymbol{\sigma}_h) + \boldsymbol{f}] \right\|_{\ell^\infty}, \ \texttt{mass}_h := \left\| \mathscr{P}_h\left[\left(c_0 + \frac{d\alpha^2}{d\lambda + 2\mu} \right) p_h + \frac{\alpha}{d\lambda + 2\mu} \mathrm{tr}\boldsymbol{\sigma}_h + \mathrm{div}(\boldsymbol{\varphi}_h) + g \right] \right\|_{\ell^\infty},$$

TABLE 1 *Example 1. Error history (degrees of freedom, mesh size, individual errors and experimental rates of convergence) in two dimensions for the formulation using the two lowest-order FE families with $PEERS_k$ elements*

k	DoFs	h	$e(\boldsymbol{\sigma})$	rate	$e(\boldsymbol{u})$	rate	$e(\boldsymbol{\rho})$	rate	$e(\boldsymbol{\varphi})$	rate	$e(p)$	rate
0	98	0.7071	3.5e+0	⋆	4.5e-02	⋆	3.7e-01	⋆	4.9e-01	⋆	2.4e-01	⋆
	354	0.3536	1.9e+0	0.86	2.0e-02	1.20	8.0e-02	2.19	2.6e-01	0.92	1.3e-01	0.92
	1346	0.1768	9.9e-01	0.96	1.0e-02	0.98	3.3e-02	1.30	1.3e-01	0.98	6.5e-02	0.98
	5250	0.0884	5.0e-01	0.99	5.0e-03	1.00	1.3e-02	1.37	6.6e-02	0.99	3.3e-02	1.00
	20738	0.0442	2.5e-01	1.00	2.5e-03	1.00	4.7e-03	1.43	3.3e-02	1.00	1.6e-02	1.00
	82434	0.0221	1.2e-01	1.00	1.3e-03	1.00	1.7e-03	1.47	1.6e-02	1.00	8.2e-03	1.00
1	290	0.7071	1.3e+0	⋆	1.3e-02	⋆	4.1e-02	⋆	1.5e-01	⋆	7.4e-02	⋆
	1090	0.3536	4.1e-01	1.61	4.2e-03	1.68	1.4e-02	1.50	3.9e-02	1.92	2.0e-02	1.93
	4226	0.1768	1.1e-01	1.94	1.1e-03	1.95	5.8e-03	1.30	9.9e-03	1.98	5.0e-03	1.98
	16642	0.0884	2.7e-02	1.98	2.7e-04	1.99	2.0e-03	1.55	2.5e-03	1.99	1.2e-03	2.00
	66050	0.0442	6.8e-03	2.00	6.8e-05	2.00	5.8e-04	1.78	6.2e-04	2.00	3.1e-04	2.00
	263170	0.0221	1.7e-03	2.00	1.7e-05	2.00	1.5e-04	1.92	1.6e-04	2.00	7.8e-05	2.00

where $\mathscr{P}_h : \mathrm{L}^2(\Omega) \to \mathrm{P}_k(\mathscr{T}_h)$ is the scalar version of $\mathscr{P}_h$. They are computed at each refinement level and tabulated in Table 2 together with the total error $\mathtt{e} := e(\boldsymbol{\sigma}) + e(\boldsymbol{u}) + e(\boldsymbol{\rho}) + e(\boldsymbol{\varphi}) + e(p)$, and its experimental convergence rate. We report on the nonlinear iteration count as well. The expected optimal convergence of the total error, and the announced local conservativity are confirmed. We also note that, at least for this parameter regime, for all the refinements and polynomial degrees the nonlinear solver takes three iterations to get a residual below the tolerance. In the last column of the same table we report on the efficiency of the global *a posteriori* error estimator designed in Section 6 $\mathtt{eff}(\Xi) = \frac{\mathtt{e}}{\Xi}$, which—in this case of smooth solutions—is asymptotically constant (approximately 0.98 for $k = 0$ and 1.52 for $k = 1$).

7.2 *Convergence in three dimensions using physically relevant parameters*

Next, we investigate the behaviour of the proposed numerical methods in a three-dimensional setting and taking model parameters more closely related to applications in tissue poroelasticity. We still use manufactured solutions to assess the accuracy of the formulation, but take an exact displacement that satisfies $\mathrm{div}\boldsymbol{u} \to 0$ as $\lambda \to \infty$. The domain is the three-dimensional box $\Omega = (0, L) \times (0, L) \times (0, 2L)$ with $L = 0.01$ m, and mixed boundary conditions were taken analogously as before, separating the domain boundary between Γ_{N} defined by the planes $x = 0$, $y = 0$ and $z = 0$, and Γ_{D} as the remainder of the boundary. The manufactured displacement and pressure head are

$$\boldsymbol{u} = \frac{L}{4}\begin{pmatrix} \sin(x/L)\cos(y/L)\sin(z/(2L)) + x^2/\lambda \\ -2\cos(x/L)\sin(y/L)\cos(z/(2L)) + y^2/\lambda \\ 2\cos(x/L)\cos(y/L)\sin(z/(2L)) - 2z^2/\lambda \end{pmatrix}, \quad p = \sin(x/L)\cos(y/L)\sin(z/(2L)).$$

First, we set again the model parameters to mild values $\lambda = \mu = c_0 = k_0 = \alpha = \mu_f = 1$, $k_1 = k_2 = 0.1$, we use the exponential permeability constitutive law, and we compare them with the

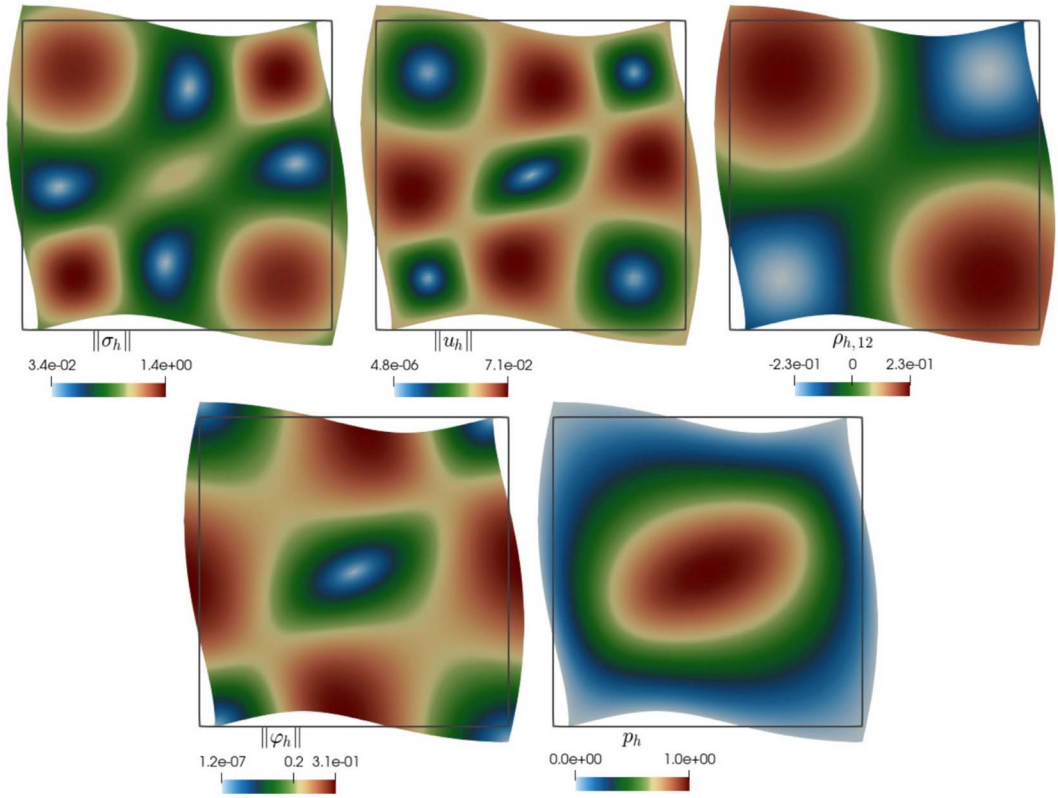

FIG. 1. Example 1. Sample of approximate solutions (stress magnitude, displacement magnitude, nonzero entry of rotation, flux magnitude and fluid pressure) computed with the second-order scheme and plotted on the deformed domain (for reference we also show the contour of the undeformed domain).

following values (from, e.g., Barnafi *et al.* (2022); Ruiz-Baier *et al.* (2022)):

$$k_0 = 2.28 \times 10^{-11}\,\mathrm{m}^3, \quad k_1 = 5 \times 10^{-12}\,\mathrm{m}^3, \quad \lambda = 1.44 \times 10^6\,\mathrm{Pa},$$
$$\mu = 9.18 \times 10^3\,\mathrm{Pa}, \quad \mu_f = 7.5 \times 10^{-4}\,\mathrm{Pa}\cdot\mathrm{s}, \quad c_0 = 0, \quad \alpha = 0.99.$$

Table 3 reports on the convergence of the method. While the magnitude of the stress errors is much higher for the second parameter regime, the discharge flux error magnitude is smaller than in the first case and the displacement, rotation and fluid pressure errors remain roughly of the same magnitude. In any case the table confirms that the optimal slope of the error decay is not affected by a vanishing storativity or large Lamé constants. The components of the numerical solution are displayed in Fig. 2.

We also test the convergence of the mixed FE scheme for a wider parametric space. We select the following ranges: $\lambda \in [1, 10^{12}], \kappa_i \in [10^{-12}, 1], c_0 \in [10^{-12}, 1], \alpha \in [10^{-12}, 1]$. Samples (81 instances) of these computations are collected in Fig. 3 and they provide a robustness analysis in terms of error history (in rate of error decay, and not in absolute errors since we are not using parameter-rescaled

TABLE 2 *Example 1. Total error, experimental rates of convergence, ℓ^∞-norm of the projected residual of the equilibrium and mass balance equations, Newton–Raphson iteration count and efficiency index of the global* a posteriori *error estimator. Tabulated results correspond to the two lowest-order polynomial degrees*

DoFs	h	e	rate	$\mathtt{equ}_h$	$\mathtt{mass}_h$	iter	$\mathtt{eff}(\Xi)$
$k = 0$							
97	0.707	4.83e+0	⋆	9.30e-16	1.94e-16	3	0.93
353	0.354	2.45e+0	0.98	9.44e-16	2.98e-16	3	0.94
1345	0.177	1.25e+0	0.98	2.64e-15	8.26e-16	3	0.96
5249	0.088	6.22e-01	1.00	5.58e-15	2.49e-15	3	0.97
20737	0.044	3.10e-01	1.00	1.46e-14	7.03e-15	3	0.98
82433	0.022	1.55e-01	1.00	1.72e-13	1.09e-13	3	0.98
328705	0.011	7.63e-02	1.00	4.25e-13	3.46e-13	3	0.98
$k = 1$							
289	0.707	1.57e+0	⋆	2.88e-15	1.20e-15	3	1.45
1089	0.354	5.08e-01	1.63	6.77e-15	2.25e-15	3	1.50
4225	0.177	1.34e-01	1.92	2.21e-14	6.60e-15	3	1.53
16641	0.088	3.42e-02	1.97	8.00e-14	1.31e-14	3	1.52
66049	0.044	8.62e-03	1.99	3.91e-13	3.83e-14	3	1.51
263169	0.022	2.16e-03	2.00	8.20e-12	7.61e-14	3	1.51
1050625	0.011	5.04e-04	2.00	2.17e-11	4.90e-13	3	1.52

TABLE 3 *Example 2. Error history (degrees of freedom, mesh size, individual errors and experimental rates of convergence) in three dimensions for the formulation using the lowest-order FE family with PEERS$_k$ elements and changing from unity (top) to physically relevant (bottom) parameters*

DoFs	h	$e(\boldsymbol{\sigma})$	rate	$e(\boldsymbol{u})$	rate	$e(\boldsymbol{\rho})$	rate	$e(\boldsymbol{\varphi})$	rate	$e(p)$	rate
Unity parameters											
328	0.0173	2.9e-02	⋆	1.1e-06	⋆	4.8e-04	⋆	3.1e+0	⋆	1.3e-04	⋆
2311	0.0087	1.5e-02	0.94	5.7e-07	0.96	1.3e-04	1.90	1.6e+0	1.00	6.3e-05	1.00
17443	0.0043	7.5e-03	0.99	2.8e-07	1.00	4.4e-05	1.54	7.8e-01	1.00	3.2e-05	1.00
135715	0.0022	3.8e-03	1.00	1.4e-07	1.00	1.8e-05	1.34	3.9e-01	1.00	1.6e-05	1.00
1071043	0.0011	1.9e-03	1.00	7.0e-08	1.00	7.7e-06	1.19	1.9e-01	1.00	7.9e-06	1.00
Physically relevant parameters											
328	0.0173	2.1e+02	⋆	1.1e-06	⋆	4.2e-04	⋆	4.8e-07	⋆	1.9e-04	⋆
2311	0.0087	1.1e+02	0.91	5.6e-07	0.99	1.1e-04	1.93	3.9e-07	0.55	9.1e-05	1.05
17443	0.0043	5.6e+01	0.98	2.8e-07	1.00	3.3e-05	1.74	2.2e-07	0.89	4.4e-05	1.04
135715	0.0022	2.8e+01	1.00	1.4e-07	1.00	1.2e-05	1.42	1.2e-07	0.93	2.2e-05	0.99
1071043	0.0011	1.4e+01	1.00	7.0e-08	1.00	5.3e-06	1.23	6.0e-08	0.97	1.1e-05	0.98

norms and for each re-parametrization the forcing terms change accordingly) and Newton–Raphson iteration count. In all cases we observe an optimal first-order convergence, and we also see that for some parameters the nonlinear solver takes less iterations to reach the desired tolerance.

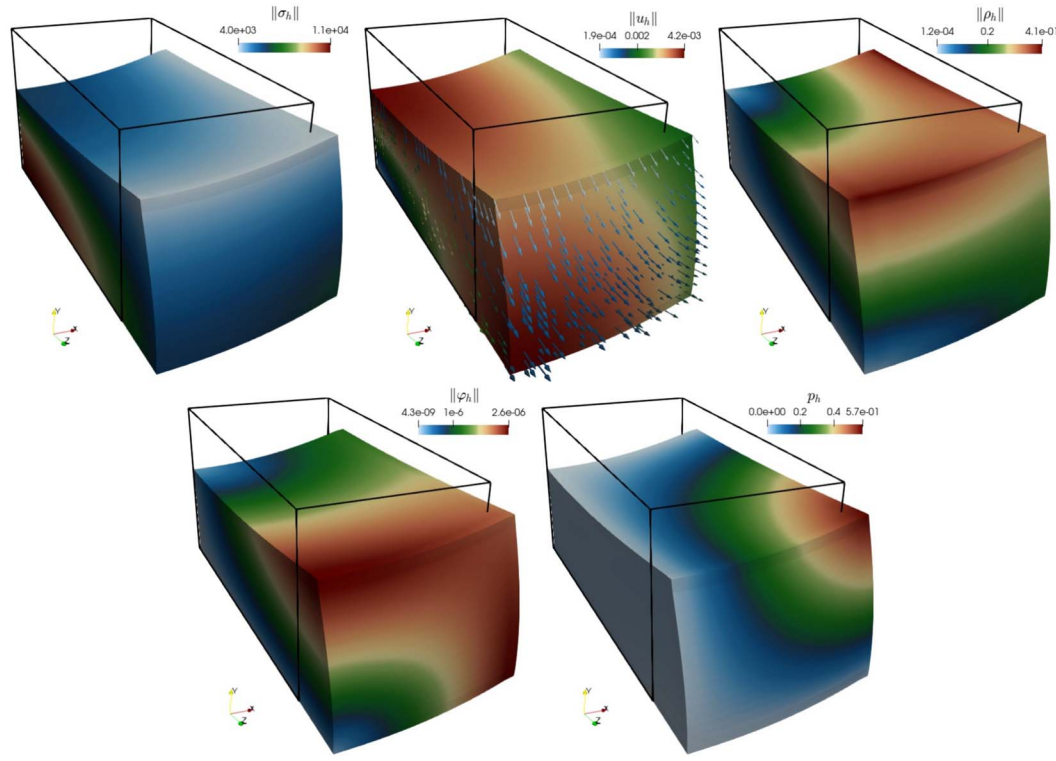

FIG. 2. Example 2. Sample of approximate solutions (stress magnitude, displacement magnitude, rotation magnitude, flux magnitude and fluid pressure) computed with the first-order scheme and plotted on the deformed domain (for reference we also show the outline of the undeformed domain).

7.3 *Convergence in the case of adaptive mesh refinement*

We continue with a test targeting the recovery of optimal convergence through adaptive mesh refinement guided by the *a posteriori* error estimator proposed in Section 6. We employ the well-known adaptive mesh refinement approach of solving, then computing the estimator, marking and refining. Marking is done as follows (Dörfler, 1996): a given $K \in \mathcal{T}_h$ is added to the marking set $\mathcal{M}_h \subset \mathcal{T}_h$ whenever the local error indicator Ξ_K satisfies

$$\sum_{K \in \mathcal{M}_h} \Xi_K^2 \geq \zeta \sum_{K \in \mathcal{T}_h} \Xi_K^2,$$

where ζ is a user-defined bulk density. All elements in $\mathcal{M}_h$ are marked for refinement and also some neighbours are marked for the sake of closure. For convergence rates we use the alternative form

$$\text{rate} = -2\log(e/\widehat{e})[\log(\text{DoFs}/\widehat{\text{DoF}})]^{-1}.$$

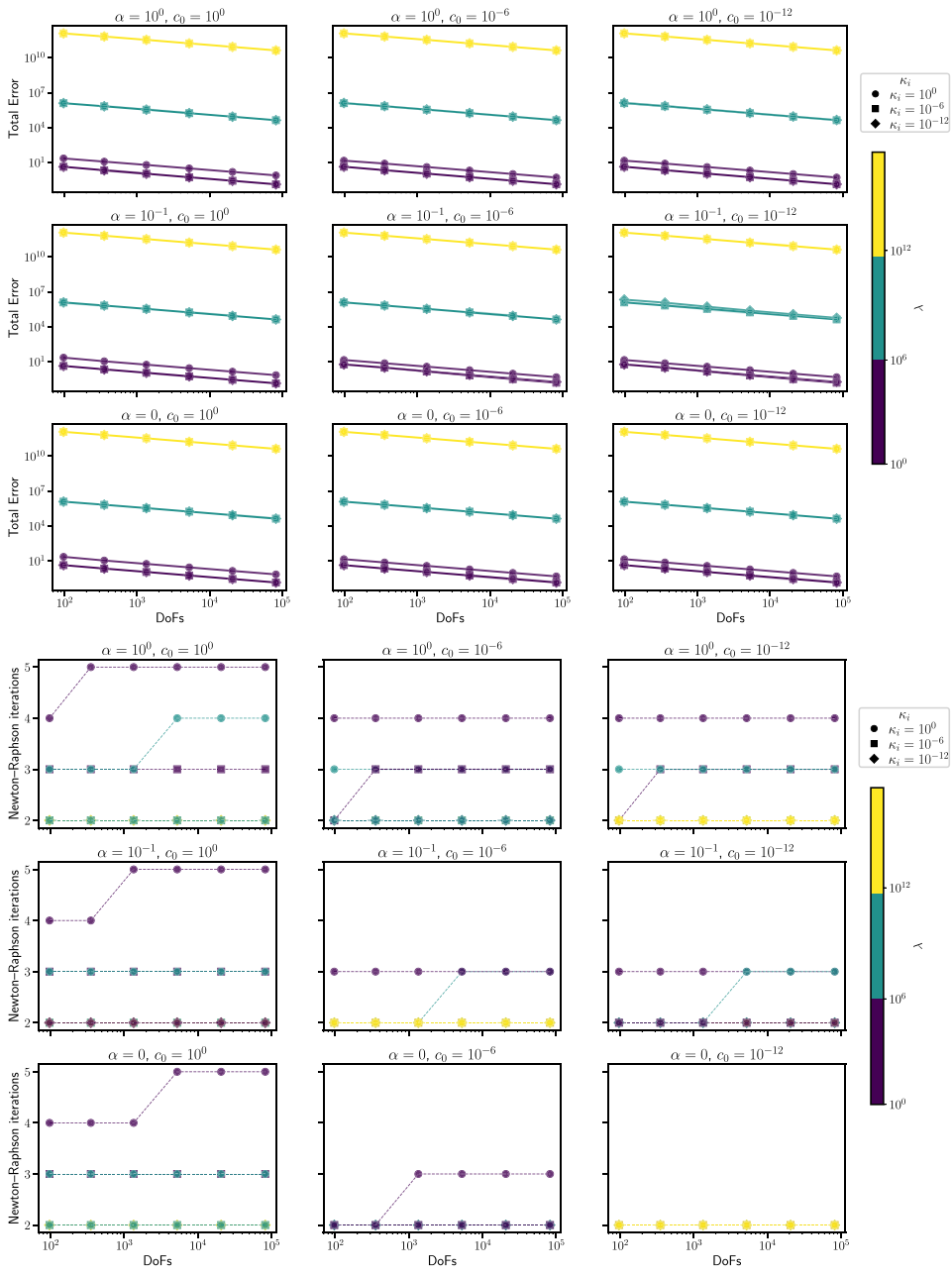

FIG. 3. Example 2. Parameter robustness of the convergence for the mixed FE method in the lowest-order case across 81 parameter configurations. The colour-bar represents the variation in λ and the different line markers the variation in the permeability parameter κ_i (here using $\kappa_0 = \kappa_1 = \kappa_2$ for the exponential permeability function). The top panels indicate total error, and the bottom panels the iteration count.

Let us consider the nonconvex rotated L-shaped domain $\Omega = (-1,1)^2 \setminus (-1,0)^2$ and use manufactured displacement and fluid pressure with sharp gradients near the domain re-entrant corner (see, e.g., Carstensen *et al.* (2000) for the displacement and Bulle *et al.* (2023) for the fluid pressure)

$$\boldsymbol{u}(r,\theta) = \frac{r^{\chi}}{2\mu}\begin{pmatrix} -(\chi+1)\cos([\chi+1]\theta) + (M_2-\chi-1)M_1\cos([\chi-1]\theta) \\ (\chi+1)\sin([\chi+1]\theta) + (M_2+\chi-1)M_1\sin([\chi-1]\theta) \end{pmatrix},$$

$$p(r,\theta) = r^{1/3}\sin\left(\frac{1}{3}\left(\frac{\pi}{2}+\theta\right)\right),$$

with polar coordinates $r = \sqrt{x_1^2+x_2^2}$, $\theta = \arctan(x_2,x_1)$, $\chi \approx 0.54448373$, $M_1 = -\cos([\chi+1]\omega)/\cos([\chi-1]\omega)$ and $M_2 = 2(\lambda+2\mu)/(\mu+\lambda)$. The boundary conditions (taking as Γ_{N} the segments at $x = \pm 1$ and $y = \pm 1$ and Γ_{D} the remainder of the boundary) and forcing data are constructed from these solutions and the model parameters are $\lambda = 10^3$, $\mu = 10$, $k_0 = \frac{1}{2}$, $\mu_f = c_0 = k_1 = 0.1$ and $\alpha = \frac{1}{4}$, where for this test we consider a Kozeny–Carman permeability form. As in Carstensen *et al.* (2000) a sub-optimal rate of convergence is expected for the mixed elasticity sub-problem in its energy norm. Note that, since the exact pressure is in $\mathrm{H}^{4/3-\epsilon}(\Omega)$ for any $\epsilon > 0$ (cf. (Grisvard, 2011, chapter 5)), it is still regular enough to have optimal convergence. However, its gradient (and therefore also the exact discharge flux $\boldsymbol{\varphi}$) has a singularity located at the reentrant corner, and therefore we expect an order of convergence of approximately $O(h^{1/3})$.

The numerical results of this test are reported in Table 4. We observe the expected sub-optimal convergence under a uniform mesh refinement, while the optimal convergence in all variables is attained as the mesh is locally refined (the first three rows are very similar as most of the elements are refined in the first three steps; this can be controlled by the bulk density, here taken as $\zeta = 9.5 \times 10^{-5}$). We also note that the individual errors are approximately of the same magnitude in the last row of each section of the table, but for the adaptive case this is achieved using approximately 5.5% of the number of degrees of freedom needed in the uniformly refined case. The last column of the table again confirms the reliability and efficiency of the *a posteriori* error estimator. Note that for this case we compute the divergence part of the error norm in the stress and fluxes as projections of the equilibrium and mass residuals onto the displacement and pressure discrete spaces, respectively. We plot in Fig. 4 the approximate displacement and pressure, as well as sample triangulations obtained after a few adaptive refinement steps that confirm the expected agglomeration of vertices near the reentrant corner.

7.4 *Adaptive computation of cross-sectional flow and deformation in a soft tissue specimen*

Finally, we apply the proposed methods to simulate the localization of stress, deformation and flow patterns in a multi-layer cross-section of cervical spinal cord. We follow the set-up in Støverud *et al.* (2016) and Meddahi & Ruiz-Baier (2023). The geometry and unstructured mesh have been generated using GMSH (Geuzaine & Remacle, 2009) from the images in Støverud *et al.* (2016). The heterogeneous porous material consists of white and grey matter surrounded by the pia mater (a thin layer, also considered poroelastic; see Fig. 5, top two left panels). All components are assumed fully saturated with cerebrospinal fluid. The transversal cross-section has 1.3 cm in maximal diameter and the indentation region is a curved subset of the anterior part of the pia mater (a sub-boundary of length 0.4 cm). Boundary conditions are of mixed load-traction type, but slightly different than the ones analysed in the previous section. We conduct an indentation test applying a traction $\boldsymbol{\sigma n} = (0,-P)^{\mathrm{t}}$, with P a

TABLE 4 *Example 3. Convergence history (degrees of freedom, mesh size, individual errors, experimental rates of convergence and effectivity index) in a rotated L-shaped domain for the formulation using the lowest-order FE family with PEERS$_k$ elements and changing from uniform (top) to adaptive mesh refinement (bottom) guided by the* a posteriori *error indicator from (6.2)*

DoFs	h	$e(\boldsymbol{\sigma})$	rate	$e(\boldsymbol{u})$	rate	$e(\boldsymbol{\rho})$	rate	$e(\boldsymbol{\varphi})$	rate	$e(p)$	rate	eff (Ξ)
Uniform mesh refinement												
77	1.4142	1.7e+3	⋆	1.7e+1	⋆	7.6e+1	⋆	9.1e+0	⋆	1.6e+0	⋆	2.67
273	0.7071	1.5e+3	0.27	7.8e+0	1.10	2.5e+1	1.61	5.8e+0	0.65	7.8e-01	1.06	2.65
1025	0.3536	1.2e+3	0.31	5.0e+0	0.63	2.1e+1	0.27	4.3e+0	0.44	3.9e-01	1.00	3.12
3969	0.1768	8.9e+2	0.40	3.6e+0	0.50	1.7e+1	0.26	3.3e+0	0.38	2.0e-01	0.99	2.82
15617	0.0884	6.6e+2	0.43	2.6e+0	0.45	1.4e+1	0.32	2.6e+0	0.35	9.9e-02	0.99	2.60
61953	0.0442	4.8e+2	0.45	1.9e+0	0.45	1.1e+1	0.35	2.0e+0	0.34	5.0e-02	1.00	2.42
246785	0.0221	3.5e+2	0.46	1.4e+0	0.46	8.4e+0	0.38	1.6e+0	0.34	2.5e-02	1.00	2.27
985089	0.0011	2.9e+2	0.45	1.1e+0	0.45	6.7e+0	0.38	1.2e+0	0.34	1.3e-02	1.00	2.40
Adaptive mesh refinement												
77	1.4142	1.7e+3	⋆	1.7e+1	⋆	7.6e+1	⋆	9.1e+0	⋆	1.6e+0	⋆	2.67
273	0.7071	1.5e+3	0.29	7.8e+0	1.20	2.5e+1	1.76	5.8e+0	0.72	7.8e-01	1.16	2.65
1025	0.3536	1.2e+3	0.33	5.0e+0	0.66	2.1e+1	0.28	4.3e+0	0.47	3.9e-01	1.04	3.12
3813	0.3536	8.9e+2	0.42	3.6e+0	0.52	1.7e+1	0.27	3.3e+0	0.40	2.0e-01	1.04	2.82
7113	0.2500	6.7e+2	0.89	2.6e+0	0.98	1.4e+1	0.68	2.6e+0	0.77	1.1e-01	1.91	2.55
11013	0.2500	5.2e+2	1.20	2.0e+0	1.31	1.1e+1	0.99	2.0e+0	1.07	6.0e-02	1.74	2.58
17449	0.2500	4.0e+2	1.10	1.5e+0	1.18	9.1e+0	0.95	1.6e+0	1.01	3.7e-02	1.79	2.52
27225	0.1768	3.1e+2	1.14	1.2e+0	1.18	7.2e+0	1.05	1.3e+0	1.05	2.1e-02	1.80	2.52
38081	0.1768	2.5e+2	1.37	9.0e-01	1.53	5.7e+0	1.38	1.0e+0	1.37	1.5e-02	1.57	2.55
54797	0.1250	2.0e+2	1.18	7.2e-01	1.21	4.6e+0	1.22	8.1e-01	1.26	1.2e-02	1.48	2.53

constant solid pressure of 950 dyne/cm^2. The posterior part of the pia mater acts as a rigid posterior support where we prescribe zero displacement. The remainder of the boundary of the pia mater is stress-free. For the fluid phase we impose a constant inflow pressure of cerebrospinal fluid of 1.1 dyne/cm^2 and zero outflow pressure at the stress-free sub-boundary, as well as zero normal discharge flux at the posterior support. For the three different layers of the domain we use the following values for Young modulus, Poisson ratio and lower bound for permeability (some values from Bloomfield *et al.* (1998), Støverud *et al.* (2016) and Meddahi & Ruiz-Baier (2023)) $E^{\text{pia}} = 23000\,\text{dyne/cm}^2$, $\nu^{\text{pia}} = 0.3$, $E^{\text{white}} = 8400\,\text{dyne/cm}^2$, $\nu^{\text{white}} = 0.479$, $E^{\text{grey}} = 16000\,\text{dyne/cm}^2$, $\nu^{\text{grey}} = 0.49$, $k_0^{\text{grey}} = 1.4 \times 10^{-9}\,\text{dyne/cm}^2$, $k_0^{\text{white}} = 1.4 \times 10^{-6}\,\text{dyne/cm}^2$, $k_0^{\text{pia}} = 3.9 \times 10^{-10}\,\text{dyne/cm}^2$. Further, we take $\boldsymbol{f} = \boldsymbol{0}$, $g = 0$, $\mu_f = 70\,\text{dyne/cm}^2 \cdot$ s (for cerebrospinal fluid at 37°), $k_1 = \frac{1}{2}k_0$, $\alpha = \frac{1}{4}$ and $c_0 = 10^{-3}$.

The initial and the final adapted mesh, together with samples of solutions are shown in Fig. 5, where we have used the mesh density parameter $\zeta = 5.5 \times 10^{-4}$. After each adaptation iteration guided by the *a posteriori* error indicator (6.2) a mesh smoothing step was included. The figure indicates that most of the refinement occurs near the interface between the heterogeneous components of the porous media, and the plots also confirm a flow pattern moving slowly from top to bottom, consistently with a typical indentation test.

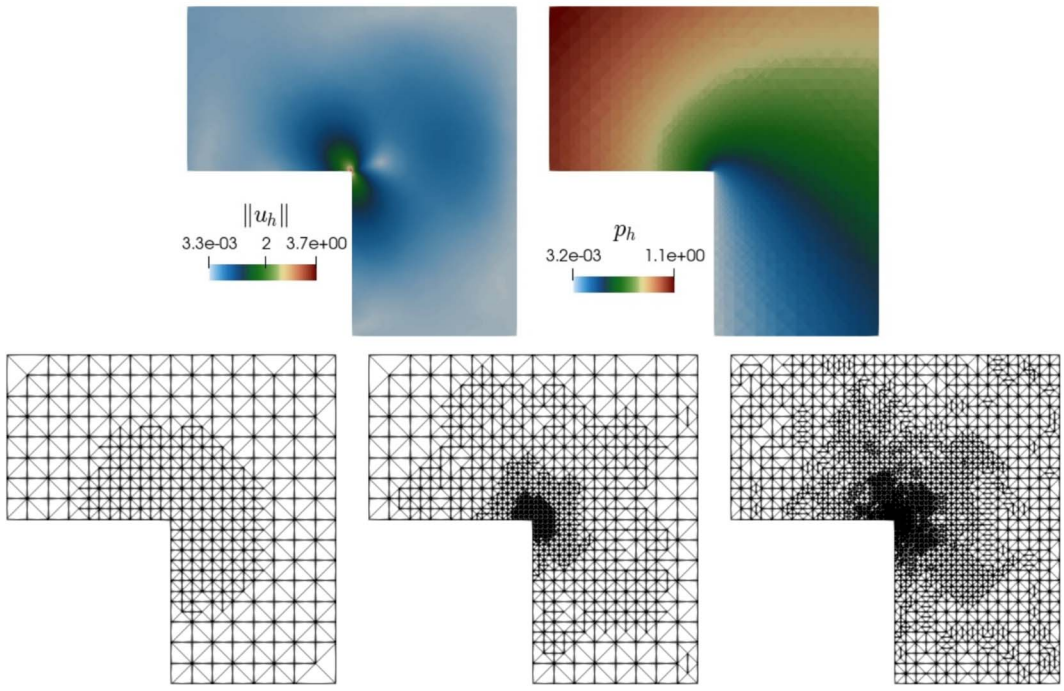

FIG. 4. Example 3. Approximate primal variable solutions (solid displacement and fluid pressure) computed with the first-order scheme, and meshes generated after two, three and four adaptive refinement steps.

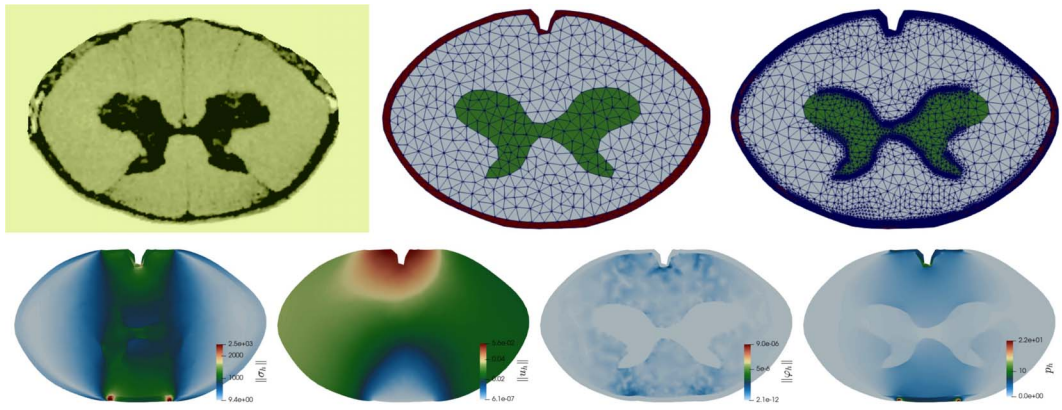

FIG. 5. Example 4. Cross-sectional area of cervical spinal cord segmented from sheep imaging data in Støverud *et al.* (2016), initial coarse mesh indicating subdomains with distinct material properties (outer layer: pia mater; middle layer: white matter; inner layer: grey matter), final adapted mesh after six refinement steps, and sample of stress, displacement, fluid flux and fluid pressure at the indentation test (bottom row figures are obtained with the lowest-order scheme and rendered on the deformed configuration).

8. Concluding remarks

In this work we developed a family of mixed FE methods for a nonlinear poroelasticity model with stress-dependent permeability. By reformulating the constitutive equations we enabled the use of a Hellinger–Reissner-type mixed formulation, ensuring robustness with respect to near-incompressibility and vanishing storativity limits. The problem structure was analysed using fixed-point theory and saddle-point formulations, leading to well-posedness results for both the continuous and discrete settings. The chosen FE spaces (PEERS_k elements for elasticity and Raviart–Thomas elements for fluid flow) provided exact equilibrium and mass conservation.

We derived *a priori* error estimates, demonstrating optimal convergence properties. Furthermore, a residual-based *a posteriori* error estimator was introduced and shown to be both reliable and efficient. This estimator guided adaptive mesh refinement strategies, which were validated through numerical experiments in both two and three dimensions.

The proposed nonlinear dependence of permeability on stress in poroelasticity is particularly relevant for soft tissues, where permeability changes due to deformation, and for subsurface reservoirs, where stress variations influence fluid transport. The current formulation can be adapted to different material systems by choosing appropriate functional forms for the permeability–stress relationship including also anisotropic permeability variations.

We are keen to follow other extensions, for instance, exploring different abstract results that would impose a less restrictive assumption on smallness of data, and extend the formulation to accommodate a nonlinear stress-strain constitutive law, transient effects and splitting algorithms following, e.g. Kraus *et al.* (2024), as well as fully coupled multiphysics systems, such as thermo-poroelasticity. Note, however, that these generalizations (useful to broaden the applicability of the proposed methods to more complex real-world scenarios) will require a substantially different theoretical framework.

Conflicts of interest

The authors declare that they have no conflict of interest.

Funding

Australian Research Council (FT220100496, DP22010316); National Research and Development Agency (ANID) (74220026); SERB/ANRF Core research grant CRG/2021/002569; SERB/ANRF MATRICS grant MTR/2020/00030.

References

Alnæs, M. S., Blechta, J., Hake, J., Johansson, A., Kehlet, B., Logg, A., Richardson, C., Ring, J., Rognes, M. E. & Wells, G. N. (2015) The FEniCS project version 1.5. *Arch. Numer. Softw.*, **3**, 9–23.

Álvarez, M., Gatica, G. N. & Ruiz-Baier, R. (2015) An augmented mixed-primal finite element method for a coupled flow-transport problem. *ESAIM: Math. Model. Numer. Anal.*, **49**, 1399–1427.

Álvarez, M., Gatica, G. N. & Ruiz-Baier, R. (2016) *A posteriori* error analysis for a viscous flow–transport problem. *ESAIM: Math. Model. Numer. Anal.*, **50**, 1789–1816.

Amestoy, P. R., Duff, I. S. & L'Excellent, J.-Y. (2000) Multifrontal parallel distributed symmetric and unsymmetric solvers. *Comput. Methods Appl. Mech. Eng.*, **184**, 501–520.

Arnold, D. N., Brezzi, F. & Douglas, J. (1984) *PEERS: a new mixed finite element method for plane elasticity*. *Japan J. Appl. Math.*, **1**, 347–367.

Ateshian, G. A. & Weiss, J. A. (2010) Anisotropic hydraulic permeability under finite deformation. *J. Biomech. Eng.*, **132**, 111004.

Bærland, T., Lee, J. J., Mardal, K.-A. & Winther, R. (2017) Weakly imposed symmetry and robust preconditioners for Biot's consolidation model. *Comput. Methods*, *Appl. Math.*, **17**, 377–396.

Barbeiro, S. & Wheeler, M. F. (2010) *A priori* error estimates for the numerical solution of a coupled geomechanics and reservoir flow model with stress-dependent permeability. *Comput. Geosci.*, **14**, 755–768.

Barnafi, N., Gomez-Vargas, B., Lourenco, W. D. J., Reis, R. F., Rocha, B. M., Lobosco, M., Ruiz-Baier, R. & dos Santos, R. W. (2022) Finite element methods for large-strain poroelasticity/chemotaxis models simulating the formation of myocardial oedema. *J. Sci. Comput.*, **92**, e92.

Bloomfield, I., Johnston, I. & Bilston, L. (1998) Effects of proteins, blood cells and glucose on the viscosity of cerebrospinal fluid. *Pediatr. Neurosurg.*, **28**, 246–251.

Bociu, L., Guidoboni, G., Sacco, R. & Webster, J. T. (2016) Analysis of nonlinear poro-elastic and poro-visco-elastic models. *Arch. Rational Mech. Anal.*, **222**, 1445–1519.

Bociu, L., Muha, B. & Webster, J. T. (2022) Weak solutions in nonlinear poroelasticity with incompressible constituents. *Nonlinear Anal.: Real World Appl.*, **67**, 103563.

Bociu, L. & Webster, J. T. (2021) Nonlinear quasi-static poroelasticity. *J. Diff. Eqns.*, **296**, 242–278.

Boffi, D., Brezzi, F. & Fortin, M. (2013) *Mixed Finite Element Methods and Applications*, vol. **44**. Berlin: Springer.

Borregales Reverón, M. A., Kumar, K., Nordbotten, J. M. & Radu, F. A. (2021) Iterative solvers for Biot model under small and large deformations. *Comput. Geosci.*, **25**, 687–699.

Brenner, S. & Scott, L. (1994) *The Mathematical Theory of Finite Element Methods*. New York: Springer–Verlag.

Bulle, R., Hale, J. S., Lozinski, A., Bordas, S. P. & Chouly, F. (2023) Hierarchical *a posteriori* error estimation of Bank–Weiser type in the FEniCS project. *Comput. Math. Appl.*, **131**, 103–123.

Camaño, J., Caucao, S., Oyarzúa, R. & Villa-Fuentes, S. (2022) *A posteriori* error analysis of a momentum conservative Banach-spaces based mixed-FEM for the Navier–Stokes problem. *Appl. Numer. Math.*, **176**, 134–158.

Camaño, J., Gatica, G., Oyarzúa, R., Ruiz-Baier, R. & Venegas, P. (2015) New fully-mixed finite element methods for the Stokes–Darcy coupling. *Comput. Methods Appl. Mech. Eng.*, **295**, 362–395.

Cao, Y., Chen, S. & Meir, A. (2013) Analysis and numerical approximations of equations of nonlinear poroelasticity. *Discr. Cont. Dynam. Syst. B*, **18**, 1253–1273.

Carstensen, C. & Dolzmann, G. (1998) *A posteriori* error estimates for mixed FEM in elasticity. *Numer. Math.*, **81**, 187–209.

Carstensen, C., Dolzmann, G., Funken, S. A. & Helm, D. S. (2000) Locking-free adaptive mixed finite element methods in linear elasticity. *Comput. Methods Appl. Mech. Eng.*, **190**, 1701–1718.

Caucao, S., Discacciati, M., Gatica, G. & Oyarzúa, R. (2020a) A conforming mixed finite element method for the Navier–Stokes/Darcy–Forchheimer coupled problem. *ESAIM: Math. Model. Numer. Anal.*, **54**, 1689–1723.

Caucao, S., Oyarzúa, R. & Villa-Fuentes, S. (2020b) A new mixed-FEM for steady-state natural convection models allowing conservation of momentum and thermal energy. *Calcolo*, **57, 4**, 36.

Caucao, S., Oyarzúa, R. & Villa-Fuentes, S. (2022) *A posteriori* error analysis of a momentum and thermal energy conservative mixed-FEM for the Boussinesq equations. *Calcolo*, **59, 4**, article: 45.

Caucao, S., Gatica, G. N. & Ortega, J. P. (2023) *A posteriori* error analysis of a Banach spaces-based fully mixed FEM for double-diffusive convection in a fluid-saturated porous medium. *Comput. Geosci.*, **27**, 289–316.

Caucao, S., Mora, D. & Oyarzúa, R. (2016) *A priori* and *a posteriori* error analysis of a pseudostress-based mixed formulation of the Stokes problem with varying density. *IMA J. Numer. Anal.*, **36**, 947–983.

Correa, C. & Gatica, G. (2022) On the continuous and discrete well-posedness of perturbed saddle-point formulations in Banach spaces. *Comput. Math. Appl.*, **117**, 14–23.

Dörfler, W. (1996) A convergent adaptive algorithm for Poisson's equation. *SIAM J. Numer. Anal.*, **33**, 1106–1124.

van Duijn, C. & Mikelić, A. (2023) Mathematical theory of nonlinear single-phase poroelasticity. *J. Nonl. Sci.*, **33**, 44.

Elyes, A., Radu, F. & Nordbotten, J. (2019) Adaptive poromechanics computations based on *a posteriori* error estimates for fully mixed formulations of Biot's consolidation model. *Comput. Methods Appl. Mech. Eng.*, **347**, 264–294.

Ern, A. & Guermond, J.-L. (2004) *Theory and Practice of Finite Elements, Applied Mathematical Sciences, 159*. New York: Springer-Verlag.

Gaspar, F. J., Lisbona, F. J., Matus, P. & Tuyen, V. T. K. (2016) Numerical methods for a one-dimensional nonlinear Biot's model. *J. Comput. Appl. Math.*, **293**, 62–72.

Gatica, G. N. (2006) Analysis of a new augmented mixed finite element method for linear elasticity allowing $\mathbb{RT}_0$-$\mathbb{P}_1$-$\mathbb{P}_0$*approximations*. *ESAIM: Math. Model. Numer. Anal*, **40**, 1–28.

Gatica, G. N. (2014) *A simple introduction to the mixed finite element method. Theory and Applications*. Berlin: Springer-Verlag.

Gatica, G. N. (2020) A note on stable Helmholtz decompositions in 3D. *Appl. Anal.*, **99**, 1110–1121.

Gatica, G. N., Gómez-Vargas, B. & Ruiz-Baier, R. (2022) *A posteriori* error analysis of mixed finite element methods for stress-assisted diffusion problems. *J. Comput. Appl. Math.*, **409**, e114144.

Gatica, G. N., Márquez, A. & Sánchez, M. (2010) Analysis of a velocity-pressure-pseudostress formulation for the stationary Stokes equations. *Comput. Methods Appl. Mech. Eng.*, **199**, 1064–1079.

Gatica, G. N., Márquez, A. & Rudolph, W. (2013) *A priori* and *a posteriori* error analyses of augmented twofold saddle point formulations for nonlinear elasticity problems. *Comput. Methods Appl. Mech. Eng.*, **264**, 23–48.

Geuzaine, C. & Remacle, J.-F. (2009) Gmsh: a 3-D finite element mesh generator with built-in pre-and post-processing facilities. *Int. J. Numer. Methods Eng.*, **79**, 1309–1331.

Gómez-Vargas, B., Mardal, K.-A., Ruiz-Baier, R. & Vinje, V. (2023) Twofold saddle-point formulation of Biot poroelasticity with stress-dependent diffusion. *SIAM J. Numer. Anal.*, **63**, 1449–1481.

Grisvard, P. (2011) *Elliptic Problems in Nonsmooth Domains*. Philadelphia, PA: SIAM.

Kraus, J., Kumar, K., Lymbery, M. & Radu, F. A. (2024) A fixed-stress splitting method for nonlinear poroelasticity. *Eng. Comput.*, 1–12. https://doi.org/10.1007/s00366-024-02030-x

Lamichhane, B. P., Ruiz-Baier, R. & Villa-Fuentes, S. (2024) New twofold saddle-point formulations for Biot poroelasticity with porosity-dependent permeability. *Results Appl. Math.*, **21**, e100438.

Lee, J. J. (2016) Robust error analysis of coupled mixed methods for Biot's consolidation model. *J. Sci. Comput.*, **69**, 610–632.

Li, T. & Yotov, I. (2022) A mixed elasticity formulation for fluid–poroelastic structure interaction. *ESAIM: Math. Model. Numer. Anal.*, **56**, 1–40.

Lonsing, M. & Verfürth, R. (2004) On the stability of BDMS and PEERS elements. *Numer. Math.*, **99**, 131–140.

Meddahi, S. & Ruiz-Baier, R. (2023) A mixed discontinuous Galerkin method for a linear viscoelasticity problem with strongly imposed symmetry. *SIAM J. Sci. Comput.*, **45**, B27–B56.

Ruiz-Baier, R., Taffetani, M., Westermeyer, H. D. & Yotov, I. (2022) The Biot–Stokes coupling using total pressure: formulation, analysis and application to interfacial flow in the eye. *Comput. Methods Appl. Mech. Eng.*, **389**, e114384.

Showalter, R. E. & Su, N. (2001) Partially saturated flow in a poroelastic medium. *Discrete Contin. Dyn. Syst. B*, **1**, 403–420.

Støverud, K. H., Alnæs, M., Langtangen, H. P., Haughton, V. & Mardal, K.-A. (2016) Poro-elastic modeling of syringomyelia—a systematic study of the effects of pia mater, central canal, median fissure, white and gray matter on pressure wave propagation and fluid movement within the cervical spinal cord. *Comput. Methods Biomech. Biomed. Eng.*, **19**, 686–698.

Yi, S.-Y. (2014) Convergence analysis of a new mixed finite element method for Biot's consolidation model. *Numer. Methods Partial Differ. Equations*, **30**, 1189–1210.